LIGNIN MODIFICATION AND DEGRADATION FOR ADVANCED COMPOSITES AND CHEMICALS

A Dissertation
Presented to
The Academic Faculty

By

Zhe Zhang

In Partial Fulfillment
of the Requirements for the Degree
Doctor of Philosophy in the
School of Chemical and Biomolecular Engineering

Georgia Institute of Technology

December 2017

Copyright © 2017 by Zhe Zhang

LIGNIN MODIFICATION AND DEGRADATION FOR ADVANCED COMPOSITES AND CHEMICALS

Approved by:

Dr. Yulin Deng, Advisor
School of Chemical & Biomolecular Engineering
Georgia Institute of Technology

Dr. Sven H. Behrens
School of Chemical & Biomolecular Engineering
Georgia Institute of Technology

Dr. Donggang Yao, Co-Advisor
School of Materials Science & Engineering
Georgia Institute of Technology

Dr. Yonathan Thio
School of Chemical & Biomolecular Engineering
Georgia Institute of Technology

Dr. Meisha Shofner
School of Materials Science & Engineering
Georgia Institute of Technology

Date Approved: August 18, 2017

ACKNOWLEDGEMENTS

Ph.D study in Georgia Tech is one of the most memorable journeys in my life. Simple words cannot express my gratitude adequately to those who supported and helped me when facing every challenge during the past five years. First of all, I would like to show my greatest appreciation to my thesis advisor, Dr. Yulin Deng, who brought me to the world of research, who provides me with wise guidance to the right direction and who inspires and supports me continuously. It is great fortunate for me to have him as the advisor of Ph.D thesis and, more importantly, the mentor for my life. Also, I would like to thank Dr. Donggang Yao as my co-advisor. He taught me how to consider from the perspective of a process engineer and offered me great ideals and guidance for my research. My thanks would extend to all of my thesis committee members: Dr. Shofner, Dr. Thio and Dr. Behrens for their invaluable suggestions, encouragements and supports on my research and thesis.

Besides, please let me show my appreciation to the School of Chemical and Biomolecular Engineering for accepting me as a Ph.D candidate and for their supporting during my study. I also would like to thank all the faculty and staff of Renewable Bioproducts Institute for their financial support (PSE fellowship) to my research and other assistance to my work and study.

Furthermore, I would like to express my thanks to all my current and former lab mates, including Dr. Jian Gong, Dr. Zeshan Hu, Dr. Yongfeng Li, Dr. ParikshitGogoi, Dr. Xinliang Liu, Xihong Zu, Xiaodan Zhang, Wei Mu, Yong Cui, Sudhir Sharma, Arie

Mulyadi, Wei Liu, Xu Du, Vincent Li, Le Yang, Bingjie Zhou, Jianyu Xia, Zhaoyun Lin and all those who have worked in Dr. Deng's group. Thanks a lot for your supporting and discussing research with me! I appreciate all the colleagues and friends in Georgia Tech whoever helps me during the past five years.

Last but not the least, please let me show my deepest gratitude to my family! Thanks to Yi Ji, my adorable girlfriend, for your accompanying through my darkest time in life! Thanks to my parents for their endless and unconditional understanding, encouragement and love!

TABLE OF CONTENTS

LIST OF FIGURES

LIST OF TABLES

LIST OF SYMBOLS ANDABBREVIATIONS

ATRP	Atom transfer radical polymerization
RAFT	Reversible addition-fragmentation chain transfer
$CDCl_3$	Chloroform, deuterated
DMF	Dimethylformamide
AIBN	Azobisisobutyronitrile
KPS	Potassium persulfate
PDI	Polydispersity
DMSO	Dimethyl sulfoxide
FTIR	Fourier Transform infrared
GC	Gas Chromatography
GPC	Gel Permeation chromatography
HSQC	Heteronuclear Single-Quantum Correlation
M_n	Number average molecular weight
MS	Mass Spectroscopy
M_w	Weight average molecular weight
NMR	Nuclear Magnetic Resonance
Pd	Palladium
Pt	Platinum
Ru	Ruthenium
RT	Room Temperature
SEM	Scanning Electron Microscopy

SW	Softwood
HW	Hardwood
T	Temperature
TGA	Thermogravimetric Analysis
DTA	Derivative of thermogravimetric analysis
THF	Tetrahydrofuran
UV	Ultraviolet
XRD	X-ray Diffraction
1 D	1 dimensional
2 D	2 dimensional
DMSO	Dimethyl sulfoxide
H_2	Hydrogen gas
N_2	Nitrogen gas
O_2	Oxygen gas
H_2	Hydrogen gas
nm	Nanometer
μm	Micrometer
wt	Weight
vol	Volume
XPS	X-ray photoelectron spectroscopy
$NaNO_3$	Sodium nitrate
$FeCl_3$	Iron(III) chloride

SUMMARY

Over centuries, our society mostly relies on fossil fuels for majority of commodity materials, chemicals, plastics as well as energy sources derived from petroleum, coal and natural gas. The overutilization of fossil fuels to fulfill the inflation will cause the inevitable issues including dwindling of available resources and global environmental problems. With the awareness of the severe consequences of the society's over-dependence on fossil fuels, identifying sustainable and renewable alternatives has attracted significant and increasing attentions. Lignocellulosic biomass is one of the most accessible renewable forms of carbon and has been regarded as one the most logical feedstock to replace traditional fossil resources.

It is suggested recently that coupling of "biomass-conversion technologies" with "land-use" could meet the nation's increasing need for fuel without affecting food, feed and fiber production. However, most of the current biorefinery products are from the first-generation cellulosic projects, where most lignin is burnt for heating directly similar as the traditional pulp and paper industrial. Consequently, the advent of biorefineries that convert cellulose into liquid fuels generate more lignin than necessary substantially, which is a major waste of natural resources. Therefore, lignin valorization into value-added products is worthy to bio-refinery concept in particular and in general to the society. With this purpose, this dissertation is focused on modification and degradation of lignin for advanced chemicals and composites. The dissertation can be divided into the following components:

I. Lignin modification and the synthesis of lignin-based surfactant

In the first part, the structure and chemistry of lignin was investigated through various advanced characterization approaches and the viability of lignin as a good candidate for surfactant and emulsifier after certain modifications was demonstrated.

Typical lignin contains both hydrophilic phenolic/aliphatic hydroxyl groups and lipophilic carbon backbone, suggesting a special affinity to polar and nonpolar phases. However, the challenge is the solubility difficulty in both water and most organic phases. The challenge was overcome by modification of lignin with different chemicals. The resultant lignin showed great potential as surfactant which decreased the interfacial tension between styrene and water dramatically. Besides, this lignin-based surfactant was further demonstrated to be effective to prepared water-in-oil emulsions, which could be kept stable for over 30 days. The excellent interfacial activity of lignin is resulted from both its unique amphiphilicity and its disordered macromolecular structure.

II. Preparation of sustainable composites with lignin as the substitution of traditional polymer

Here, an effective route to prepare lignin/polystyrene composites foam via high internal phase emulsion (HIPE) polymerization was disclosed and their major properties were evaluated.

The incorporation of renewable materials as fillers and substitutions has attracted strong interest to promote sustainability for the existing plastic industry and to save the limited reserves of fossil fuel resources. However, the challenge is the poor compatibility between traditional polymer and natural materials, which can also be overcome by lignin

modification. We modified the lignin and the corresponding solubility in different media was exemplified by using theoretical model (Hassan solubility parameter model). Furthermore, the modified lignin was demonstrated to be good fillers and substitution of polystyrene through the investigation of its effects on the mechanical, thermal, and dimensional stability properties of the composites.

III. Catalytic degradation of lignin into aromatic chemicals by redox ion pairs

In this project, a new catalytic system which could degrade lignin into aromatic compounds under very mild conditions was designed.

Lignin is the only natural aromatic macromolecular feedstock of large production and therefore, is supposed to be good sources of sustainable aromatic chemicals. Till now no commercially available processes have been developed in our knowledge due to its unknown complicated structural pattern and its changes during the depolymerization process. Some oxidative chemicals were used in the literature to degrade lignin. However, most of the degradation processes suffer from low reactions kinetics and harsh conditions. Through research, we offered a low temperature oxidative degradation of lignin to form vanillic compounds by using $FeCl_3/NaNO_3/O_2$ as catalyst under mild conditions. The addition of $NaNO_3$ serves as a bridge between oxygen (gaseous phase) and iron salts (liquid phase) to improve the re-oxidation rate of Fe^{2+} and thus promote the overall degradation rate.

IV. Wood chips pretreatment by redox ion pairs under mild conditions

In this project, the new catalyst system was further used in biomass pretreatment, where wood chips were pretreated directly without grinding.

Based on the results of lignin degradation, we found this catalyst system was also effective in the biomass pretreatment. In biorefinery, pretreatment is an important step towards the accessibility of hydrolytic enzymes to cellulose for glucose conversion. However, in all the pretreatment process, biomass is grinded into powders first, which consumes energy and increase the cost. Using the novel catalyst system described here, the process where wood chips could be pretreated directly without grinding under mild conditions with a glucose yield of 70 % was first discovered.

In summary, this dissertation focuses on the valorization of lignin through modification and degradation approaches. It contributes on the colloid and interfacial science by preparation of lignin-based surfactant and studying on its interface phenomenon. Also, in this dissertation, the miscibility between lignin and polymer are investigated and the corresponding properties of the as-prepared composites are discussed. Besides, a new catalyst system to degrade lignin and pretreat wood chips is proposed and demonstrated to be effective, which contributes on the study of bonding cleavage in lignin and biomass materials.

CHAPTER I

INTRODUCTION

Over centuries, our society mostly relies on fossil fuels for majority of commodity materials, chemicals, plastics as well as energy sources derived from petroleum, coal and natural gas. The overutilization of fossil fuels to fulfill the inflation will cause the inevitable issues including dwindling of available resources and global environmental problems. With the awareness of the severe consequences of the society's over-dependence on fossil fuels, identifying sustainable and renewable alternatives has attracted significant and increasing attentions.

Lignocellulosic biomass is one of the most accessible renewable forms of carbon and has been regarded as one the most logical feedstock to replace traditional fossil resources. The annually production of biomass from both forestry and agricultural was reported to be over 1.3 billion tons, which suggests that biomass might be the most abundant source of carbohydrate. Previously, biomass is mainly used in the traditional agricultural field and pulp and paper manufacture. However, it has been demonstrated that the biomass resource is much more than what needed in these two industrials. It is suggested recently that coupling of "biomass-conversion technologies" with "land-use" could meet the nation's increasing need for fuel without affecting food, feed and fiber production. The biomass conversion into biofuels has been developed for over decades and several plants have been built to realize its commercialization.

However, most of the current biorefinery products are from the first-generation cellulosic projects, where most lignin is burnt for heating directly. Consequently, the

advent of biorefineries that convert cellulose into liquid fuels generates more lignin than necessary substantially. Besides, in the traditional pulp and paper industrial, lignin is generally regarded as a waste-product left in the black liquor with a production of 50 million tons annually. Similar as the biorefinery industrial, over 90 % of lignin is used as fuel directly. Indeed, lignin is an energy-rich compound and is supposed to have potential in various areas. Burning directly without further utilization suggests a major waste of natural resources. Therefore, lignin valorization into value-added products is worthy to bio-refinery concept in particular and in general to the society. With this purpose, this work is focused on modification and degradation of lignin for advanced chemicals and composites.

Lignin is a polymeric component in biomass, serving as a linker between cellulose bundles and functioning to give strength and rigidity to the cell walls, conduct water in plant stems and resist microorganisms attack. The structure of lignin is amorphous and highly branched by carbon-carbon bonds and ether bonds forming with three phenylpropanolic monomers (monolignols): p-Counmaryl alcohol, Coniferyl alcohol and Sinapyl alcohol. Based on the structure of lignin and the corresponding properties, study on value-added application of lignin has drawn great scientific attention and some progress has been achieved to convert lignin into value-added products, including liquid fuels, carbon fiber and chemicals. However, most of the technologies are far from commercial practice and much more efforts are needed in this area.

Chapter II of this dissertation is a brief review of some basic concepts and a state-of-the-art of the lignin modification by chemicals as well as its applications. This chapter aims to introduce the fundamental knowledge and current technologies on this topic,

which is the basis of the following researches. The Chapter III is “Problem Analysis and Objectives”, where the challenges of this research are listed and the corresponding solutions are proposed. Besides, detailed objectives are also described in this chapter. In Chapter IV, a study on synthesis of lignin-based surfactant via chemical modification is explored. The modified lignin shows great potential as a surfactant which decreases the interfacial tension between styrene and water dramatically. Besides, this lignin-based surfactant is further demonstrated to be effective to prepared stable water-in-oil emulsions. In Chapter V, an effective route to prepare lignin/polystyrene composites foam through high internal phase emulsion (HIPE) polymerization is disclosed. Lignin is demonstrated to be good fillers and substitution of traditional polymer through the investigation of its effects on the properties of the composites. Chapter VI describes a new catalytic system which can degrade lignin into aromatic compounds under very mild conditions. Furthermore, in Chapter VII, this catalyst system was used in biomass pretreatment, where wood chips were pretreated directly without grinding. It is demonstrated that the addition of $NaNO_3$ into $FeCl_3$ and O_2 serves as a bridge between oxygen (gaseous phase) and iron salts (liquid phase) to improve the re-oxidation rate of Fe^{2+} and thus promote the overall degradation rate. The finally Chapter VIII will summarize the overall conclusion of this research and provide the potential directions of the future work.

CHAPTER II

LITERATURE REVIEW

2.1 Problem Statement

Until 2011, over 80% of the total energy consumption in U.S., which has increased by 28% in the last 37 years[1], was generated from the three major fossil fuels. Along with the increasing in human demand, the overutilization of fossil fuels will cause two inevitable issues: dwindling of available resources and global environmental problems.[2-5] With the awareness of the severe consequences of the society's over-dependency on fossil fuels, finding sustainable and renewable alternatives has attracted significant attentions. Lignocellulosic biomass is the most accessible renewable form of carbon[6] and has been regarded as one the most logical feedstock to replace traditional fossil resources.[7]

A recent national report pointed the U.S. domestic production of biomass from forestry and agricultural industrials is over 1.3 billion tons annually.[8] The currently used and potential biomass (at $60 per dry ton or less) under baseline assumption is summarized in Table 2.1 and it is noticed that the annually biomass potential increases sharply. This suggests that, potentially, there is enough biomass to be utilized to replace fossil fuels. Furthermore, it is claimed that the coupling of "advanced biomass-conversion technologies" with "land-use changes" will not affect the production of food and fiber and, more importantly, it will provide more resources to the society.[9, 10]

Table 2.1 Summary of Currently Used and Potential Forest and Agriculture Biomass at $60 per Dry Ton or Less, under Baseline Assumptions[8]

Feedstock (million dry tons)	2012	2017	2022	2030
Forest resources currently used	129	182	210	226
Forest biomass & waste resource potential	97	98	100	102
Agricultural resources currently used	85	103	103	103
Agricultural biomass & waste resource potential	162	192	221	265
Energy crops	0	101	282	400
Total currently used	214	284	312	328
Total potential resources	258	392	602	767
Total – baseline	473	676	914	1094

Recent researches focus on the biomass conversion into biofuels or bioethanol, which can contribute to the area of liquid transportation fuels.[2, 10, 11] Indeed, the cellulose-based bioethanol technology has been commercialized and the bioethanol production of the first commercialized plant is located in Italy having 75 million liters per year capacity.[12] In the United States, the Department of Energy set a target that bio-based fuels would replace 30% of the conventional transportation fuel derived from petroleum by

2025.[2, 13] Beside of biofuels, bio-based chemicals and materials can also be produced from biomass, such as plastics, solvent and lubricants.[2] For example, polylactic acid has been manufactured in a U.S. company on the scale of million-kilogram.[14] Another goal set by the U.S. Department of Energy and Department of Agriculture is to increase the percentage of bio-based chemicals and materials to 25% in 2030 from 5% in 2005.[15]

However, most of the current biorefinery products are from the first-generation cellulosic projects, where most lignin is burnt for heating directly similar to the traditional pulp and paper industry. Actually, the generation of lignin is about 1.6 times of the amount needed for the internal energy use of these biorefinery projects[16], suggesting a highly underutilization of lignin resources. In 2010, the production of lignin from pulping process was 50 million tons, among which only around 2% was developed into specialty products.[17] The U.S. Energy Security and Independence Act of 2007 mandate the production of 79 billion of biofuels, which suggests an expected utilization of around 223 million tons of biomass and a lignin production of 62 million tons of lignin.[10, 18] In order to avoid the waste of natural resources, more attentions should be given on engineering lignin-based value-added products.

Actually, study on value-added application of lignin has drawn great scientific attention and some progress has been achieved to convert lignin into value-added products, including liquid fuels,[19] carbon fiber[20] and chemicals, such as phenol,[21] vanillin,[22] styrene[23] and etc. More specifically, lignin molecules have both hydrophilic functional groups and lipophilic carbon backbone, suggesting an amphipathic property to polar and nonpolar phases and great potential as a surfactant.[24, 25] Furthermore, as a natural polymeric material providing mechanical supports in wood, lignin can be used as

fillers or substitution in the polymer composites in order to make the composites more sustainable with certain desired properties.[10, 26] Additionally, lignin is the only scalable natural feedstock composed with aromatic units[22] and it is highly expected to obtain valuable aromatic components from lignin through some thermal, chemical or catalytic approaches. Figure 2.1 summarized some pathways of converting biomass into value-added products.[10] Although some progress of lignin upgrading has been achieved, most of the technologies are far from commercial practice and much more efforts are needed in this area.

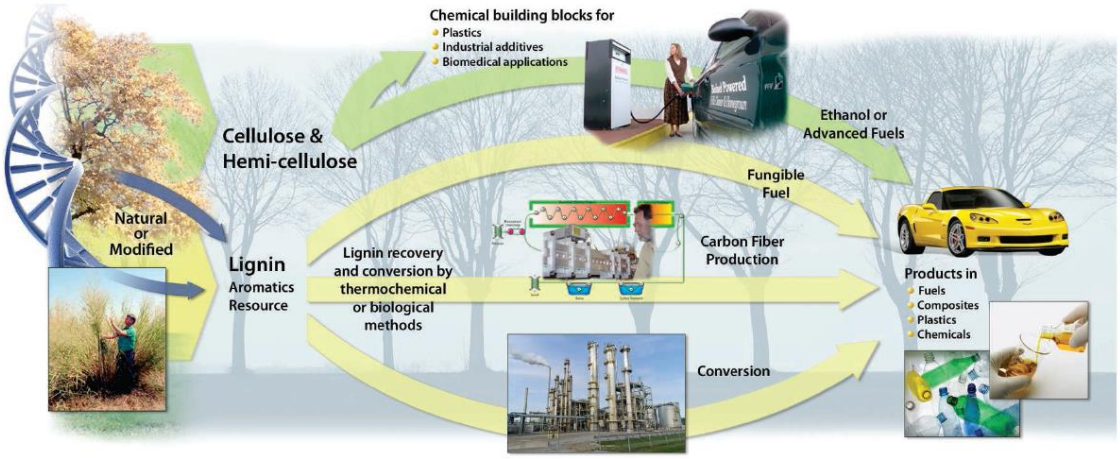

Figure 2.1 Development of value-added products from lignocellulosic biomass[10]

2.2 Lignocellulosic Biomass

Lignocellulosic biomass captures and stores the solar energy directly, which is one of the most abundant and sustainable resources on the earth. The major components of lignocellulosic biomass are cellulose, hemicellulose and lignin (shown in Figure 2.2[27]) with minor quantity of some other compositions, such as pigment, resin, tannin, etc. Among all the components, cellulose, composed with linked glucose units, comprises 30-

50 wt % of the dry biomass. Hemicellulose is another macromolecular polysaccharide, which constitutes 20-35 wt % of biomass. The remaining 15-30 wt % of biomass is lignin, which has highly cross-linked hetero-polymeric structure.[26, 28, 29]

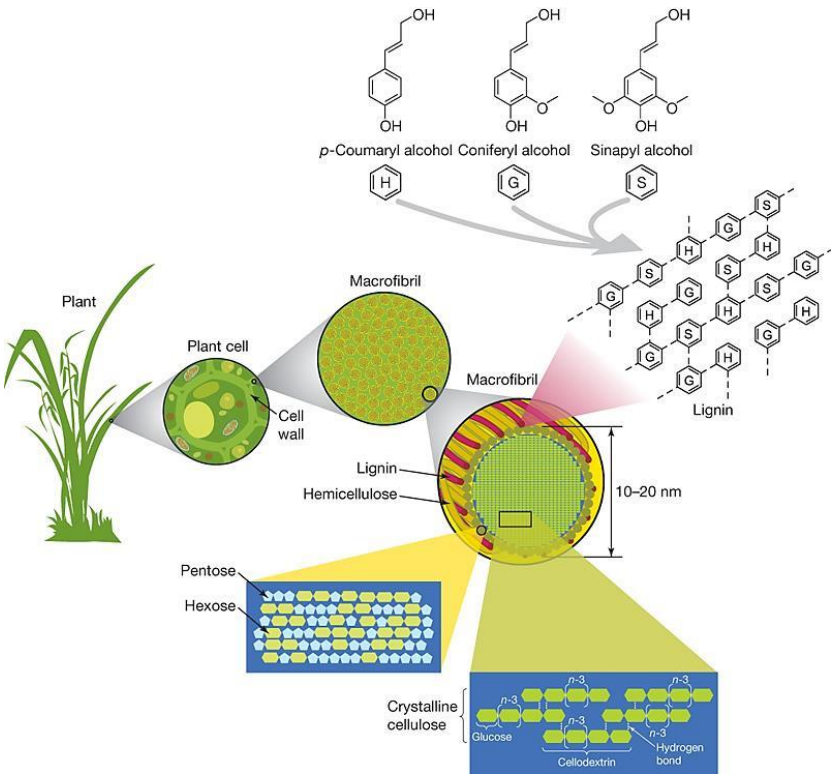

Figure 2.2 Structure of Lignocellulose[27]

2.2.1 Cellulose

Cellulose is the main structural component in the biomass cell walls and is the most abundant natural polymeric material distributed in plants, algae, fungi, bacteria and etc.[30], with an annual production of 75-100 billion tons in the world.[31-33]

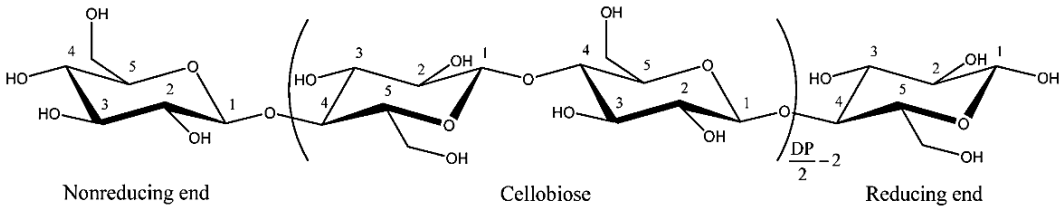

Figure 2.3 Chemical structure of cellulose[30]

In 1938, cellulose was first discovered and isolated by AnselmePayen[34] and the researches on its physical and chemical properties were made constantly since then. Technically, cellulose is a well-defined polymer linked by β-1-4 bonds of thousands of anhydro-D-glucose unites, as shown in figure 2.3.[30, 35] The polymerization degree of wood cellulose reaches up to 20 000.[28] In cellulose, the hydrogen atoms are positioned in the vertical plane and the hydroxyl groups are in the ring plane, which can form strong hydrogen bonds resulting in a stable structure. Besides, due to the high molecular homogeneity, the crystallization degree of cellulose can reach up 70%.[36] Cellulose was mainly used in the traditional pulp and paper industrial for centuries, but, during the recent decades, more and more cellulose stocks are converted into value-added products in the areas of chemicals, plastics and fuels through chemical, thermal or bio-treatments.[10] Until now, several cellulosic ethanol plants have been commercialized.

2.2.2 Hemicellulose

Another polysaccharide macromolecular component in biomass is hemicellulose, which is composed of different unites, including xylans, arabinans, mannans, galactans and etc.[37] The composition of hemicellulose varies significantly depending on the species or types of plants. In hardwood, the dominant hemicellulose structure is xylan (shown in

Figure 2.4 (a)), which may amount to 80-90% of hardwood hemicellulose[38], while glucomannan (shown in Figure 2.4 (b)) domains in softwood.[39, 40] Compared with cellulose, the polymerization degree of hemicellulose is relatively lower (~200) and the hydrogen bonds are much weaker.

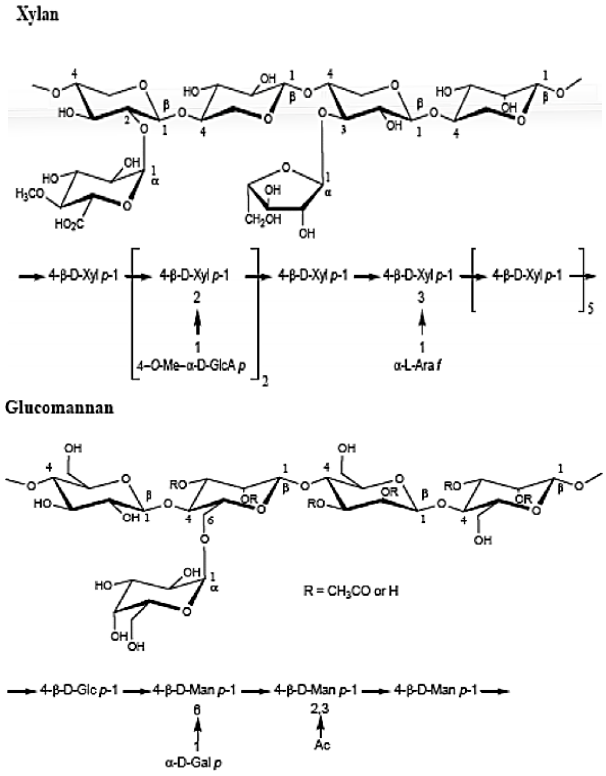

Figure 2.4 The dominant hemicellulose in hardwood-xylan (a) and softwood-glucomannan (b)[38]

In plant cell walls, hemicellulose promotes to connect cellulose fibrils together and contributes flexibility to the overall composites materials. In the traditional pulp and paper industrial, hemicellulose is produced as a byproduct and is not utilized optimally.[41]

2.2.3 Lignin

Lignin is another major polymeric component in biomass, which acts as a linker between cellulose bundles and is usually bonded to hemicellulose. In wood, lignin functions to give strength and rigidity to the cell walls, conduct water in plant stems and resist microorganisms attack.[42] The structure of lignin is amorphous and highly branched by carbon-carbon bonds and ether bonds and formed through an oxidative radical polymerization[43] with three phenylpropanolic monomers (monolignols): p-Counmaryl alcohol, Coniferyl alcohol and Sinapyl alcohol[44], as shown in Figure 2.5. Typically, lignin in grasses contains all three monomers, lignin from hardwood contains both Coniferyl and Sinapyl alcohol and softwood lignin mainly contains Coniferyl alcohol.[45] Different covalent bonds link between each monolignol[46], including β-O-4, 5-5, β-5, 4-O-5, β-1, β-β and dibenzodioxocin[47], leading to the complex lignin structure.

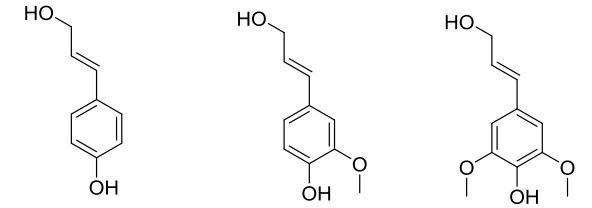

Figure 2.5 Three primary monolignols: p-Counmaryl alcohol, Coniferyl alcohol and Sinapyl alcohol

Until now, there is no certain conclusion to its original structure because the chemical composition of lignin changes according to the resources and isolation method employed.[48] Lignin can be classified into different types accordingly, such as enzymatic

lignin, kraft lignin, pyrolysis lignin, lignosulphonate, organosolv lignin and etc.[49] Therefore, the molecular weight (MW) of natural lignin is still a matter of debate and the MWs of lignin products vary highly dependent on the separation process. Table 2.2 shows the monomer molecular weights, molecular weights and polydispersities of different types of lignin. Kraft lignin, a primary byproduct extracted from black liquor during kraft pulping process through precipitation by controlling the pH value of the liquor, is the lignin mostly used in this research and the proposed structure of kraft lignin is shown in Figure 2.6. Compared with other types of lignin, the degradation by NaOH and Na_2S during the kraft pulping process leads to a relatively low molecular weight of kraft lignin, which is in the range of 1000-3000 Da.[49]

Table 2.2 Molecular weight and polydispersity of different lignins[49]

Lignin type	Monomer MW/[Da]	MW/[Da]*	Polydispersity
Milled wood lignin	198	2800–14200	3.7–12.9
Cellulolytic enzyme lignin	187	~1900	5.7–6.7
Enzymatic mild acidolysis lignin	187	~2000	~3
Kraft lignin	180	1000–3000	2–4
Lignosulfonate (softwood)	215–254	36000–61000	4–9
Lignosulfonate (hardwood)	188	5700–12000	4–9
Organosolv lignin	188	>1000	2.4–6.4
Pyrolysis lignin	n.d.	300–600	2.0–2.2
Steam explosion lignin	188	1100–2300	1.5–2.8

* Number-average molecular weight

The original lignin in natural biomass may be soluble in some certain mixtures of water and organic solvents. However, lignin products, especially kraft lignin, which are chemically modified and fragmented during the isolation process, can only dissolve in alkali aqueous solution and very limited organic solvents, such as dimethylformamide, dimethyl sulfoxide and furfural.[33]

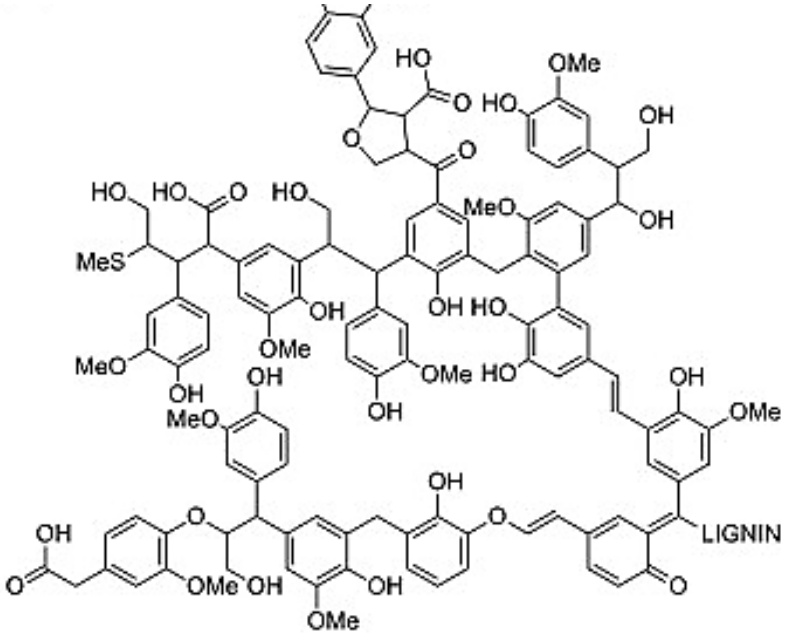

Figure 2.6 Proposed kraft lignin structure[49]

During the recent decades, study on value-added application of lignin has drawn great scientific attention and some progress has been achieved to convert lignin into value-added products, including liquid fuels,[19] carbon fiber[20] and chemicals, such as phenol,[21] vanillin[22] and styrene.[23]. However, much more efforts need to be done before these researches translating into commercial practice.

2.3 Characterization of lignin

As described in Section 2.2.3, the structures of lignin products will vary depending on the plant species and isolation process, yielding diversity and uncertainty of chemical compositions and physical properties. In order to be optimally applied in the following modification or degradation processes, it is crucial to identify the details of lignin structure both qualitatively and quantitatively through advanced characterization approaches.

Fourier transform infrared spectroscopy (FTIR) is widely used to study the chemical bonds in lignin by obtaining its infrared spectrum of absorption or emission. A wide band at 3450 cm^{-1} for O-H and a peak at 2935 cm^{-1} for the vibration of methoxyl groups[50] are the characterized peaks of raw kraft lignin. Besides, peaks at 1615 and 1514 cm^{-1} were assigned to the C-C stretching of aromatic rings in lignin[51].

Thermogravimetric analysis (TGA) and differential thermal analysis (DTA) can be applied to study the thermal properties of lignin. Raw kraft lignin shows a typical decomposition region of 300-450 ^{o}C with a solid residue of 30-40% at 900 ^{o}C in N_2 atmosphere.[25, 52]

Gel permeation chromatography (GPC), one type of size exclusion chromatography (SEC), is generally used to determine the lignin molecular weight depending on the basis of size.[53, 54] The mobile phase used in GPC can be deionized water (DI water), tetrahydrofuran (THF) or dimethylformamide (DMF), which is decided by the solubility of as-tested lignin.

As an amorphous polymeric material, lignin is supposed to have the glass transition temperature (T_g) which can be determined by differential scanning calorimeter

(DSC). Nevertheless, T_gs of lignin may vary drastically caused by the difference on lignin types, cross-linking degree and molecular weight.[55] A generally accepted range of T_g is reported between 70-170 ^oC[56], which seems very wide and difficult to use.

UV-Vis spectrophotometric analysis is exploited to measure the solubility of lignin in water. A calibration curve of standard lignin with different concentrations corresponding solution is needed at UV adsorption of 280 nm, which is considered as primary wavelength for quantification of lignin. [25, 57]

Recently, tremendous researches interests are focused on the lignin depolymerization into small chemicals.[58-61] To investigate the degraded chemicals in the solution, some chromatography methods are very helpful, including gas chromatography (GC), High-performance liquid chromatography (HPLC) coupled with mass spectrometry (MS), as shown in Figure 2.7.[60-62]

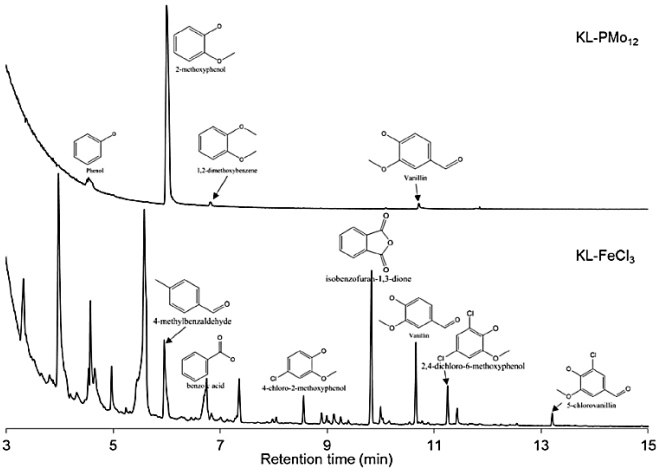

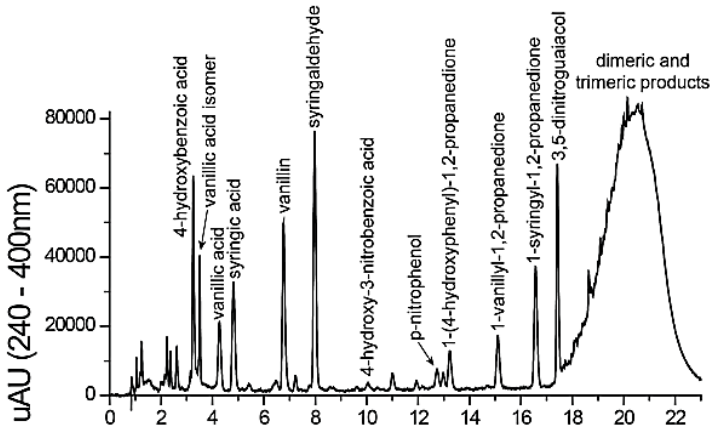

Figure 2.7 Investigation of small molecules produced by lignin degradation though GC-MS (a)[62] and HPLC (b)[60]

Among all the characterization approaches, nuclear magnetic resonance spectroscopy (NMR) is probably the most important and powerful technique to conduct the lignin structure analysis. NMR measurements of lignin can be classified on the basis of excited isotope (^{1}H NMR, ^{13}C NMR, ^{31}P NMR), nuclear dimensional resonance (1D NMR, 2D NMR) as well as sample statues (solid-state, solution-state). The solution-state ^{1}H NMR, ^{13}C NMR, ^{31}P NMR and hetero-nuclear single quantum coherence (HSQC) are most widely used to obtain the details of lignin structure.[63-65]

^{1}H NMR and ^{13}C NMR are obtained with the respects to hydrogen-1 nuclei and carbon-13 nuclei, respectively, in the lignin molecules. ^{1}H NMR shows the difference between hydroxyl, carbonyl, carboxylic acid, methoxyl, aromatic and aliphatic groups by the difference of proton chemical shifts.[66-68] Compared with ^{1}H NMR, ^{13}C NMR has a better resolution and is always used a quantification tool to determine the amount of carbon atoms in different chemical environments.[69]

^{31}P NMR is a general approach to quantitatively determine the content of hydroxyl groups in the lignin by forming derivatives with phosphitylation agent, 2-chloro-4,4,5,5-tetramethyl-1,3,2-dioxaphospholane (TMDP).[70-73] The reactions of TMDP and hydroxyl groups are summarized in Figure 2.8.[74] The contents of the hydroxyl groups in different chemical environments were determined by comparing relative areas with authentic internal standard.

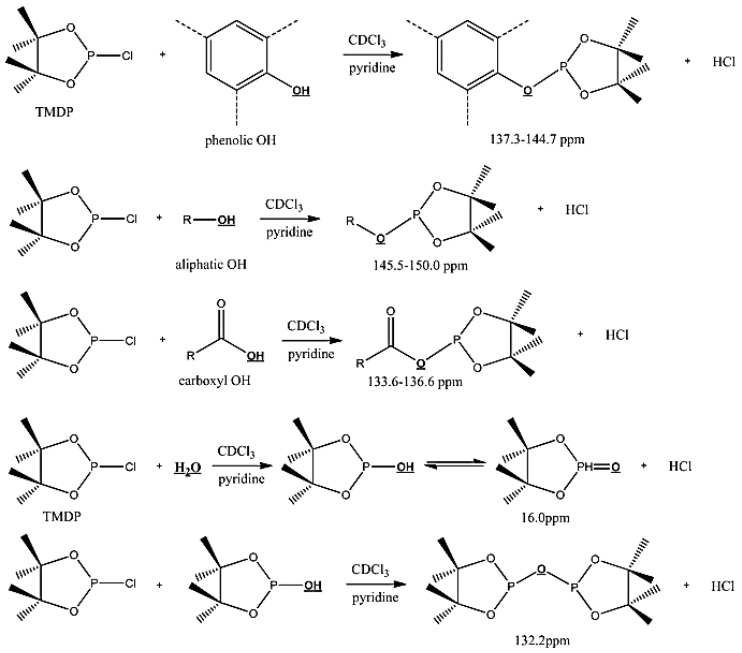

Figure 2.8 Reactions of TMDP with hydroxyl functional groups and the ^{31}P NMR assignment of lignin derivative[74]

HSQC NMR suggests its unique advantage by show the separation of heavily overlapped peaks in 1D NMR spectra caused by the complex of lignin structure.[75, 76] In the HSQC technology, the magnetization between H-1 and C-13 nuclei is transferred by two polarization transfer delay periods and the obtained spectra provide the information

of directly bonded protons and carbon atoms.[77] Therefore, the information of different structural units and lignin inter-unit linkages can be obtained with HSQC, as shown in Figure 2.9.[60]

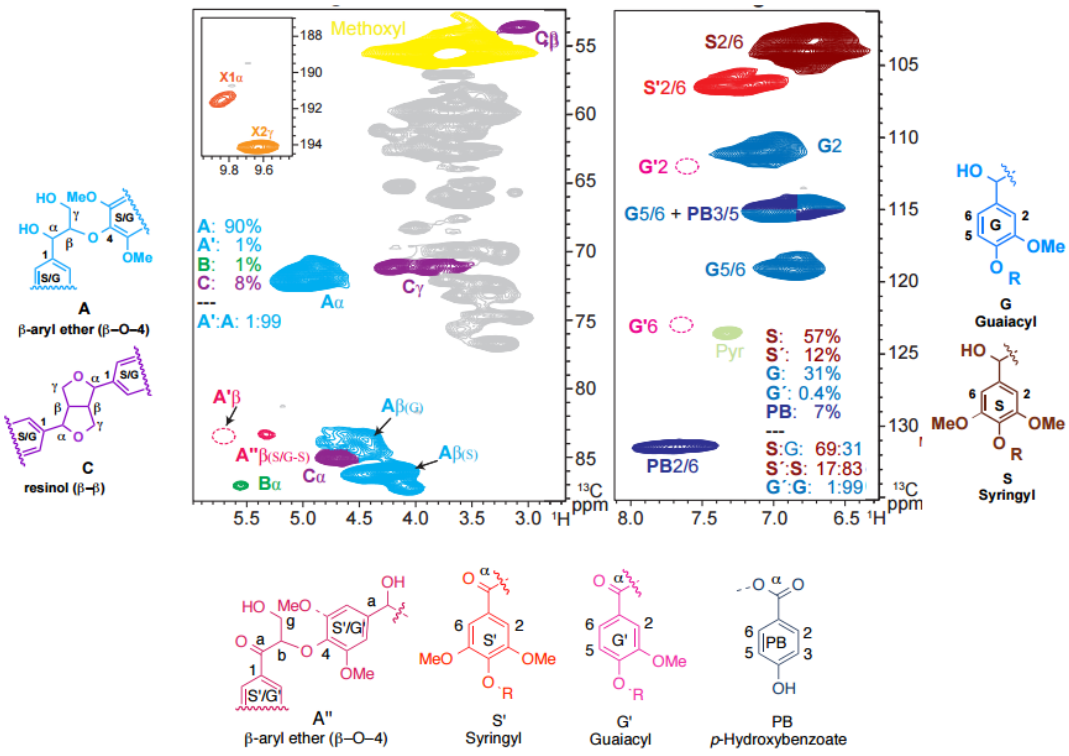

Figure 2.9 HSQC NMR of isolated Aspen lignin[60]

2.4 Lignin modification and lignin-based surfactant

Lignin contains both hydrophilic functional groups as well as lipophilic carbon backbone, suggesting a special affinity to aqueous and organic phases. Therefore, lignin is expected to be a good candidate of surfactant. However, the challenge is the limited lignin solubility difficulty in both aqueous phase of neutral or low pH value and most organic solvents and monomers, which hinders its practical application. Recently, many scientific investigations have been conducted on lignin to control its amphiphile by modification

and the resultant modified lignins show good potential in the field of dispersion and emulsification as bio-based surfactants.[24]

2.4.1 Lignin modification by chemicals

Although the detailed structural pattern for different types of lignins are not similar, most lignins contain some common functional groups, including of hydroxyl, methoxyl, carbonyl, ether and carboxylic acid groups. The diversity of functional groups combined with its carbon backbone may cause the difficulty in solubility, however it also provides the possibility of various kinds of modification approaches, such as esterification, acylation, halogenation and sulfonation.[78] In order to tune the chemical and physical properties, different modification approaches have been carried out to introduce functional sections onto lignin, as shown in Figure 2.10[79].

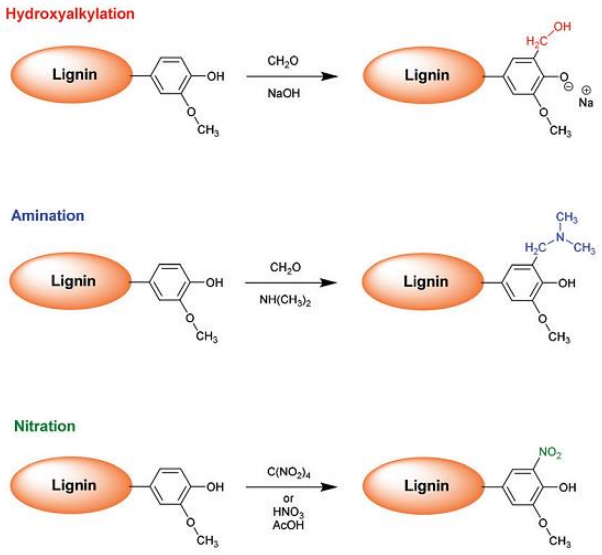

Figure 2.10 Summary of the chemical modification of lignin[79]

The hydroxyl groups in kraft lignin are generated by the fragmentation of lignin macromolecules through the bonding cleavage of the phenylpropane units in kraft cooking digester by NaOH and Na_2S.[80, 81] There are both aliphatic and phenolic hydroxyl groups in lignin, which can be functionalized by reactions with different chemicals, as shown in Figure 2.11. Alkylation and alkoxylation modifications are proposed to occur easily on these hydroxyl sites through nucleophilic aromatic substitution reactions.[82] The resultant lignin derivatives can be used as pre-polymers in the co-polymer preparation.[83, 84] Nitration of lignin can be achieved by reacting with nitric acid and the as-obtained lignin is proposed to be used as the fillers of polyurethane matrix.[85, 86] With amine and formaldehyde, lignin amination can be carried out through the Mannich reaction and the modified lignin shows great potential as a cationic surfactant as well as a reinforcement filler of polymer composites.[87-89]

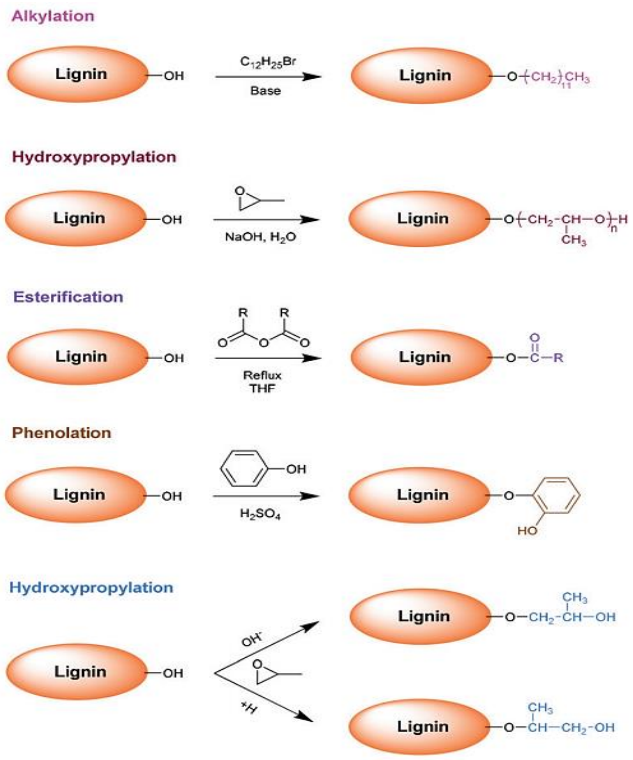

Figure 2.11 Functionalization of hydroxyl groups[79]

Another important and effective modification approach is esterification, which can convert the hydroxyl groups into esters.[90] Acids, acid anhydrides and acidic compounds have been demonstrated to be good esterifying agents.[52, 91-93] In purpose of preparing novel macropolyols, propylene oxide is used to esterify lignin with alkaline catalysts.[94, 95] In the area of lignin-based resins, lignin phenolationis carried out to enhance its chemical reactivity by introducing more –OH groups onto lignin structure.[96] Typically, the corresponding properties of the modified lignin can be tuned by adjusting grafting chemical, reaction conditions and esterification extent.[79] For example, a fully esterification of hydroxyl groups in kraft lignin by butyric anhydride makes lignin completely soluble in styrene while raw kraft lignin is not soluble.[90] Modification by

esterification has been demonstrated to be a good strategy to functionalize lignin, however, it is noticeable that the properties of resultant lignin derivatives are highly dependent on the amount of hydroxyl groups as well as other types of functional groups in lignin.

2.4.2 Lignin-based surfactant

In the typical lignin molecules, there are both hydrophilic phenolic/aliphatic hydroxyl groups and lipophilic carbon backbone, proposing a special affinity to polar and nonpolar phases as a surfactant. However, a certain modification step is often necessary to further control its amphiphilicity and solubility. Recently, many researches have been conducted to control the amphiphilicity of lignin so that the resultant derivatives can be applied in the field of dispersion and emulsification as bio-based surfactants.[24] These obtained sustainable surfactants would not only extend the application of lignin, but they also show better environmental compatibility compared with traditional chemical surfactants.

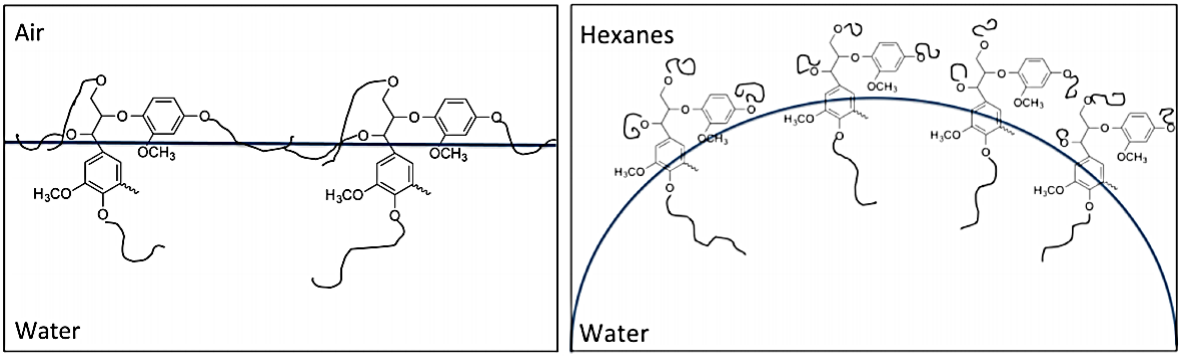

Figure 2.12 Schematic representations of polymer-grafted lignin at an air−water interface (left) and a hexanes−water interface (right)[24]

Homma *et al.* used poly(ethylene glycol) to functionalize kraft lignin.[97] The resultant lignin derivative successfully lowered the critical aggregation concentration in gypsum by 2~4 orders of magnitude. Zhou *et al.* prepared a water-soluble lignin-based surfactant through the alkylation with 1-bromododecane in alkali pyridine/isopropanol/water system.[98] They found that the water/air surface tension was reduced from 72.8 to 28.2 $mN \cdot m^{-1}$ when the resultant lignin derivative was applied. Besides, Gupta *et al.* grafted polyacrylamide and poly(acrylic acid) onto kraft lignin through reversible addition-fragmentation chain-transfer (RAFT) polymerization.[24] The grafted lignin was used to prepare emulsions of water and hexane where the low grafting density in the modified lignin was hypothesized to favor partitioning into hexane side of the oil-water interface, as shown in Figure 2.12. In another study, copolymerization between kraft lignin and acrylic acid was conducted by Kong *et al.*[99] The lignin copolymer product is water-soluble under acidic condition (pH=4).

Another strategy of enhancing its surface activity performance is to introduce highly hydrophobic groups onto lignin molecules. Lignin-based anionic/cationic surfactant was synthesized by Zhou *et al.*, [100] where a hydrophobic polyethylene glycol chain was introduced to sodium lignosulphonate (CA-PEGs). The surface tension in water/air interface decreased to 39 $mN \cdot m^{-1}$ when SL-PEG was used with CTAB. Surface-active organosiloxanolates were chosen as modifiers to improve the hydrophobicity of lignin by Telysheva *et al.*[101] These studies demonstrated that the interfacial activities of lignin could be improved by effective chemical modification.

Additionally, the lignin-based cement dispersant was successfully synthesized through calcium lignosulfonate oxidization by hydrogen peroxide and the corresponding

dispersibility was improved by 34 %.[102] Besides, more cement dispersants were prepared from lignin by grafting with ethoxy (2-hydroxy) propoxy polyethylene glycol glycidylether, polyethylene glycol diglycidylether and dodecyloxy-polyethylene glycol glycidyl ether and reported by Aso *et al.*[103-105] Furthermore, Ouyang and Fatechi modified kraft lignin by sulfomethylation and the resultant product also showed great potential as cement dispersant.[106]

However, to the best of our knowledge, only few publications related to oil-soluble lignin with good surface activity and stable W/O emulsion are reported in the literature. In Chapter IV, we tried to improve the compatibility of lignin and organic monomers by chemical modifications and synthesize bio-based surfactant which can be used as an emulsifier to prepare W/O emulsion.

2.5 Lignin-polymer composites

2.5.1 Polymer blending

Blending is one of the most commonly applied approaches to prepare polymer composites with desired properties. With its rigid structure and high polarity, lignin has been demonstrated to show great potential as an organic component in the area of polymer blends.[107] The blends of lignin and polystyrene (PS) were simply prepared by melting mixing in an internal batch mixer by Mohamad *et al.*[108] and they investigated the chemical and physical properties of the as-obtained blends with different lignin content. Maurizio *et al.*[109] blended lignin with poly(ethylene terephthalate) (PET) through a single-screw extruder. The influence of lignin on the crystallization of PET and thermal properties of the lignin/PET composites were studied. Another example is the blend of

lignin and poly(ethylene oxide) (PEO) synthesized by John *et al.*[110] where lignin and PEO were miscible due to the hydrogen bonds between these components. Actually, the miscibility of lignin with many other polymers is poor, which seems to be a big challenge hindering the further development of lignin/polymer blends. Charlyse *et al.*[111] studied the compatibility of lignin with different polymers and concluded that in order to obtain the expected blends, researchers needed to make careful choices on both technical lignin type and polymer structure.

The bad miscibility of lignin and polymer in the blends is resulted from the poor interfacial binding between these two components.[79] To overcome this challenge, chemical modifications are carried out to tune the structural affinity of lignin, which is further employed in the thermoplastic composites. Atul *et al.*[112] modified lignin with maleic anhydride first and prepared the blends of commercial polypropylene (PP) with the resultant lignin and found that its mechanical properties had less deterioration compared with the blends of PP and raw lignin. Furthermore, poly(methyl methacrylate) grafted lignin was blended with polyethylene (LDPE) by RRN Sailaja[113] and the as-obtained composites showed improved mechanical and thermal properties. Yang *et al.*[114] reported that films of nanocomposites blended by poly(lactide) (PLA) and modified lignin could be obtained through casting in chloroform. The addition of lignin was found to increase the elongation at break and toughness.

Beside of the thermoplastic materials, lignin is also demonstrated to show potential as reinforcement agent in the rubbery polymers. Alkyl esters were used to modify lignin in the work of Teramoto *et al.*[115] and the resultant lignin was blended with poly(ε-caprolactone) (PCL). They found that when the ratio of lignin and PCL was 1:1,

the mechanical properties of the composites, including strength and elongation at break, were improved significantly. Suo *et al.*[116] prepared the lignin-reinforced styrene-butadiene rubber (SBR) where lignin was first modified into lignin-layered double hydroxide composites by in situ method. In this research, lignin was demonstrated to be well dispersed in the composites by different characterization approaches. And most of the major mechanical properties of the composites were improved.

Lignin/polymer blends can also be applied in other functional areas, including UV protection, antioxidant as well as carbon precursors. Pouteau *et al.*[117] reported that the antioxidant activity of lignin/PP blends would decrease first and then increase with the increasing of lignin content. Furthermore, in the case of lignin/PLA blends[118], the addition of lignin into PLA would create the antioxidant capability while the pure PLA showed no this kind of property. The phenol groups in lignin can serve as the radical scavengers and therefore, lignin owns the potential as the agent for UV protection, which has been demonstrated by blending with PCL through high-energy ball milling conducted by Rachele *et al.*[119] Besides, the blend of PCL and lignin (PMMA grafted lignin) was found to be biocompatible, which could be applied as one biomedical material.[120] Lignin is also a good precursor of activated carbon in the energy storage area. Su-Xi *et al.*[121] prepared the lithium ion battery electrodes through the carbonization of lignin/PEO blend, which showed good conductivity and electrical properties.

2.5.2 Chemical grafting

Using lignin molecules as monomers by grafting polymerization on lignin is another strategy to synthesize lignin-polymer composites. Since lignin has a relatively high T_g due to the rigid aromatic structure, the copolymers of lignin with some soft elastomeric

polymers may result in thermoplastic properties of which the mechanical strength is provided by lignin and the rubbery characteristics are from the soft synthetic polymer.[82] The lignin-based polyurethane is one of the most important examples. The synthesis of lignin-based polyurethane can be realized through the grafting of isocyanate groups onto hydroxyls group sites of lignin and forming the urethane bonds via mixing lignin, diisocyanate and another diol monomer[122] or polymerizing lignin with isocyanate-based prepolymers[123]. Nakamura et al. studied the thermal properties of lignin-PEG-based polyurethane and found their T_g could be tuned by changing the content of lignin.[124] Saito *et al.*[125] discovered that the tensile strength of the as-prepared polyurethane would improve as they increased the lignin content up to 75%.

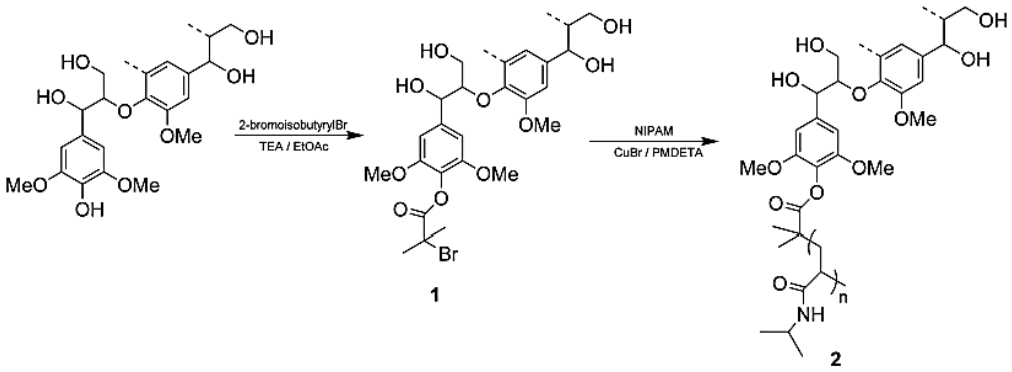

Figure 2.13 Two-step synthesis of lignin-N-isopropylacrylamide copolymer[126]

In the atom transfer radical polymerization (ATRP) and ring opening polymerization processes, lignin molecules are used as both one copolymer component as well as macro-initiators. The copolymer of kraft lignin and N-isopropylacrylamide was synthesized through a two-step process, as shown in Figure 2.13[126], where lignin was first modified with 2-bromoisobutyryl bromide and then the ATRP was carried out with the

as-modified lignin as initiator. The solubility of the obtained copolymer material could be controlled by the ratio of lignin and N-isopropylacrylamide. Besides, Shayna *et al.*[127] demonstrated that ATRP could be applied to prepare nano-particles of lignin-polymer composites with an average diameter of 5 nm, which also showed improved mechanical properties, including T_g and modulus. Lignin-poly(lactide) (PLA) composites can be prepared through ring opening polymerization, which was reported by Yi-Lin *et al.*[128] on the initial purpose of increasing the compatibility of lignin and other polymer. The toughening mechanism and mechanical improvement of the lignin-PLA composites were further studied by Yang *et al.*[114] and they reported that the crazing, the stereocomplex and the rubber phase were the major factors which resulted in the enhancement.

Additionally, as describe in Section, reversible addition-fragmentation chain-transfer (RAFT) polymerization was also employed to graft polyacrylamide and poly(acrylic acid) onto kraft lignin, which was carried by Gupta *et al.*[24] The obtained lignin was used to prepare emulsions of water and hexane as surfactant. Satvinder *et al.*[129] reported the copolymerization of lignin and vinyl acetate with $(NH_4)_2Fe(SO_4)_2 \cdot 6H_2O$ as catalyst in the aqueous phase. They investigated the effects of reaction parameters on grafting extent in detail.

2.6 Biomass pretreatment

The diminution of fossil fuels has attracted the use of plant biomass as an alternative sustainable source of building blocks for chemicals, materials and biofuels. Lignocellulosic biomass which is readily available in large amounts represents a potentially sustainable source of liquid fuels could satisfy the energy needs for

transportation and electricity generation with green chemistry perspectives. Potentially cellulose and hemicellulose in abundant feedstock include crops (corn, sugar cane), agricultural wastes, forest products, grasses, and algae etc[38, 130], can be converted to ethanol, 5-hydroxymethylfurfural (HMF), 2,5-dimethylfuran (DMF), levulinic acid and methyl furan, along with other energy platform molecules. The conversion process of lignocellulosic biomass to fuel typically consists of three steps: (1) pretreatment; (2) hydrolysis of cellulose and hemicellulose into fermentable sugars; and (3) fermentation of the sugars into liquid fuels (ethanol) and other commodity chemicals. Efficient conversion of lignocellulosic biomass to fermentable sugar depends largely upon the physical and chemical properties of biomass, pretreatment methods, effective microorganisms, and optimization of processing conditions.[131] The ideal pretreatment should break the lignocellulosic complex, increase the active surface area and decrease the cellulose crystallinity, while limiting the generation of inhibitory byproducts and minimizing hazardous wastes and wastewater.[132-134]

The largest technical hurdle for the efficient utilization of lignocellulosic biomass is the recalcitrance of lignocellulose to enzymatic degradation. Nowadays, one of the most critical needs for the commercialization of lignocellulosic biofuels is an efficient biomass pretreatment technology. In general, pretreatment can account for up to 40% of the total processing costs in the bioconversion of lignocellulosic biomass.[135] The traditional pretreatment methods of lignocelluloses mainly include steam explosion, dilute acid, ammonia fiber expansion, hot water, lime and organic solvent pretreatment technologies.[136] However, most of these processes require high temperatures or harsh chemical environments, leading to the formation of side products and being remarkably

energy intensive. Recently, cellulose solvents have attracted more and more attention, because they can break the recalcitrant structures of biomass effectively under relatively gentle conditions.[137] They can break the linkages among cellulose, hemicellulose and lignin, and also dissolve highly-ordered hydrogen bonds in cellulose fibers, thus leading to the great increases in enzyme accessibility.[138]

To the best of our knowledge, in most of the current pretreatment processes, wood chips are first grinded into powers before the chemical/thermal treatment, which is highly energy-consuming. Therefore, finding an effective pretreatment method where wood chips can be used directly will save a large amount of energy and cost and be a promising direction.

2.7 Thermochemical conversion of lignin into aromatic components

Lignin is the only large-volume natural feedstock composed with aromatic units,[22] which are cross-linked through the enzymatic mediated dehydrogenation polymerization.[139] The high aromatic nature makes lignin as one of the few natural large-scale sources for production of aromatic compounds and its extraction from lignin is recognized as crucial aspect to the economic sustainability of integrated biorefineries. Generally, the amorphous structure of lignin is formed by the couplings reactions of oligomer-oligomer, oligomer-monomer as well as monomer-monomer.[140] The major linkages in lignin include β-O-4, β-5, β-1, β-β, 5-5, and 4-O-5 (as shown in Figure 2.15[26, 47, 48]), among which β-O-4 is regarded as the most important target during the degradation process since it may account up to 50 % of the total linkages of lignin.[141] Besides, the diversity of the linkages types makes it more difficult and complicated to degrade lignin effectively

and selectively. Recently, the research interest on lignin upgrading to yield aromatic chemicals has increased through different techniques, such as oxidation[142], reduction[143], electrolysis[62], hydrothermal treatment[144] and biological treatment[145], as shown in Figure 2.14[146]. Until 2007, the major commercial products generated from lignin degradation processes were vanillin, dimethyl sulfide, and dimethyl sulfoxide.[146] In this research, we only focused on two major thermochemical approaches, oxidation and reduction, to convert lignin into value-added aromatic components.

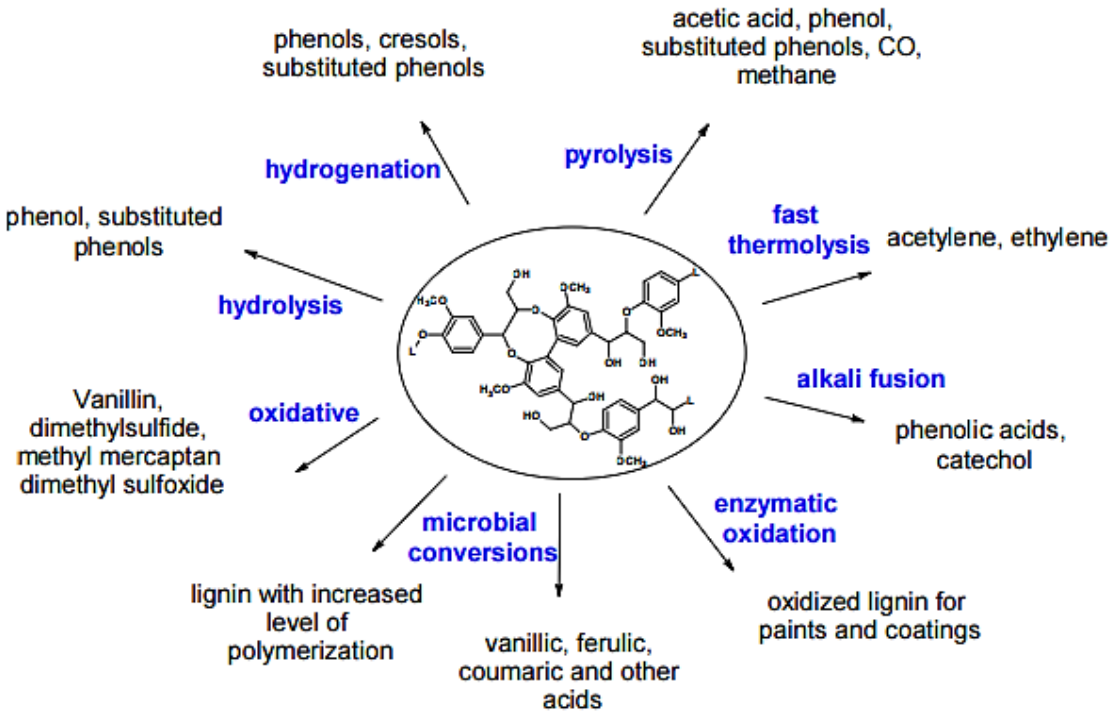

Figure 2.14 Brief summary of lignin degradation approaches and products[146]

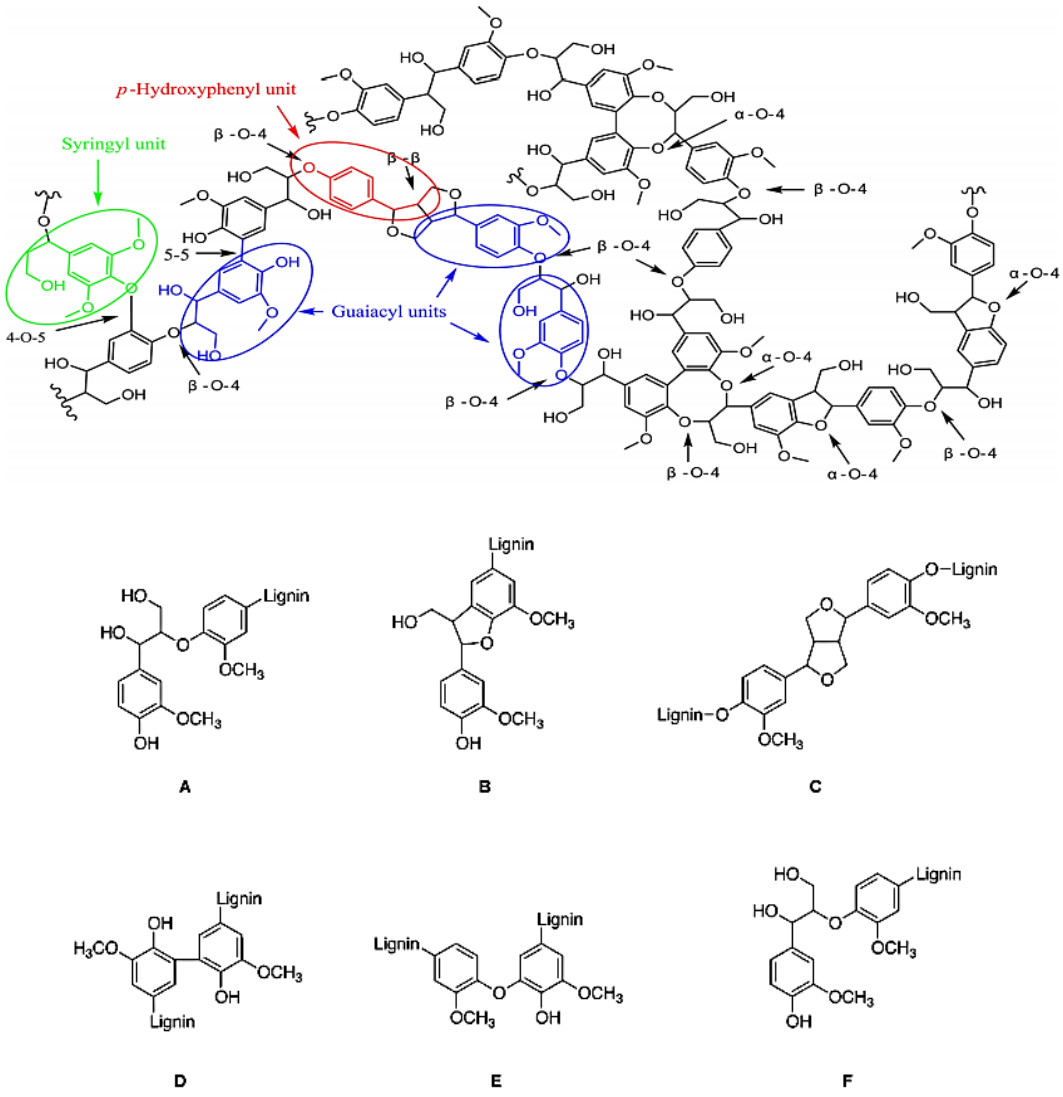

Figure 2.15 Major linkages in lignin: β-O-4; B: β-5; C: β-β; D: 5-5; E: 4-O-5; F: β-1.[26, 47, 48]

2.7.2 Lignin degradation by oxidation

Lignin depolymerization by oxidation is an important strategy to isolate aromatic components from lignin through the oxidative cracking reactions and cleavage of the chemical bonds.[142] The most commonly used oxidative agents include oxygen gas, metal oxides, nitrobenzene and hydrogen peroxide.[26] The products from lignin oxidation processes may vary depending on the reaction conditions, ranging from vanillin,

syringaldehyde, 4-hydroxybenzaldehyde to carboxylic acids. As the most abundant and cheapest oxidative agents, oxygen is proposed to be the ideal candidate to oxidize lignin. However, without a catalyst, the low rate kinetics of overall reactions and the poor selectivity of the as-obtained products hinder the practical application of oxygen.[147, 148] Therefore, numerous researches have been focused on the development of novel catalyst systems to optimize the lignin oxidative degradation process, including metal salts catalysis, metal-free organic catalysis, acid or base catalysis, organometallic catalysis as well as photocatalysis.

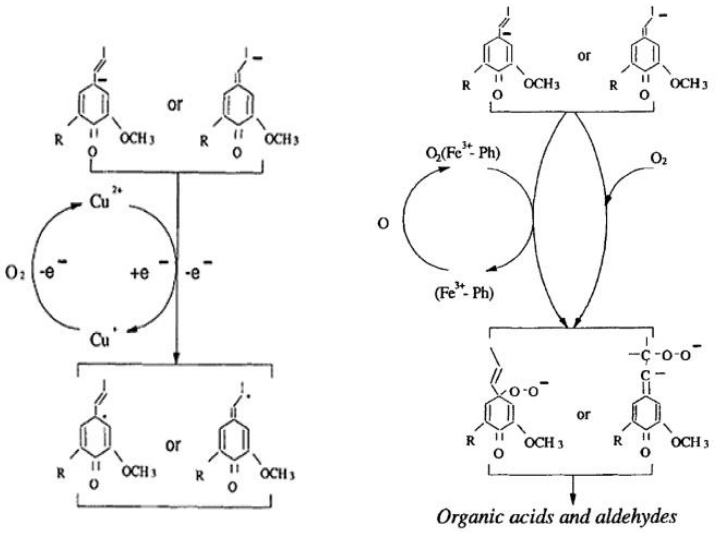

Figure 2.16 Proposed oxidation mechanism with Cu^{2+} and Fe^{3+} as the Catalysts[149]

Transition metal salts are an important category of lignin degradation catalysts. Metal ions with bivalence, such as Co^{2+}, Mn^{2+} and Zn^{2+}, can generate moderate yield of products through lignin model compounds in acids with the presence of oxygen.[150] However, the yield from hardwood organosolv lignin was low, which was around 10.9 %.[151] Besides, $CuSO_4$ and $FeCl_3$ were used in an alkaline solution by Wu *et al.*[148,

[152]to oxidize steam-explosion hardwood lignin and the yield of aromatic aldehydes was improved to 14.6 %. The proposed mechanism of Cu^{2+} and Fe^{3+} on lignin degradation is shown in Figure 2.16[149]. Compared with the traditional metal oxides, the perovskite-type oxides (ABO_3), such as $LaCoO_3$, $LaMnO_3$, and $LaFeO_3$, show more advantages in the lignin oxidation area due to their high catalytic activity and improved stability.[153] The catalytic activity of the perovskite-type oxides can be further improved by the substitution of A- or B- cations.[142] It was reported that the hollow nano-spheres of $LaFe_xMn_{1-x}O_3$ and $La_{0.9}Sr_{0.1}MnO_3$ was demonstrated to be more effective to oxidize lignin in the wet air condition compared with conventional perovskite-type oxides.[154] Furthermore, the substitution of Co-based ($LaCoO_3$)[155] and Fe-based ($LaFeO_3$)[156] oxides by Cu- ions ($LaFe_{1-x}Cu_xO_3$, $LaFe_{1-x}Cu_xO_3$) was proposed to promote the lignin degradation by increasing oxygen vacancies concentration and, thus, increasing the amount of adsorbed oxygen surface active site.

Polyoxometalates (POMs) are a class of anionic metal-oxo polyhedral clusters formed with metal centers and oxygen atoms at the vertices.[157-159] Recently, POMs are also explored to oxidize lignin in O_2 atmosphere.[160, 161] $[SiW_{11}VO_{40}]^{5-}$ was reported to be able to degrade phenolic lignin model compounds only by Weinstock *et al.*[162] while $[PMo_7V_5O_{40}]^{8-}$ showed catalytic activity on both phenolic and nonphenolic units[163]. The reaction mechanism was further investigated using β-aryl ether dimers and was disclosed to differ for phenolic and nonphenolic units. In the case of phenolic β-O-4 units, the cleavage of the linkages involves both hydrolytic cleavage of the alky-phenyl bonds and the typical acid-catalyzed splitting, as shown in Figure 2.17 (up). In the case of nonphenolic units, the cleavage of β-aryl ether proceeds through VO^{2+} one-electron

oxidation of aromatics followed by homolytic cleavage of C_{α}-$C_{ß}$ and β-O-4 linkages, as shown in Figure 2.17 (bottom). Besides, another POM, $H_3PMo_{12}O_{40}$ was applied as the oxygen vehicle to degrade lignin since its redox potential is higher than lignin and lower than oxygen.[160] They also discovered that the addition of small alcohol molecules into the degradation system could effectively prevent the re-polymerization of lignin fragments in aqueous phase and, therefore, promote the product yield.

Another strategy of lignin oxidation is focused on the combination of oxidative agents with ionic liquids. Zhu *et al.*[164] reported a lignin oxidation catalysis system of palladium (0) and iron bis(dicarbollide) pyridinium salt in the mixture of [Bmim]PF_6/[Bmim][$MeSO_4$]. This catalysis system was demonstrated to be effective and enhanced the conversion of the lignin model compounds by increasing the lignin solubility. The use of ionic liquids as solvent of the oxidation process can not only promote the solubility of lignin, it will also make the degradation extent controllable.[165] Weckhuysen *et al.*[166] compared the effects of different metal salts, such as $CoCl_2 \cdot 6H_2O$, $Co(acac)_3$, FeC_2O_4, $Ni(NO_3)_2$, $Cu(acac)_2$, and $Mn(NO_3)_2$, in 1-ethyl-3-methylimidazolium diethylphosphate ([Emim]DEP). They reported that the $CoCl_2 \cdot 6H_2O$ showed the highest reactivity in [Emim]DEP with high selectivity and also the activity order of different metal ions was Co > Cr > Fe > Ni >Mn≫ Cu.

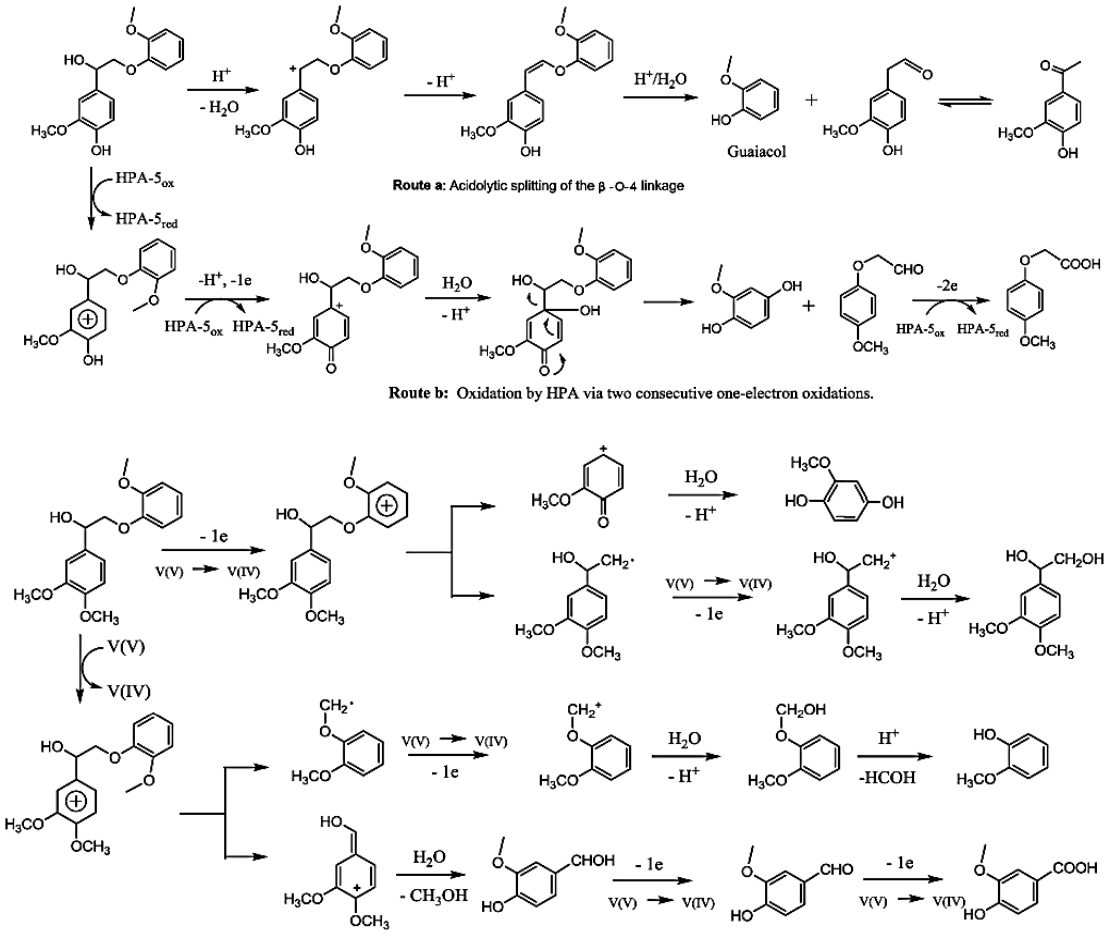

Figure 2.17 Cleavage of phenolic (up) and nonphenolic (bottom) β-O-4 linkages by POM[142]

2,2,6,6-tetramethylpiperidine-1-oxyl radical (TEMPO) is an effective metal-free catalyst to convert primary hydroxyl groups into carboxyl groups[167], which is further applied for lignin depolymerization.[58, 168] It was reported by Zhai *et al.*[169] that in the TEMPO oxidation system, the conversion was supposed to be decide by three factors: TEMPO, oxidative agents and reaction environment. The mechanism of a TEMPO-mediated lignin catalytic system in the aerobic condition was proposed by Stahl *et al.*[58] They proposed that the system combined with HNO_3 and HCl should have high chemo-

selectivity on secondary benzylic alcohols and they tested various lignin model compounds, as shown in Figure 2.18.[58] They further developed another process where formic acid was used in the system and the resultant yields increased up to 60 wt %.[60]

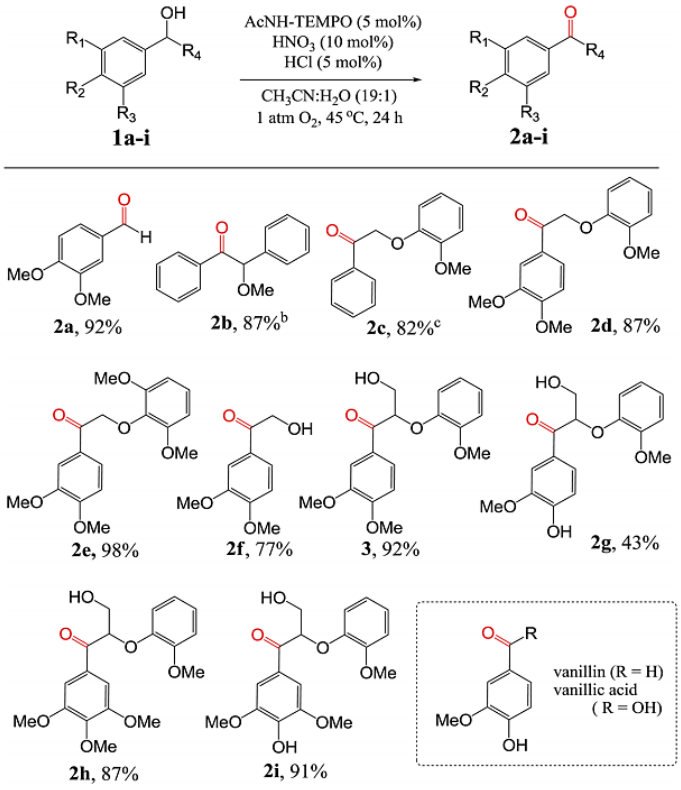

Figure 2.18 Chemo-selectivity of TEMPO-mediated oxidative system on lignin models[58]

2.7.3 Lignin degradation by reduction reaction

Benzene, toluene and xylene are the three major ideal chemicals derived from lignin since they are the starting chemicals and act as the building blocks of other aromatic compounds.[26] However, the chemicals produced from current lignin oxidation processes, such as vanillin and syringaldehyde, still possess some extent of oxygenation. In order to

obtain the completely deoxygenated aromatic compounds, reduced depolymerization or hydroprocessing cleavage is crucial in the lignin upgrading process. Technically, hydrogenolysis is the process where hydrogen atoms break the C-C or C-heteroatom bonds and add to the new-formed molecules.[142] This process is further developed into hydrodeoxygenation when combined with oxygen removal.

As one of the most popular hydrogenolysis catalyst, Nickel-based catalysts were applied in the area of lignin degradation starting back to the 1940s.[170] Sergeev *et al.*[171] demonstrated that the Ni-based complex could catalyze the hydrogenolysis of aryl ethers at 100 ^{o}C under 0.1 MPa H_2 atmosphere with yields of 54-99%. Another SiO_2 supported Ni catalyst was reported to break aryl ether bonds selectively, including α-O-4, β-O-4 and 4-O-5.[172] Beside of the model compounds, activated carbon supported Ni catalyst were reported to selectively cleave β-O-4 linkage of lignosulfonate in methanol by Song *et al.*[173] They further studied the effects of different alcohols as solvent on lignin depolymerization with Ni-carbon catalysts and indicated that alcohols served as proton-donors and H_2 gas wouldn't affect the lignin conversion.[174]

Another important category of hydrogenolysis catalysts are the metals in platinum group, including Pd, Pt, Ru, Rh and Ir, which have higher intrinsic catalytic activity compare with Ni.[142] Toledano *et al.*[175] reported that monomers, dimers and oligomers were successfully prepared from organosolv lignin through cleavage of aryl-O-aliphatic and aryl-O-aryl bonds by Al-SBA-15 supported Pd, Pt and Ru catalysts. Bouxin *et al.*[53] studied the impact of different types of lignin on the products of catalytic degradation by Pt/Al_2O_3 and suggested that yields of monomers were highly related to the proportion of β-O-4 linkages in lignin. However, due to the high catalytic activity of hydrogen, the

selectivity of catalysts in this group is not very high since they will not only promote hydrogenolysis of lignin and they also affect the rate of other hydrogen related reactions as well as side reactions.[53] Therefore, mild reaction conditions are preferred. Parsell *et al.*[176] introduced Zn into Pd-based catalysts and discovered that the new catalyst showed high synergistic effects on lignin conversion as well as a high selectivity on hydrodeoxygenation of aromatic alcohols without the impact on arenes.

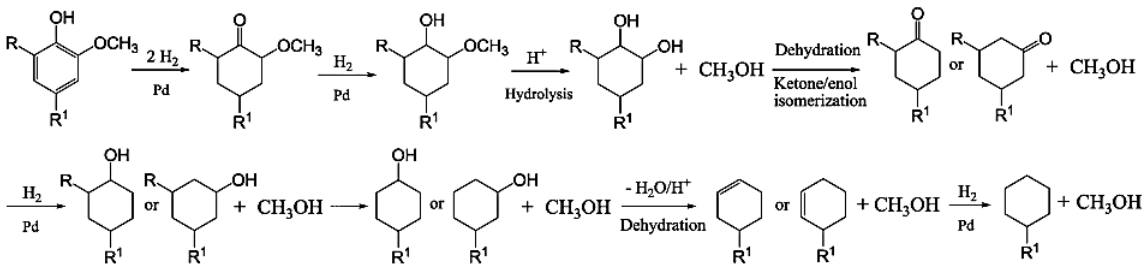

Figure 2.19 Proposed mechanism for phenolic aromatics hydrodeoxygenation with Pd/C and acid

Other types of catalysts, such as molybdenum-based compounds[177] and metal phosphides[178, 179] also show potential in lignin hydrodeoxygenation. Besides, some bimetallic catalysts, including PtRh[180], PtSn[181], PtRe[182], NiRe[183] and etc., can improve the selectivity of hydrodeoxygenation compared with monometal catalysts. It is also reported that the bifunctional catalysts containing both metal and acid components can increase the reaction kinetics and product selectivity. For example, Zhao *et al.*[184] studied the bifunctional catalysts of carbon supported Pd, Pt, Ru and Rh with phosphoric acid and found that they could convert phenolic compounds into cycloalkanes and methanol through hdyrodeoxygen process with the mechanism shown in Figure 2.19. However,

most of these catalytic reactions were carried out on lignin model compounds and very few hydrodeoxygenation researches were conducted on lignin complex. Oasmaa *et al.*[185] reported the catalytic hydrotreatment on organosolv lignin and kraft lignin with ammonium heptamolybdate and the hydrodeoxygenation degree reached 98%.

Using hydrogen-donating solvents, such as the mixture of phenol-water[186] and supercritical methanol or water[187], is an alternative strategy of lignin hydrogenolysis. Huang *et al.*[188] combined the metal catalysts ($CuMgAlO_x$) and supercritical ethanol and found an effective approach to lignin hydrodeoxygenation with an aromatic monomer yield of 23 wt % of lignin. Another kind of solvents is the ionic liquid. Binder *et al.*[189] conducted the hydrogenolysis of lignin model compounds in 1-ethyl-3-methylimidizolium chloride and triflate with metals and acids as catalyst systems and were able to isolate the expected products with relatively high yields.

However, most of the lignin degradation processes are carried out at very harsh conditions. Therefore, it is necessary to develop a new and effective method that can convert lignin into aromatics under very mild conditions.

CHAPTER III

PLOBLEM ANALYSIS AND OBJECTIVES

3.1 Problem analysis

As reviewed in Chapter 2, the production of biomass from agricultural and forestry sources is more than 1.3 billion tons annually. A study proposed that the coupling "biomass-conversion technologies" and "land-use" could not only meet the nation's increasing need for fuel, and also it would not affect the production of food, feed and fiber. Recently, the advent of biorefineries that convert cellulose into liquid fuels generates more lignin than necessary substantially. Over 90 % of the lignin generated is burnt for heating directly, which is a great waste of natural resources. Therefore, lignin valorization into value-added products is of great significance to the society.

It is indicated from the literature that the limited solubility, poor miscibility with other polymers and structure heterogeneity are the major obstacles hindering the further application of lignin. Besides, the strong covalent bonds between various units in lignin make it difficult to degrade lignin into small aromatic compounds under mild conditions. The primary objective of this thesis is to prepare value-added products from lignin. There are two common strategies: the first is to use lignin as a natural macromolecular material and the second it to decompose its complex structure into low molecular weight chemicals.

In order to use lignin in its macromolecular status, we seek to find some special properties from lignin. Lignin contains both hydrophilic functional groups as well as lipophilic carbon backbone, suggesting a good candidate of surfactant. Also lignin can

provide mechanical support in woods due to its rigid aromatic structure, which shows potential as fillers in the polymer composites. Hence, the desired solubility in aqueous or oil phase and good miscibility are crucial, which is actually affected by the heterogeneous structure. To overcome these challenges, we seek different modification reactions to tune the structure of the lignin and obtain the desired properties. We further demonstrate its application as the emulsifier for water-in-oil emulsion and substitution of traditional polymers in the porous aerogel.

In order to prepare useful chemicals from lignin, we seek to find some good catalysts that can degrade lignin in a green and sustainable method. As mentioned in Chapter 2, lignin is the only natural aromatic macromolecular feedstock of large production; however, all the aromatic units are linked with carbon-carbon or ester bonds, which can only be cleaved with high energy. There are two common chemical degradation methods: oxidation and reduction. Oxygen is the most ideal oxidative agent due to its universal availability and environmental-friendliness; however, the challenge is the low oxygen solubility in solvent and limited reaction kinetics at the liquid-gas interface. To overcome this challenge, we design the catalyst system with the combination of $FeCl_3$ and $NaNO_3$, which serves as the molecular vehicle to transfer oxygen onto the reaction sites and to increase the overall reaction rate. We further apply this system in the application of wood chips pretreatment. In the case of reduction, we choose anthraquinone and formaldehyde as the catalyst system to overcome the similar challenge.

3.2 Objectives

3.2.1 Objective 1

To prepare organic phase soluble lignin though modification with different chemicals and investigate its interfacial activities as surfactant.

Lignin is supposed to a good candidate of surfactant since it contains both hydrophilic and oleophilic units in the structure. However, most researches are focused on the aqueous phase soluble surfactant. In this objective, we will study the structure in detail with different characterization approaches and seek chemicals to graft onto lignin in order to make it soluble in organic monomers. The effects of modified lignin as surfactant on interfacial tension between aqueous and organic phases will be investigated. Further, we will apply it in the area of emulsification and study the stability of as-prepared emulsion.

3.2.2 Objective 2

To substitute traditional polymer with lignin and prepared the aerogels of the lignin-polymer composites. Also to study the effects of lignin on the properties of the as-prepared composites.

Lignin is supposed to be a good substitution of traditional polymer due to its rigid structure and mechanically supporting role in the wood. However, the fabrication of lignin-based emulsion-derived composite foams has not been fully disclosed. In this objective, we will increase the compatibility of lignin with other polymers and further design an effective route to prepare lignin-based polystyrene composites, in form of films and porous structures. The effects of lignin on the mechanical, thermal, physical and dimensional stability will be investigated.

3.2.3 Objective 3

To prepare aromatic compounds through lignin oxidation using redox ion pairs as catalyst under mild condition.

Lignin is supposed to be good sources of aromatic chemicals since it is composed with aromatic units. However, the degradation process is challenging due to its complicated structural pattern and strong covalent bonds. In this objective, we will offer a low temperature oxidative degradation of lignin to form vanillin by using a redox couple catalyst under mild conditions. The reaction parameters, such as catalyst content, temperature and reaction time will be studied. We will discuss the mechanism of the catalysis process.

3.2.4 Objective 4

To pretreat and break the lignocellulosic complex of hardwood and softwood chips directly by redox ion pairs under mild conditions.

Pretreatment of lignocellulosic biomass, especially for softwoods and hardwoods, plays the vital role in conversion of cellulosic biomass to bioethanol. Although many pretreatment technologies have been reported, almost all effective pretreatment methods cannot handle large sized woodchips directly. In this objective, we will report a simple, effective and low temperature (~100 ^{o}C) process for pretreatment of hardwood (HW) and softwood (SW) chips directly by using a catalytic system of $FeCl_3/NaNO_3$ redox couple. The working mechanism and understanding the structural changes of hard and softwoods during the process will be provided.

CHAPTER IV

BUTYRIC ANHYDRIDE MODIFIED LIGNIN AND ITS OIL-WATER INTERFACIAL PROPERTIES

4.1 Introduction

With an increasing concern over the fossil fuel shortage and environmental sustainability, great efforts have been made to utilize materials from renewable resources, such as bio-based surfactants.[79] Lignin is the second most abundant biomass resources on earth and the production is around 50 billion tons annually.[73] However, over 90% of lignin is currently disposed directly as a cheap fuel.[190] Studies on value-added application of lignin have drawn great scientific attention, and some progress has been made to convert lignin into value-added products.[19-23] Recently, many scientific investigations have been conducted on lignin to control its amphiphilicity so that the resultant lignin can be applied in the field of dispersion and emulsification as bio-based surfactants.[24] These sustainable surfactants would not only extend the application of lignin, but they also show better environmental compatibility compared with traditional chemical surfactants. Homma *et al.* used poly(ethylene glycol) to functionalize kraft lignin. [97]The resultant lignin derivative successfully lowered the critical aggregation concentration in gypsum by 2~4 orders of magnitude. In another study, Gupta *et al.* grafted polyacrylamide and poly(acrylic acid) onto kraft lignin through reversible addition-fragmentation chain-transfer (RAFT) polymerization.[24] The grafted lignin was used to prepare emulsions of water and hexane where the low grafting density in the modified lignin was hypothesized to favor partitioning into hexane side of the oil-water interface.

Naturally, most lignin is formed through an oxidative radical polymerization[43] by three main monolignols: p-counmaryl alcohol, coniferyl alcohol and sinapyl alcohol[44]. The functional groups of lignin may change depending on its biomass resources and isolation process[48]. Kraft lignin, used herein, is a primary byproduct extracted from black liquor during the kraft pulping process in the conventional paper and pulp industry. The hydroxyl groups in kraft lignin are generated by the fragmentation of lignin macromolecules through the bonding cleavage of the phenylpropane units in kraft cooking digester by NaOH and Na_2S.[80, 81] Kraft lignin can only be dissolved in a very limited selection of organic solvents and basic aqueous solution.[24] This problem often hinders the strategic utilization of lignin for various industrial applications. Nevertheless, on the other hand, the diversity of functional groups allows the possibility of many different modifications, such as esterification, acylation, halogenation and sulfonation. [78]

Typical lignin contains both hydrophilic phenolic/aliphatic hydroxyl groups and lipophilic carbon backbone, which suggests a special affinity to polar and nonpolar phases. Therefore, it owns great potential to be used as a surfactant. However,a certain modification step is often necessary to control its amphiphilicity and solubility. Zhou *et al.* prepared a water-soluble lignin-based surfactant through the alkylation with 1-bromododecane in alkali pyridine/isopropanol/water system. [98]. They found that the water/air surface tension was reduced from 72.8 to 28.2 $mN \cdot m^{-1}$ when the resultant lignin derivative was applied. In another study, copolymerization between kraft lignin and acrylic acid was conducted by Kong *et al.*[99]in an aqueous solution using $K_2S_2O_8$–$Na_2S_2O_3$ as an initiator. The lignin copolymer product is water-soluble under acidic condition (pH=4). Another strategy of enhancing its surface activity performance is to

introduce highly hydrophobic groups onto lignin molecules. Lignin-based anionic/cationic surfactant was synthesized by Zhou *et al.*,[100] where a hydrophobic polyethylene glycol chain was introduced to sodium lignosulphonate (CA-PEGs). The surface tension in water/air interface decreased to 39 $mN \cdot m^{-1}$ when SL-PEG was used with CTAB. Surface-active organosiloxanolates were chosen as modifiers to improve the hydrophobicity of lignin by Telysheva *et al.*[101] These studies demonstrated that the interfacial activities of lignin could be improved by effective chemical modification.

However, to the best of our knowledge, only few publications related to oil-soluble lignin with good surface activity and stable W/O emulsion are reported in the literature. The objective of this work is to improve the compatibility of lignin and organic monomers by chemical modifications and synthesize bio-based surfactant which can be used as an emulsifier to prepare W/O emulsion. Lignin solubility was investigated by chemical analysis. Reactions of lignin with BA, MPS, and BIBB were studied in detail by determining hydroxyl group content in lignin. Moreover, the interfacial tension between water and organic monomers was investigated and the modified lignin showed great potential in enhancing interfacial stability. Herein, we successfully synthesized a series of bio-based surfactants derived from kraft lignin. These surfactants are effective in reducing interfacial tension between aqueous/organic phases and preparing stable W/O emulsions.

4.2 Experimental and methods

4.2.1 Materials

Kraft lignin (lignin, alkali) was purchased from Sigma-Aldrich and used without any further pretreatment. Butyric anhydride (98%), tetrahydrofuran (THF), 1-Methylimidazole (1-MIM) and dichloromethane (spectrophotometric grade) were purchased from Alfa Aesar and used as received. Dimetylformamide (DMF) and anhydrous ethyl ether were obtained from J.T. Baker. 3-(trimethoxysilyl)propyl methacrylate (MPS), 2-bromoisobutyryl bromide (BIBB) and triethylamine were purchased from Sigma-Aldrich. Cyclohexane was purchased from BDH. Three monomers, styrene (stabled with 4-tert-butylcatechol), methyl methacrylate (MMA) (stabled) and butyl acrylate (BA) (stabled with 4-methoxyphenol) were purchased from Alfa Aesar and purified by passing through an alumina column to remove inhibitors before the interfacial tension measurements.

4.2.2 Lignin modification with butyric anhydride

In this reaction, the esterification reaction was carried out between lignin and butyric anhydride. Briefly, 5g of lignin was mixed with 15g of butyric anhydride in a 50ml two-headed flask. 0.25g of 1MIM was then added to the system as a catalyst. The reaction was performed at 70 °C in nitrogen atmosphere under vigorous stirring. After 10 hs, the reaction was quenched by adding diethyl ether. The reaction mixture was washed three times with water to remove the catalyst. Then cyclohexane was added to the solution to precipitate modified lignin from ether phase. After filtration, the product was dried under vacuum (50^{o}C) for 24hs. In the product separation process, 200 mL ethyl

ether, 3×200 mL water and 200 mL cyclohexane were used for each 100 mL reaction mixture.

4.2.3 Lignin modification with 3-methacryloxypropyltrimethoxysilane (MPS) and 2-bromoisobutyrylbromide (BIBB)

To compare with the butyric anhydride, another two chemicals (MPS and BIBB) were used to modify lignin in this section. In the case of MPS, 2g of original kraft lignin was first dissolved in the mixture of 80 mL THF and 12 mL water, and then 6 g of MPS was added to the system. The reaction was carried out at 60°C for 6hs under stirring and reflux. Dichloromethane was used to remove all the unreacted reactants. Most derivatized lignin precipitated and formed a granular layer between the organic and aqueous phases. After filtration, the products were washed with water for three times and then dried at 50 ^{o}C under vacuum for 24hs.

Another esterification reaction was performed between lignin and BIBB. Briefly, 3g of lignin was dissolved in 50 mL DMF in a 200 mL three-necked flask containing 16mltriethylamine. 12mLBIBB was added to the system dropwise under stirring. The reaction was performed at 70 °C under nitrogen atmosphere with stirring for 24 hs. After the evaporation of solvent, dichloromethane and water was used to wash the product for three times and then the product was dried at 50 ^{o}C under vacuum for 24hs.

4.2.4 Characterization of products

The structures of kraft lignin and modified lignin were verified by Fourier Transform Infrared Spectroscopy (FTIR) and proton Nuclear Magnetic Resonance (^{1}H NMR). Samples were dried at 105^{o}C for overnight before measurements. FTIR analysis was obtained by a Bruker Vertex 80V in the range of 500 to 6000 cm^{-1} with 32 scans. For ^{1}H NMR measurements, lignin samples (~100 mg) were dissolved in 600 μL DMSO-d6

and the spectra were recorded by a Bruker Avance/DMX 400MHzNMR spectrometer with 16 scans and 1s pulse delay.

Lignin pellets were prepared by pressing modified lignin powder (6000 psi). One drop of DI water was dropped onto the surface of each pellet. Then the contact angle of each lignin was measured by FTA200 dynamic contact angle analyzer (First Ten Angstroms). For each contact angle, three repeated tests were conducted, and the experimental error among the tests was less than 5%.

Thermogravimetric analysis (TGA) was performed to study the thermal stability of lignins. Approximately 15 mg of lignin samples were heated from 35 to 900 ^{o}C at a heating rate of 10 ^{o}C/min under N_2 atmosphere.

Gel permeation chromatographic (GPC) analysis was performed in THF with a flow rate of 1mL/min at 40^{o}C. Detection was achieved using a diode array detector (SPD‐M20A) and RI detector (RID‐10A). The instrument was calibrated with EasiVial polystyrene standards (Agilent).

4.2.5 Determination of hydroxyl group content

The contents of hydroxyl group in lignin were determined quantitatively by ^{31}P NMR as reported by Ben *et al.*[70] Specifically, lignin samples (~20 mg) were dissolved in 500 μL of the mixture of pyridine/$CDCl_3$ (1.6:1, v/v) with chromium acetylacetonate (1.75 mg)as relaxation agent and endo-N-hydroxy-5-norbornene-2,3-dicarboximide (NHND) (1.98 mg) as internal standard.100 μL of 2-chloro-4,4,5,5-tetramethyl-1,3,2-dioxaphospholane (TMDP) was injected to react with lignin. The spectra were obtained by a Bruker Avance/DMX 400MHzNMR spectrometer with an inversegated decoupling pulse sequence, 90^{o} pulse angle, 25 s pulse delay, and128 scans. The contents of the

hydroxyl groupsin different chemical environments were determined by comparing relative areas with authentic internal standard.

4.2.6 Conversion ratio

In this work, three chemicals were used to modify kraft lignin to convert its hydroxyl groups(–OH) into hydrophobic groups. The lignin conversion ratio (χ) was calculated based on the contents of hydroxyl group in lignin structure:

$$\chi(\%) = \frac{[-OH]_{total} - [-OH]_{remain}}{[-OH]_{total}} \times 100\%$$

where, $[-\mathrm{OH}]_{\mathrm{total}}$ is the total content of hydroxyl groups in original kraft lignin, mmol·g^{-1}; $[-\mathrm{OH}]_{\mathrm{remain}}$ is the content of unreacted hydroxyl groups after modification reactions, mmol·g^{-1}.

4.2.7. Solubility measurement of lignin in water at different pH values

The solubility of lignin in water was measured by UV-Vis spectrophotometric analysis. A calibration curve of standard lignin with different concentrations (0-1.05 g·L^{-1}) in 0.1 M NaOH solution was made at UV adsorption of 280 nm, which is considered as primary wavelength for quantification of lignin. [57]

Aqueous solutions of different pH values were prepared and adjusted by using 0.5 M H_2SO_4 and 0.5 M NaOH solution. When measuring the solubility, 1 g of lignin (original lignin and lignin-B) was added into 10mL aqueous solution and the mixtures were ultrasonicated for 1 h at room temperature. Then the mixtures were centrifuged and the supernatant was diluted with 0.1 M NaOH solution to achieve the corresponding concentrations (0-1.05 g·L^{-1}). UV absorbance at 280 nm was recorded.

4.2.8. Measurement of interfacial tension at the oil-water interface

The dynamic interfacial tension was measured via axisymmetric drop shape analysis of pendant drops with a Ramé-hart goniometer (model-250). This method is useful to determine the evolution of the interfacial tension due to the adsorption of surfactants or particles to the interface. Briefly, an inverted pendant drop of oil (styrene, MMA, or BA) immersed in the water was created by a syringe with a steel needle, and a high speed CCD camera was programmed to capture the variation of drop shape with time. The interfacial tension was obtained by analyzing the contour shape resulting from the balance of gravitational forces and tension forces. All experiments were performed at 21 °C. The oils used in this study were styrene, MMA and BA. They were purified before the testing by shaking with basic alumina for 2 minutes and kept for overnight. Ultrapure water with a resistivity of 18.2 MΩ·cm (Barnstead) was used in this study.

4.2.9. Emulsion preparation and measurements of droplet size distribution

A certain amount (0.5 wt % or 5 wt %) of lignin-B was dissolved in 4 mL of styrene and the mixture is stirred in an ice bath for 30 min to ensure complete dissolution of lignin. The resultant solution was added to 4mL deionized water (volume ratio equals to 1:1) and then the emulsion was prepared by vigorous stirring with homogenizer at 20,000 rpm for 5 min. The type of emulsion (O/W or W/O) was determined by adding one drop of emulsion into a volume of pure water or styrene and then observing its dispersion status. The results confirmed that the emulsion made from modified lignin surfactant was W/O emulsion.

A tube sedimentation test was used to determine the emulsion stability. Initially, the emulsion was milky and homogeneous and only one phase exists in the system. The

downward movement of the oil-emulsion boundary was measured to investigate the stability of emulsion to sedimentation. The coalescence rate was determined by the movement of the position of the oil-emulsion boundary as a function of time.

Size distribution of emulsion droplets was measured using a 90 Plus Brookhaven dynamic light scattering (DLS) instrument. The emulsions were diluted 100 times with styrene containing same amount of lignin-B before light scattering measurements. The measurements were performed at room temperature (20^{o}C) and the refractive index of the dispersion medium is 1.55. Ten runs were carried out for each sample.

4.3 Results and Discussion

4.3.1. Modification of kraft lignin

Theoretically, kraft lignin owns large amount of hydroxyl groups, which can react with chemicals like anhydride, silanes[191] and halogens [192]. Figure 4.1 shows possible pathways of lignin modifications with butyric anhydride, MPS and BIBB. The esterification reaction of lignin and butyric anhydride was carried out under closed nitrogen atmosphere at 70 ^{o}C with 1-MIM as a catalyst, as shown in Schematic 1(a). Butyric anhydride was used as both reactant and solvent. Initially, the original kraft lignin could not dissolve in the butyric anhydride solution before the reaction. However, as the reaction progressed, -OH groups of the lignin started to be converted into ester groups that would led to the completely dissolved lignin in the solution. Schematic 1(b) shows the reaction between kraft lignin and MPS, where the mixture of THF and water were used as the reaction medium. The reaction was performed at 60°C for 6h under stirring and reflux. In this reaction, –Si-O-C- bonds could be formed and the hydrophobic groups

of C=C bonds and ester linkages were introduced onto lignin. Another modification reaction was performed between kraft lignin and BIBB in DMF under a nitrogen atmosphere with trimethylamine as catalyst, as shown in Schematic 1(c). Ester bonds were formed with the reaction. After each reaction, the products were separated, purified and then characterized with FTIR, NMR, TGA and GPC to investigate their structures and to determine the conversion ratios.

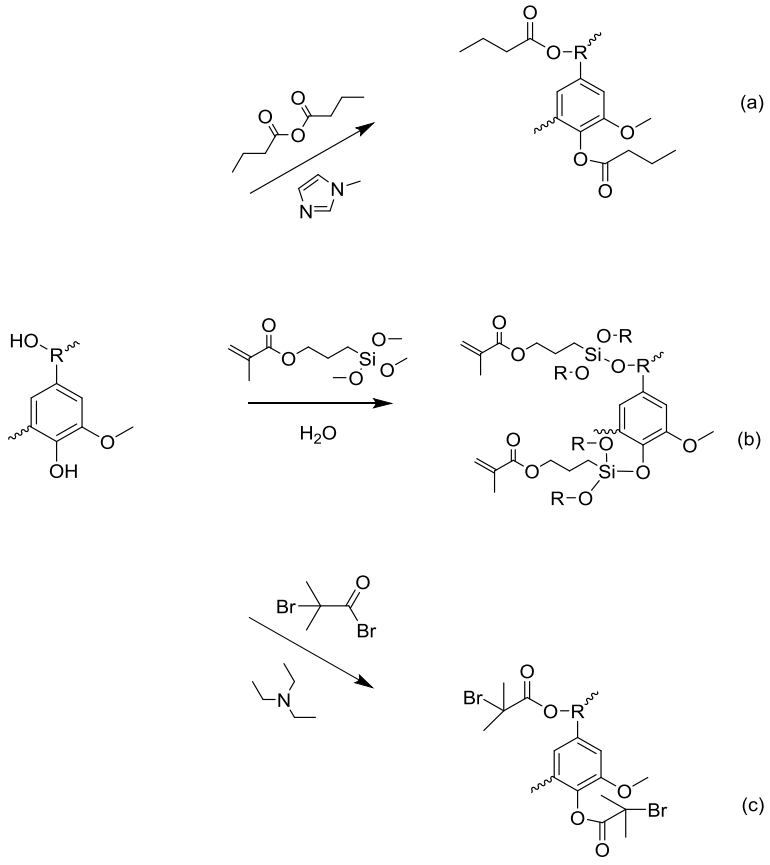

Figure4.1 Approaches of kraft lignin modification with three chemicals: (a) Butyric anhydride; (b) MPS; (c) BIBB. (Chemicals over the arrows are modifiers and molecules beneath the arrows are catalysts used in the reactions)

FTIR spectra of kraft lignin, lignin-B, lignin-MPS and lignin-BIBB are shown in Figure 4.2(A). A wide band at 3450 cm^{-1} for O-H and specific peak at 2935 cm^{-1} for the vibration of methoxyl groups could be used to characterize original kraft lignin.[193] Furthermore, peaks at 1615 cm^{-1} and 1514 cm^{-1}indicate the presence of C-C stretching in the aromatic rings.[51] A weak band at 1710 cm^{-1}represents the stretching of unconjugated carbonyls (C=O).[194, 195] Compared with the original lignin, the modified lignin can be identified by two aspects: (1) the relative strength of the absorbance bands at 2800-3000 cm^{-1} (O-H) to the strength in the range of 3000-3700 cm^{-1} (C-H stretching); (2) the shift of peak for carbonyls (C=O). The decrease of peak area in the range of 3000-3700 cm^{-1} indicates the removal of hydroxyl groups. In addition, the shifted peak of C=O from 1710 cm^{-1} to 1740 cm^{-1} suggests the introduction of esters (O-C=O) after reactions. [194]. It is also noticeable that the band in the range of 3000-3700 cm^{-1} is very weak indicating a high hydroxyl groups' conversion.

An increase in the molecular weights (MW) of modified lignin was observed in comparison with that of original lignin. As shown in Figure 4.2(B), the MW of lignin-B, lignin-MPS, and lignin-BIBB are centered on 2701 $g \cdot mol^{-1}$, 2665 $g \cdot mol^{-1}$ and 796 $g \cdot mol^{-1}$, respectively, while the MW of original lignin is centered on 461 $g \cdot mol^{-1}$. The increase of MW is another indication of the grafting of chemicals onto lignin. Figure 4.2(C) illustrates the TGA curves for kraft lignin and modified lignin. While the original lignin, Lignin-B and lignin-MPS have similar decomposition profile, in which they start at 300 ^{o}C and end at 450 ^{o}C, lignin-BIBB sample shows a two-step thermal degradation process. An early thermal weight loss starting at 200 ^{o}C was caused by the decomposition of BIBB molecules.[196, 197]

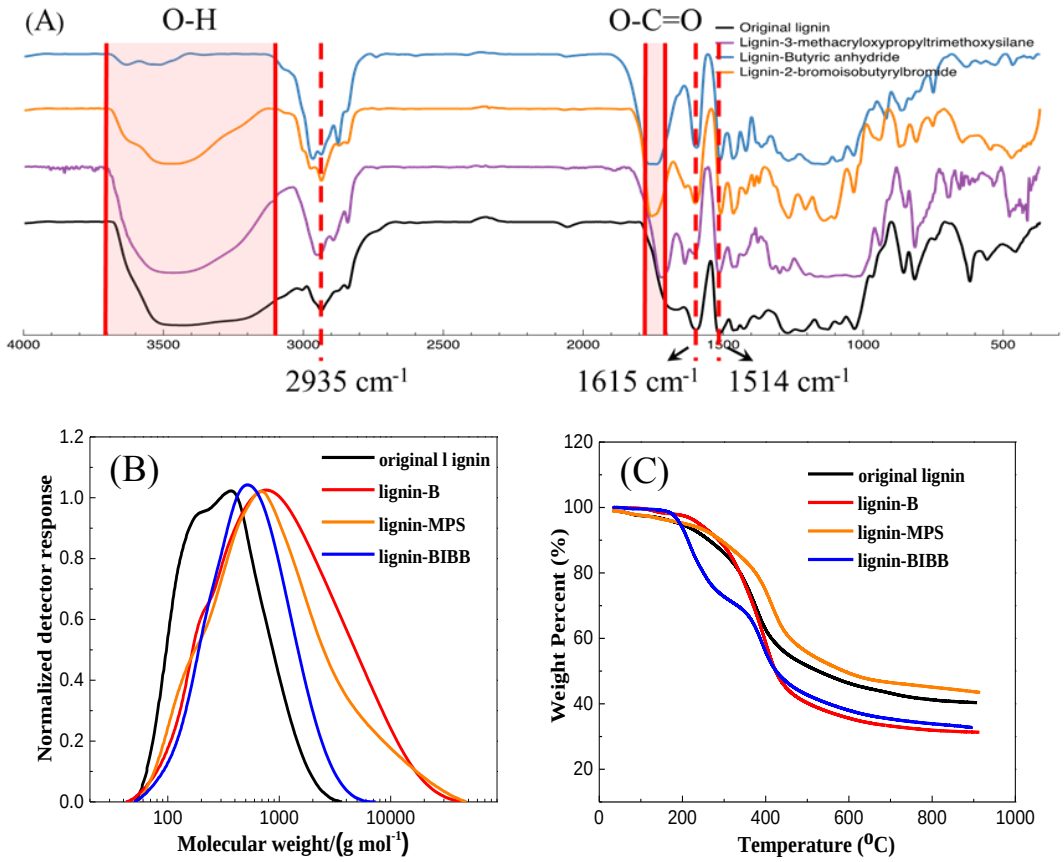

Figure 4.2 (A) FTIR spectra for different lignin (dash lines for specific peaks of lignin; solid lines for characterized peaks of modified lignin): lignin-B (blue), lignin-BIBB (orange), lignin-MPS (purple) and original lignin (black); (B) Molecular weights distribution by GPC for original lignin and modified lignin; (C) TGA curves for original lignin and modified lignin.

The ^{1}H-NMR spectra offer confirmation for the formation of the intended products, as shown in Figure 4.3. In the spectrum of original lignin (Figure 4.3(a)), protons at different chemical environments are quantified, including: hydroxyl protons (8.0-9.4 ppm), aromatic protons (6.3-7.7 ppm), methoxyl protons (3.81 ppm) and hydrocarbon chains (0-2.0 ppm).The result has been found to be consistent with the

results reported in the literatures. [198-2001]H-NMR spectra for lignin-B, lignin-MPS and lignin-BIBB are listed in Figure 4.3(b), 2(c) and 2(d), respectively. In the case of lignin-B, the relative strength of peaks in the range of 0-2.0 ppm significantly increases, corresponding to the increasing content of hydrocarbons (-CH_2-, -CH_3), [51] while the peak at ~9 ppm is no longer observed, attributed to the removal of hydroxyl groups. Peaks for specific protons are listed in the figure. In Figure 2(c), the peaks at 5.6 ppm, 1.5 ppm, 0.7 ppm, 1.35 ppm and 3.6 ppm are assigned to vinyl proton, methyl proton, α-CH_2-, β-CH_2- and γ-CH_2-, [201, 202] respectively. The spectrum confirms the successful grafting of MPS onto kraft lignin through the hydrolysis of silane groups. In the case of lignin-BIBB, only a proton of methyl groups is introduced at the chemical shift of 1.9 ppm. [203]

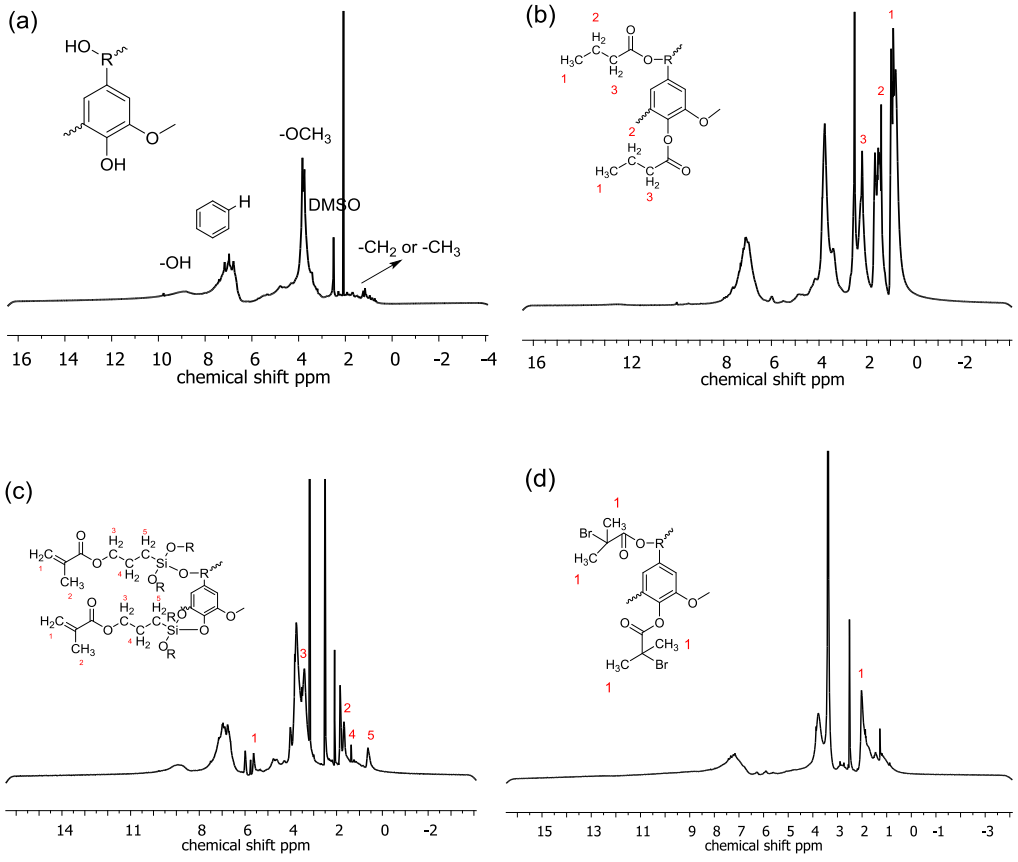

Figure 4.3 ^{1}H NMR spectroscopy for modified lignin: (a) original lignin; (b) lignin modified with butyric anhydride; (c) lignin modified with MPS; (d) lignin modified with 2-bromoisobutyrylbromide

Based on the results above, we conclude that the modification reactions occurred for all three modifiers (butyric anhydride, MPS and BIBB) under the given conditions.

4.3.2. Investigation of lignin solubility in oil

The solubility of both original kraft lignin and modified lignin was investigated by adding a small amount of lignin samples (~1.5 wt % of monomer) into styrene, MMA or BA. Figure 4.4 shows the photographs of different lignin solubility in styrene. The original kraft lignin is unable to dissolve in any of the monomers as indicated by the clear and colorless organic phase of the mixture after centrifugation. This is due to the presence of a large amount of hydrophilic groups, such as –OH, -SH and -COOH, in the unmodified lignin.[47] On the contrary, homogeneous solutions were obtained when lignin-B was mixed with styrene, MMA or BA monomers. The solubility test conducted by centrifugation followed by gravity measurement indicated that lignin-B is totally soluble at a concentration of 15 wt.%, which is similar with the result of Thielemans *et al.*[51] They conducted the similar reaction and explained the results using the Flory-Huggins solubility theory. However, they did not provide detailed information about its structure. In this work, ^{31}P NMR was applied to analyze the amount of hydroxyl groups on lignin structure and the change of its hydrophobicity was investigated through the difference of –OH contents before and after the reactions.

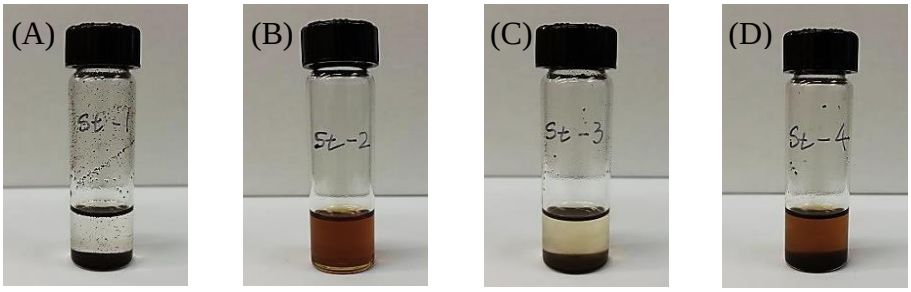

Figure 4.4. Photos of lignin dissolving in styrene: (A) original kraft lignin; (B) lignin-B; (C) lignin-MPS; (D) lignin-BIBB

In the case of MPS and BIBB modification, only partial lignin samples were dissolved. The partial solubility of lignin-MPS and lignin-BIBB in organic monomers was originated from the low reaction extent, resulting in an incomplete conversion of hydroxyl groups in kraft lignin. Therefore, to understand the extent of reaction for each modification, the content of –OH lignin after reaction need to be determined.

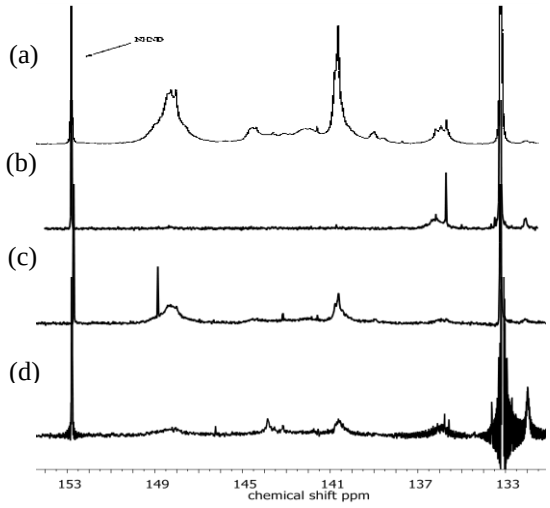

Figure 4.5 ^{31}P NMR spectroscopy for modified lignin: (a) original lignin; (b) Lignin-B; (c) Lignin-MPS; (d) Lignin-BIBB

^{31}P NMR is a general approach to quantitatively determine the content of hydroxyl groups in the lignin. [70-73]The ^{31}P NMR spectra of lignin samples, as shown in Figure 4.5 and Table 4.1, provide the information of unreacted–OH groups after the modification. Initially, one gram of kraft lignin contains 6.62 mmol hydroxyl groups. After the reaction with butyric anhydride, the hydroxyl group content reduced to 0.30 mmol/g, indicating over 95% of –OH groups were reacted. It is also believed that the residual hydroxyl groups were due to the trace amount of acid, which might be originated from the reaction of anhydride with water. In the case of lignin-MPS, more than 55% of the total hydroxyl groups in lignin were unreacted, in which 55% of aromatic hydroxyl groups and 27% of aliphatic hydroxyl groups were consumed. The result indicated that a higher reaction activity of aromatic –OH groups was observed in comparison to that of aliphatic –OH in this reaction condition. In the case of lignin-BIBB, 77% of hydroxyl groups were consumed. A relatively high but not fully converted hydroxyl groups was applied to both aliphatic and aromatic –OH. Thus, these data explained the solubility difference among lignin in styrene after modification with different chemicals. The high degree of esterification of –OH on lignin through the reaction with butyric anhydride reduces its hydrophilicity and made lignin-B soluble in styrene. In contrast, the partially –OH conversion in the case of MPS and BIBB promote only partial solubility. The overall conversion of hydroxyl groups is listed in Table 4.2.

In summary, kraft lignin was successfully modified by grafting anhydride, MPS and BIBB. The expected structures of derivatized products were confirmed by different

characterizations, including FTIR, NMR, TGA and GPC. According to the results of solubility measurements, lignin-B was demonstrated to be completely soluble in styrene while lignin-MPS and lignin-BIBB dissolved partially. The solubility of three modified lignins on oil were explained by extent of –OH conversion as calculated with the help of ^{31}P NMR. Butyric anhydride showed the highest reactivity and over 95% –OH groups were converted and the conversions were much less in the other two cases.

Table 4.1 Contents of hydroxyl groups at different positions of modified lignin

Chemical shift (ppm)	Assignment	(a) (mmol g^{-1})	(b) (mmol g^{-1})	(c) (mmol g^{-1})	(d) (mmol g^{-1})
150.0 – 145.5	Aliphatic OH	2.36		1.71	0.43
144.70 – 142.92	β-5	0.58		0.76	0.40
142.92 – 141.70	4-O-5	0.38			
141.70 – 140.20	5-5	0.69			
140.20 – 138.81	Guaiacyl	1.63	0	1.16	0.37
138.81 – 138.18	Catechol	0.22			
138.18 – 137.30	p-hydroxyl-phenyl	0.22		0.09	
136.60 – 133.60	Acid OH	0.54	0.30	0.05	0.31
	Total	6.62	0.30	3.77	1.51

(a) Original kraft lignin; (b) lignin modified with butyric anhydride; (c) lignin grafted with MPS; (d) lignin modified with 2-bromoisobutyrylbromide

Table 4.2 Conversion of hydroxyl groups for each modification reaction

	Lignin-B	Lignin-MPS	Lignin-BIBB
Conversion (%)	95.47	43.05	77.19

4.3.3. Study on the interfacial activity of modified lignin

While lignin-B is soluble in organic monomers due to the removal of most hydroxyl groups, the material still contains both hydrophobic backbones and hydrophilic function groups (–SH and –COOH).The amphiphilic structure of the material may suggest a promising surfactant functionality. In addition, the disordered high molecular weight structure of lignin is supposed to adsorb at the interface and consequently, reduces the overall interfacial tension.[24, 204]As shown in Figure 4.6(a), original lignin became soluble in aqueous solution when pH> 9, caused by the formation of sodium salt of phenol and its solubility increased sharply with the increasing pH. Nevertheless, lignin-B was insoluble at any pH value resulted from the high degree of phenol group conversion. The result indicates the potential utilization of lignin-B to provide both steric and electrokinetic stabilization at the oil-water interface.

The dynamic interfacial tensions of styrene-water interface for the modified lignin-monomer solutions were measured by the pendant drop shape analysis using a Rame-hart tensiometer. Figure 4.6(b) shows that the interfacial tension of 5 wt % of modified lignin in different monomers which decreased with time and then reached steady state. The decrease in the interfacial tension may be due to the progressive adsorption of modified lignin at the respective interface over the course of the

measurement series. As the interface reaches a saturated coverage by modified lignin, the interfacial tension reached a steady value. The steady state interfacial tensions of oil (styrene, MMA, or BA)-water interface as a function of lignin-B concentrations from 1 wt % to 15 wt % are given in Figure 4.6(c). The data demonstrate that the steady state interfacial tensions of all three systems first decreased and then reached a plateau.

The reduction of interfacial tension of oil-water interface suggests that modified lignin molecules adsorb onto the oil-water interface. The accumulation of modified lignin molecules in the interface may function effectively as emulsion stabilizer since it can prevent the droplet coalescence through electrostatic repulsion, mechanical barrier and formation of the viscoelastic skin around the droplets of the dispersed phase.

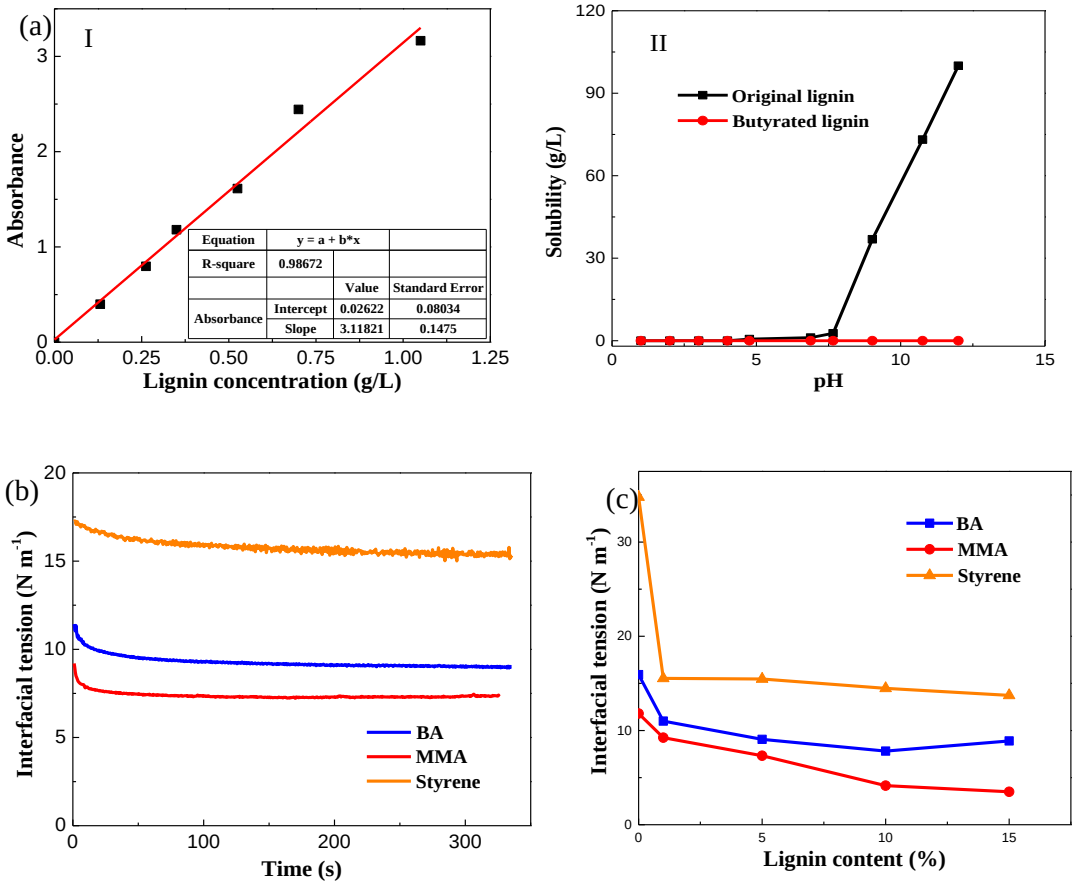

Figure 4.6 (a) Solubility of lignin: (I) Calibration curve of lignin solution with different concentrations; (II) solubility of original lignin and lignin-B at different pH values; (b) The change of interfacial tension on O/W interface with time: lignin-B (5 wt %) was used as surfactant; interfacial tension decreased with time first and then reached steady state; (c) Interfacial tension on O/W interface at steady state as a function of lignin-B concentrations from 1 wt% to 15wt%.

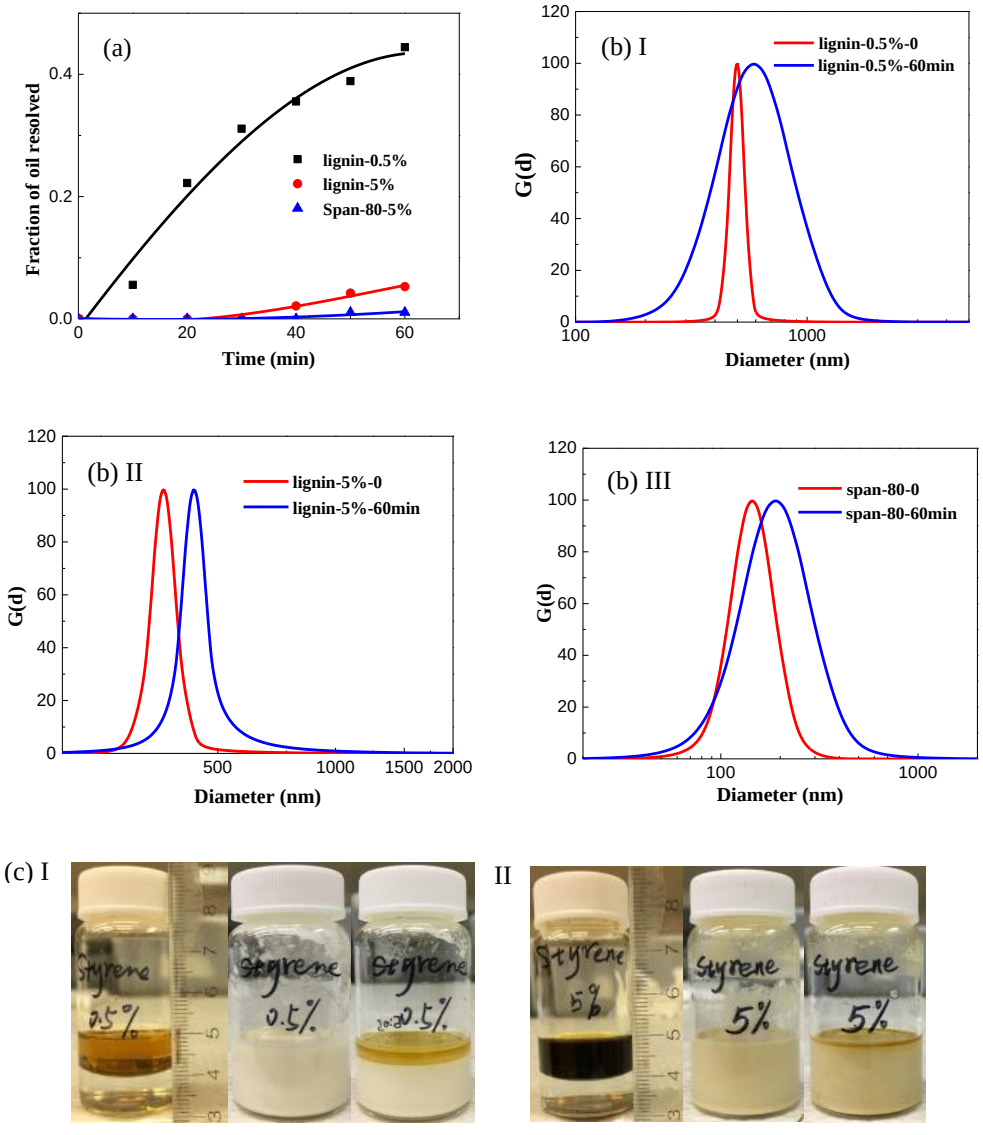

Figure 4.7 (a) Fraction of oil phase resolved versus time for styrene-water emulsion stabilized by lignin-B (0.5 wt % and 5 wt %) or span-80 (5 wt %). (b) Size distribution for styrene-water emulsion immediately after emulsification and 60 minutes after emulsification stabilized by lignin-B or span-80: (I) lignin-B, 0.5 wt % to styrene; (II) lignin-B, 5 wt % to styrene; (III) span-80, 5 wt % to styrene. (c) Photos for styrene-water system stabilized by lignin-B: before emulsification, immediately after emulsification and 60 minutes after emulsification (from left to right): (I) 0.5 wt %; (II) 5 wt %.

Before emulsification, two clear phases existed in the system with a mixture of lignin-styrene solution as upper phase and water as the bottom phase. After stirring at high speed (25,000 rpm), a homogeneous emulsion was obtained, as shown in Figure 4.7(c). The type of emulsion was verified by dispersing emulsion into the continuous phase; the prepared emulsion was able to be diluted by styrene (with stabilizer of same concentration) and formed a stable suspension, which indicates good water-in-oil (W/O) emulsion. Figure 4.8 shows the possible mechanism of emulsion system with styrene as the continuous phase and water as the dispersed phase. A thin layer is formed by lignin molecules at the O/W interface to decrease interfacial tension and stabilize water droplets.

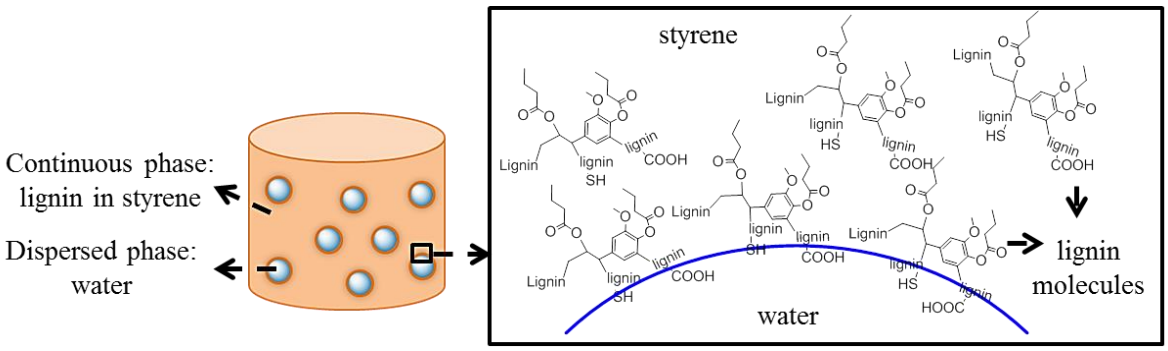

Figure 4.8 Schematic representations of lignin-B at the water droplet surface in the W/O emulsion system. Layer of lignin molecules were formed at the interface.

In order to investigate the sedimentation stability of the emulsions prepared with lignin-B, the fraction of top oil layer (φ_{oil}) separated from the emulsion was measured. As shown in Figure 4.7(a), the sedimentation stability increased progressively with the increasing of lignin-B content. After 1 h from the emulsification, φ_{oil} reached 0.4 when 0.5 wt % lignin-B was used as surfactant while φ_{oil} reduced to 0.06 when lignin content increased to 5 wt %. It has been known that the emulsion droplet dimension and the continuous phase viscosity are the two major factors that affect sedimentation stability of the emulsion. Dynamic light scattering (DLS) was applied to determine the droplet size of emulsions, as indicated in Figure 4.7(b). The diameters (intensity average) of water droplets were 499.4 nm and 363.9 nm for 0.5 wt % and 5 wt % lignin respectively when measured immediately after emulsification. The smaller droplets size (363.9 nm) in high-lignin-content (5 wt %) case suggested a slow sedimentation of the droplets in the emulsion. On the other hand, the viscosity of organic phase (continuous phase) increases with increasing lignin concentration, [205, 206]and thus hinders the sedimentation movement.

[207]Thus, high lignin content facilitated an increase in mixture viscosity and a decrease of emulsion droplet diameter, which enhanced the sedimentation stability of the emulsion.

In order to investigate the emulsion coalesce stability, the fraction of water layer at the bottom of the emulsion was measured. It is noticeable that a good coalescence stability was obtained in both cases (0.5 wt % and 5 wt %). No resolved aqueous phase was observed in 60 minutes. Furthermore, no water was separated from emulsion in 30 days, indicating lignin-B was a promising stabilizer to prepare W/O emulsion. The DLS data were in line with the good coalescence stability, since the average diameter increased a little to 630.2 nm and 435.6 nm for 0.5 wt % and 5 wt %, respectively. A broader distribution was obtained when measuring the droplets size in 60 minutes after emulsification in the case 0.5 wt % modified lignin (Figure 4.7(b)I). A proposed explanation is due to the incomplete coverage of lignin on the surface of water droplets at this low content and the lignin molecular re-assembly during the static time.

Span-80 is a widely used emulsifier to prepare W/O emulsion and it was used as comparison in this study. The result indicated that the emulsions prepared by 0.5 wt % span-80 easily collapsed in 4 minutes after emulsification and clear three layers were observed: oil on the top, water on the bottom and a very thin milky emulsion layer in the middle. Only when 5 wt % span-80 was applied, the corresponding emulsion was stable with φ_{oil} equal to 0.015 after 60 minutes without aqueous phase in the bottom. Compared with Span-80, it was noted from the sedimentation measurement that the emulsion droplets were more likely to sediment when lignin-B was used with concentration of 5 wt %. This is mainly due to the higher degree of molecular branching occurring with high-molecular-weight emulsifier since inter-molecular bridges are easy to form with long

molecules.[204, 208, 209] Nevertheless, at low concentration (0.5 wt %), span-80 alone failed to stabilize emulsion while lignin-B could form stable emulsion. This indicates that, with low concentration, the lignin-based surfactant shows better performance.

4.4 Conclusion

Grafting of butyric anhydride, MPS and BIBB onto kraft lignin can change lignin's amphiphilicity. FTIR, ^{1}H NMR, GPC and TGA analysis confirmed the grafting reactions and ^{31}P NMR analysis was applied to determine the extent of reaction. While lignin modified with MPS and BIBB could dissolve partially in styrene due to the significant amount of hydroxyl groups remained in lignin molecules. In contrast, a conversion of over 95% of hydroxyl groups was achieved when butyric anhydride was used and the resultant product (lignin-B) was found to be completely soluble in oil up to 15 wt %.

The lignin-B was demonstrated to be good surfactant with strong interfacial activity between oil-water interfaces. Stable water-in-oil emulsion was prepared with lignin-B as emulsifier. The significant reduction in the interfacial tension at W/O interface through both steric and electrokinetic stabilization contribute to the W/O emulsion stability up to 30 days. This suggests lignin-B has promising potential to be applied as a bio-based surfactants and emulsifier.

CHAPTER V

LIGNIN-POLYMER COMPOSITES FOAMS THROUGH HIGH INTERNAL PHASE EMULSION POLYMERIZATION

5.1 Introduction

With the increasing attention toward "green" biocomposites material, the incorporation of renewable materials as fillers and substitutions has attracted strong interest to promote sustainability for the existing plastic industry and to save the limited reserves of fossil fuel resources.[210] Lignin, as the second most abundant natural components accounting for 20−30% of wood by weight[211], is often used by combustion for heating directly or even disposed as industrial waste in the previous decades.[212] Therefore, the utilization of lignin as value-added products in different areas of industries has recently attracted significant attentions, including the preparation of lignin-polymer composites.[126, 213-215]

Raw kraft lignin is immiscible with most monomers and polymers. Its molecules tend to aggregate as a result of strong intermolecular hydrogen bonds caused by the presence ofa large amount of hydroxyl groups.This often hinders the utilization of lignin for some industrial applications.[128, 216]Nevertheless, these functional groups could beeasily modified using various method to improve its compatibility with monomers and polymers, accordingly.[25]

Polystyrene and its derivatives, as one of the commodity polyolefins, have been widely used in the global market as the matrix resin to fabricate molded sheets or foams. Its low production cost and some desirable attributes make it economically un-feasible to fully replace this synthetic polymers with emerging biodegradable polymers, such as

poly(lactic acid). Alternatively, the utilization of low-cost, renewable materials has been promoted to alleviate the sustainability issue by helping to conserve the petrochemicals usage. Efforts on understanding the utility of lignin within a polymer matrix allow the practical realization of industrial lignin as sustainable filler for the plastic manufacturers. Aside from inducing partial biodegradability, the incorporation of lignin in composite fabrication could facilitate reinforcement impact. The increase in the modulus of lignin-based thermoplastics, in particularpoly(lactic acid) and polyurethane, has been previously reported.[125, 128, 217] In addition, the high aromatic structure of lignin is capable of yielding high char upon heating. The presence of char residue could reduce the combustion rate of the polymeric materials as it suppresses the diffusion of heat and oxygen.[218-220] As a result, the addition of lignin in the polymer matrix could also be beneficial acting as a flame retardant additive.

As one of the most common colloidal systems, foams are widely used in different applications, such as pharmaceutical formulations, food packaging, water purification and water-oil separation. In rigid foam industry, lignin has also been successfully used as a feedstock material to generate lignin-based polyurethane foams. Literature has reported an excellent dimensional stability of the close-cell structures.[221, 222] Emulsion-derived foam is another type of porous polymeric materials that offer open-cell structures. The high internal phase emulsions (HIPE) can trap more oils and thus form more porous structure after curing.[223] The formation of such structures is originated by solidifying the continuous phase of the emulsion.[224] The characteristics of low density with a very high porosity up to 98% can be easily achieved by polymerized high internal phase emulsions (HIPE) polymerization with more than 74 vol % dispersed phase.[225, 226] Potential use of

these materials includes filter media[227], ion exchange modules[228], and catalysis support[229]. Most common HIPEs are based on styrene/DVB formulation and utilize 5-50 vol.% of a suitable non-ionic surfactant.[225] Alternative synthesis strategies have also been extensively investigated to yield different foam properties. However, to the best of authors' knowledge, the fabrication of lignin-based emulsion-derived composite foams has not been fully disclosed.

Herein, we described an effective route to prepare lignin-based polystyrene composites porous structures with enhanced mechanical properties. The work revolved around functionalization of lignin and investigated the effects of modified lignin on the mechanical, thermal, and dimensional stability properties of the composites. The mechanism of modified lignin as renewable fillers in the composite system is also discussed in this paper.

5.2 Experiments and method

5.2.1 Materials

Kraft lignin (lignin, alkali) was obtained from Sigma-Aldrich and used as received. Butyric anhydride (98%), 1-Methylimidazole (1-MIM) and Dimethyl sulfoxide-d_6 (DMSO-d_6, 99.5%, a solvent of lignin for NMR experiments) were purchased from Alfa Aesar. Anhydrous ethyl ether was purchased from J.T. Baker. Cyclohexane was provided by BDH. Hexane was obtained from EMD Millipore. Styrene (inhibited by 4-tert-butylcatechol, 99%) was purchased from Alfa Aesar and used after purification through an alumina column. 1,4-Dioxane (stabilized with BHT, >99.0%) was supplied by TCI America. Divinylbenzene (DVB, 55%, a crosslinking agent), 2,2'-Azobis(2-

methylpropionitrile) (AIBN, 98%), Sorbitanmonooleate (Span® 80) and anhydrous Calcium chloride ($CaCl_2$) were purchased from Sigma-Aldrich.

5.2.2 Lignin modification

Lignin modification was carried out with a reaction between lignin and butyric anhydride, which is similar as we described in Chapter IV.

5.2.3 Hansen Solubility Parameter Modeling

Hansen solubility parameter (HSP), which is widely applied to describe the thermodynamic behavior of polymers, was used to investigate the compatibility between lignin and styrene or polystyrene. In this theory, the solubility parameter (δ) of one component was separated into three different contributions[230-232]: the nonpolar dispersion interactions (δ_D), permanent dipole-permanent dipole interactions (δ_P) and the hydrogen bonding interactions (δ_H) and can be expressed as:

$$\delta^2 = (\delta_D)^2 + (\delta_P)^2 + (\delta_H)^2 \qquad (1)$$

Solubility properties of one component can be visualized through HSP solubility sphere in a three-dimensional coordinate system with axes δ_D, δ_P and δ_H. The center of the solubility sphere of a solute (lignin herein) is its HSP factors ($\delta_{D,1}$, $\delta_{P,1}$ and $\delta_{H,1}$) and the radius (R_o) is the maximum difference in affinity with solvent. The coordinates of goodsolvents are within the sphere while bad ones are outside of it. To quantitatively determine the miscibility of two components, the relative energy difference (RED) will be calculated as:

$$RED = \frac{R_a}{R_o} \qquad (2)$$

where, R_o is the radius of solute HSP solubility sphere; R_a is the modified difference between solute and solvent, which can be calculated as:

$$(R_a)^2 = 4(\delta_{D,1} - \delta_{D,2})^2 + (\delta_{P,1} - \delta_{P,2})^2 + (\delta_{H,1} - \delta_{H,2})^2 \qquad (3)$$

The subscript 1 is for the solute (lignin) and 2isfor the solvent. The value of RED is less than 1 for good solvents and greater than 1 for badsolvents.

5.2.4 Preparation of PS-lignin composites

5.2.4.1 Preparation of PS-lignin film through bulk polymerization

9.371 grams of styrene was mixed with 7.809 grams of divinylbenzene (DVB, 54%) to form the monomer mixture. A certain amount of modified lignin was added to monomer mixture in the ratio of 0 (L0'), 2 wt % (L2'), 5 wt % (L5'), 8 wt % (L8'), 10 wt % (L10'), and 15 wt % (L15') under stirring to form homogeneous solution. 5 grams of the monomer solution was addedto an aluminum dish containing 0.05 grams of AIBN. Then the aluminum dish was sealed with aluminum foil and kept at 70 ^{o}C for 48 hrs.

5.2.4.2 Preparation of the porous foams through emulsion polymerization

Oil phase: 9.371 grams of styrene was mixed with 7.809 grams of divinylbenzene (DVB) to form the monomer mixture. A certain amount of modified lignin was added to monomer mixture in the ratio of 0 (L0), 2 wt % (L2), 5 wt % (L5), 8 wt % (L8), 10 wt % (L10), and 15 wt % (L15) under stirring to form homogeneous oil solution. **Aqueous phase:** 1.8 grams of $CaCl_2$were dissolved in water (162 ml). Then the aqueous phase was purged with N_2 for 30 min. In a specific polymerization run, 0.02 grams of AIBN and 0.4 grams of Span-80 were added into 2 grams of oil solution in a 100 mL vial. The porous

lignin-PS composites were prepared by oil-in-water (O/W) or inverse high-internal phase emulsion polymerization (*i*-HIPE) approach. Specifically, the aqueous solution (18 mL) was added dropwise for 30 min under mechanical stirring (400 rpm), during which process, the homogeneous emulsion was obtained. After complete addition of the aqueous phase, the as-prepared emulsion was transferred into a 15 mL plastic tube and a vortex mixer was used to make the mixture more uniform. The emulsion was polymerized at 70 ^{o}C for 24 hours. After polymerization, the polyHIPE composite samples were washed with DI water and by Soxhlet extraction with methanol for 24 hours, respectively. Finally, the resulting porous polyHIPE composites were dried at 60 ^{o}C for overnight.

5.2.5 Characterization and mechanical properties tests

The structures of lignin and polyHIPE were studied by Fourier Transform Infrared Spectroscopy (FTIR), Thermogravimetric analysis (TGA) and ^{1}H NMR. The methods and equipments are described in Chapter IV.

X-ray photoelectron spectroscopy (XPS) was used to analyze the binding energy of C and O elements in lignin, which was carried out through a Thermo K-Alpha instrument equipped with a monochromatic AlKα radiation at 1486.6 eV X-ray source. A low energy flood gun was applied to perform the charge neutralization. Cu substrates were used to support the samples. The spectra were calibrated with a binding energy of 284.8 eV for C 1s.

The morphology of the polyHIPE composites was imaged by LEO 1530 thermally assisted field emission scanning electron microscope (SEM). All samples were gold-sputtered for 60 s before SEM.

The liquid absorption capacity of porous composites was examined by solvent immersion. Specifically, initial mass of dry composite (m_0) was recorded and immersed in 50 mL of solvent for 1 min. The solvent-saturatedporous composite was removed and excess liquid on the surface was blotted using blotting paper. Mass of wet composite (m_w) was measured. The liquid absorption capacities (C_{abs}) were calculated as

$$C_{abs}(w/w) = \frac{m_w - m_0}{m_0}$$

The thermomechanical properties were tested on a DMA Q800 (TA Instruments) using single cantilever mode. Rectangular specimens measuring about 30 mm × 6mm × 1.5 mm were used. All runs were performed in a ‘‘multi-frequency-strain’’ mode at 1 Hz, amplitude of 10 um, and a scan rate of 3 ^{o}C/min from 20 °C to 200 °C under N_2atmosphere.

Uniaxial tensile tests were performed to evaluate the mechanical properties the lignin-polystyrene composites. The rectangular samples with a dimension of about 30 mm × 6 mm × 1.5 mm were tested on an MTS (Model Insight 10, Thermcraft, U.S.) Universal Materials Testing Machine with a load capacity of 10 kN at room-temperature. The tensile rate was 1 mm/min for all cases.

Compression tests of polyHIPE composites were performed using Instron 5566 equipped with a 10kN load cell. Cylindrical samples were compressed with a speed of 1 mm/min to their deformation form.

5.3 Results and discussion

5.3.1 Lignin modification and characterization

Commercial kraft lignin is immiscible with most monomers and polymers because of the aggregation caused by the intermolecular hydrogen bonding, π–π stacking of benzene rings as well as Van der Waals interactions.[128, 216] Lignin is supposed to react with anhydride easily since it contains a large amount of hydroxyl groups, which offers an effective solution to improving lignin solubility in monomers and polymers. The modification reaction used herein was carried out between kraft lignin and butyric anhydride, where esterification occurred at 70 ^{o}C in N_2 atmosphere with 1-MIM as a catalyst.

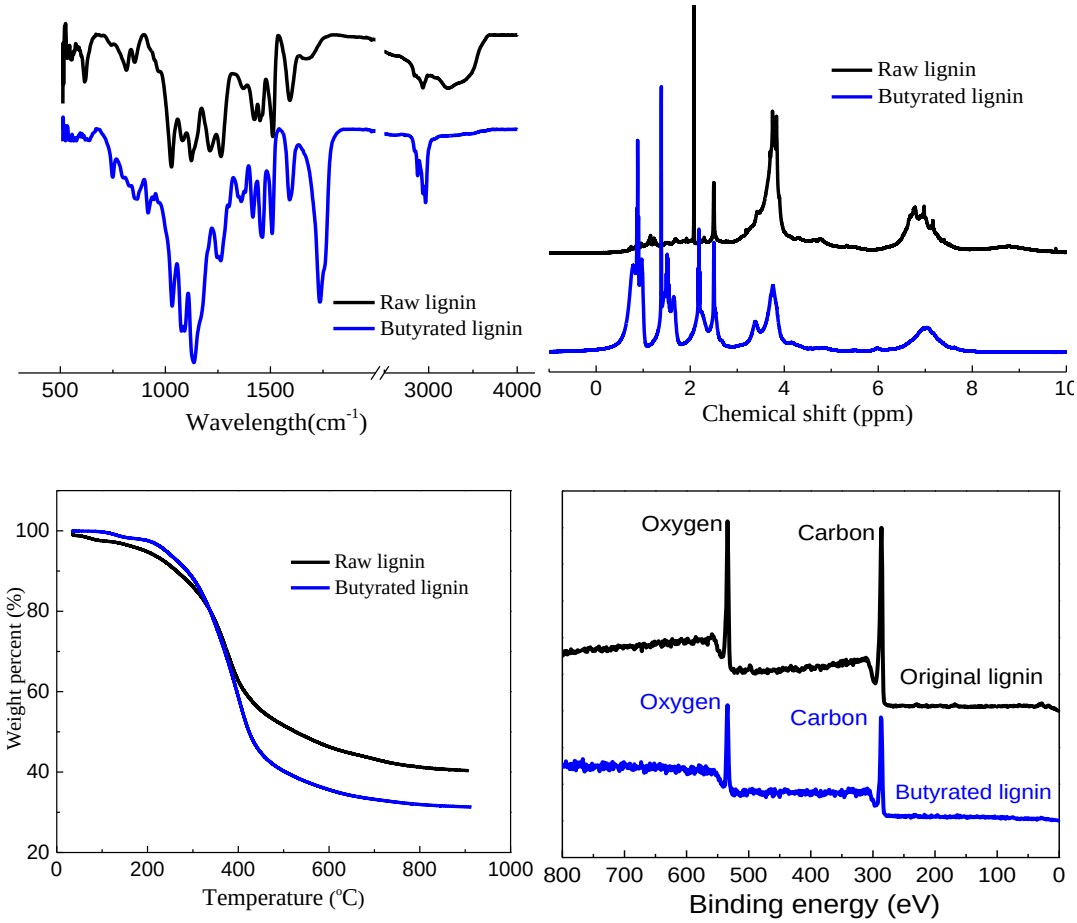

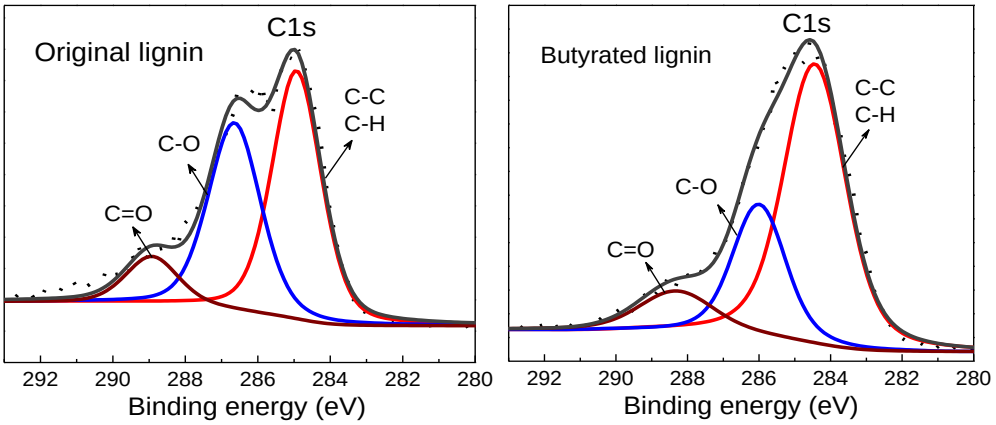

Figure 5.1 Characterizations for both original lignin and modified lignin: (a) FTIR; (b) ^{1}H NMR; (c) TGA; (d) XPS survey; (e) C 1s scans; (f) C 1s scans.

FTIR was used to investigate the structure of lignins before and after modification. As shown in Figure 5.1(A), the characterized peaks on raw kraft lignin is a broad band at 3450 cm^{-1} for O-H and a peak at 2935 cm^{-1} for the vibration of methoxyl groups.[50] Besides, peaks at 1615 and 1514 cm^{-1} were assigned to the C-C stretching of aromatic rings in lignin.[51] In the spectrum of original lignin, the peak representing the stretching of unconjugated carbonyls (C=O)[194, 233] is at 1710 cm^{-1} while this peak shifted to 1740 cm^{-1} in the spectrum of modified lignin. This was caused by the formation of ester groups (O-C=O) during the modification process. Furthermore, compared with raw lignin, the widebrand in the range of 3000-3700 cm^{-1} disappeared in the modified lignin, which suggested the conversion of most hydroxyl groups. The difference between FTIR spectra provides the evidence of successful chemical modification on lignin. Furthermore, the structure of lignin was studied by ^{1}H NMR spectra, as shown in Figure 5.1(B). In the spectrum of raw lignin, peaks at 8.0-9.4 ppm, 6.3-7.7 ppm, 3.81 ppm and 0-2.0 ppmare assigned to protons in hydroxyl groups, aromatic rings, methoxyl groups and

hydrocarbon chains (-CH_3, -CH_2), respectively.[60, 61, 234, 235] In the spectrum of modified lignin, the peak at ~9 ppm disappeared, indicating the removal of –OH groups, while the relative strength of peaks in the range of 0-2.0 ppm increases significantly, attributed to the increasing content of hydrocarbons (-CH_2-, -CH_3)[51]. Figure 1(C) shows the TGA curves of raw lignin and modified lignin, and both of them started the decomposition at 300 ^oC and ended at 450 ^oC. The ash content of butyrated lignin was less than that of raw lignin, which was caused by the grafting of butyl components. The survey of XPS spectrum of lignin (Figure 5.1 (c)) exhibits the presence of C 1s and O 1s at around 286 and 534 eV, respectively. To further investigate the chemical valences of carbon in lignin, the XPS C 1s curve is deconvoluted into three peaks of C-C (at 284.95 eV), C-O (at 286.68 eV) and C=O (at 288.88 eV)[236-239] and the percentage of each carbon type is 50%, 40% and 10% for raw lignin. For the butyrated lignin, the percentage changes to 64%, 26%, and 11%, respectively. In the process of lignin modification, the amount of C-O kept constant and therefore, the relatively increasing of C-C and C=O intensities demonstrates the successful grafting. The XPS spectra of O 1s further confirm the expected structure of modified lignin, as shown in Figure 5.9 (appendix).

5.3.2 Hansen Solubility Parameter (HSP) Modeling

The chemical modification process is expected to improve the lignin-organic compatibility by converting hydrophilic hydroxyl groups into lipophilic ester groups. In contrast to the commercial kraft lignin, the modified lignin is demonstrated to be soluble in styrene monomer experimentally, as shown in Figure 5.10 (appendix). In order to further confirm the solubility and predict the compatibility of lignin and polystyrene,

HSP theory was used to investigate the thermodynamic behavior with lignin as solute and styrene/polystyrene as a solvent. The HSP factors of different compounds (kraft lignin, modified lignin, styrene, and polystyrene) were from literature[51, 230] and listed in Table 5.1 and 13.7 $MPa^{-0.5}$is generally used as R_o for different kinds of lignin[230, 236, 240, 241].

Table 5.1 Hassan solubility parameter factors of different compounds

	δ_D ($MPa^{-0.5}$)	δ_P ($MPa^{-0.5}$)	δ_H ($MPa^{-0.5}$)	δ_t($MPa^{-0.5}$)
Kraft lignin	16.7	13.7	11.7	24.57
Modified lignin	16.4	11.1	9.3	21.88
Polystyrene	21.3	5.8	4.3	22.49
Styrene	18.6	1	4.1	19.07

Table 5.2 R_a and calculated RED numbers

	Polystyrene		Styrene	
	R_a	RED	R_a	RED
Kraft lignin	14.21	1.04	15.28	1.12
Modified lignin	12.21	0.89	12.18	0.89

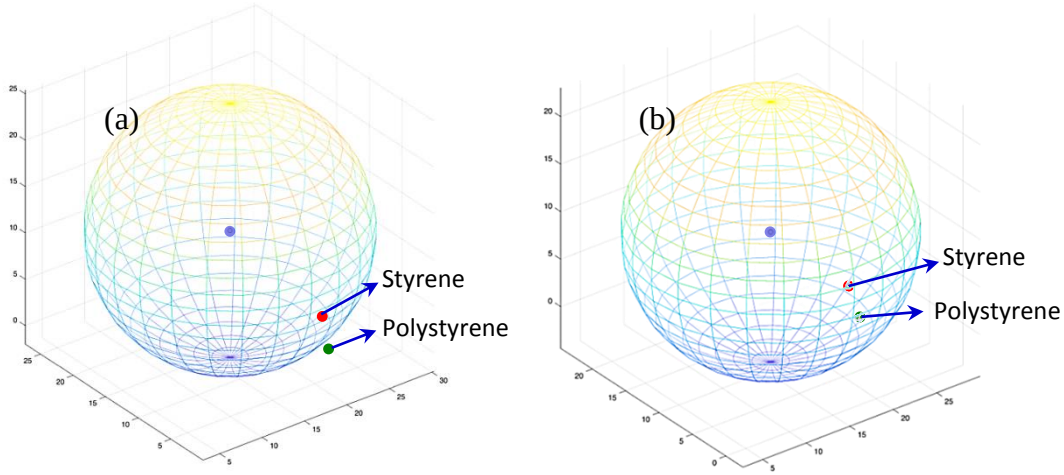

Figure 5.2 Solubility spheres for unmodified lignin (a) and modified lignin (b)

The RED and R_a values were calculated through Equation (2) and Equation (3), respectively and listed in Table 5.2. In the case of kraft lignin, RED=1.04 when polystyrene is used as solvent and RED=1.12 when styrene monomer is used as a solvent, suggesting that both polystyrene and styrene monomer are not goodsolvents. However, in the case of modified lignin, RED=0.89 when either styrene or polystyrene is used as a solvent, which indicates that the modified lignin can dissolve completely in both polystyrene and styrene, theoretically according to the HSP model. The visualized plots of solubility spheres in a 3D diagram for kraft lignin and modified lignin are presented in Figure 5.2, showing that both the coordinates of styrene and polystyrene are out of the kraft lignin solubility sphere while they are within the affinity sphere for modified lignin. The solubility difference is caused by a combination of a reduction in hydrogen bonding interactions (δ_H) and a reduction in polar forces (δ_P). Therefore, according to the results of HSP theory, we can expect that lignin and polystyrene are mixed homogeneously at the molecular level.

5.3.3 Preparation of lignin-polymer HIPEs foam

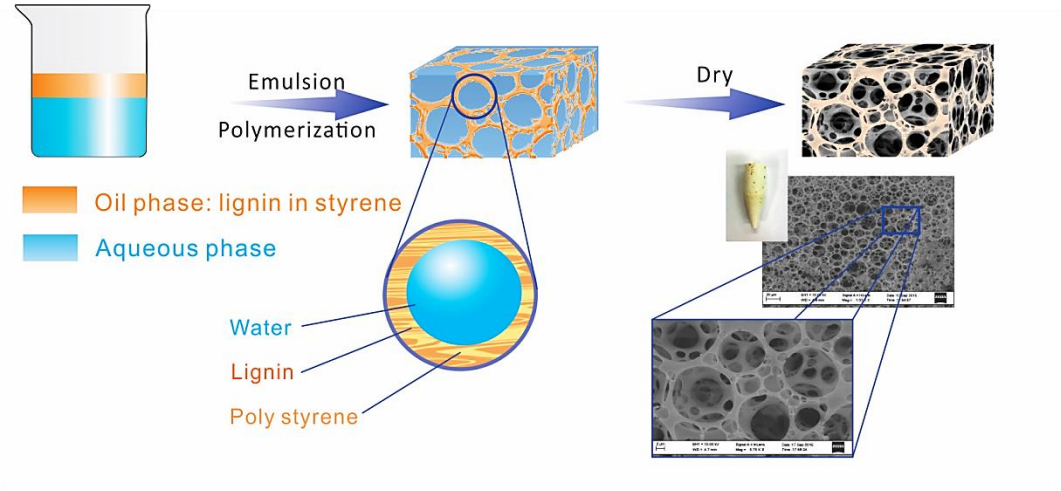

Figure 5.3 Schematic of the preparation process of lignin/polymer foam through HIPEs

The porous polyHIPE composites were prepared through reverse emulsion polymerization approach, as shown in Figure 5.3. Typically, a certain amount of as-modified lignin sample was dissolved in styrene containing the cross-linker and stabilizer. The homogeneous emulsion was prepared by adding aqueous solution dropwise into monomer mixture under mechanical stirring (300 rpm). Then the emulsion was transferred into an oven at 70 ^{o}C and kept for 24 h in order to let the monomer be polymerized completely. The final products were obtained after washing and drying.

The chemical structure of the foams is investigated by FTIR, as shown in Figure 5.4 (a). In the spectrum of Sample-L0, bands at 1600, 1489, 1450 cm^{-1} are assigned to the stretching of the aromatic C=C; bands at 756 and 700 cm^{-1} are assigned to the substituted phenyl rings[244]; bands at 3021 and 2918 cm^{-1} are assigned to the C-H stretching in

aromatic and aliphatic structure; bands at 1024 and 900 cm^{-1} are assigned to the C-H in-plane and out-of-plane bending.[245] Compared with the pure PS sample, the spectra of lignin-PS samples have two special peaks – the peak at 1173 cm^{-1} is for the butyrated group[51]; another peak at 1740 cm^{-1} is for the ester structure (O-C=O). These two peaks can be used to characterize lignin in the composites, and the intensities of these peaks increase with the increasing of lignin content as expected. Figure 5.4 (b) illustrates the TGA curves of both pure PS and lignin-PS composites, and they show similar decomposition profiles where the dominant decomposition range is in 300 – 400 ^{o}C. However, the char yield of the lignin-PS composites increases with the increasing of lignin content, which is resulted from the high content of aromatic components in lignin.

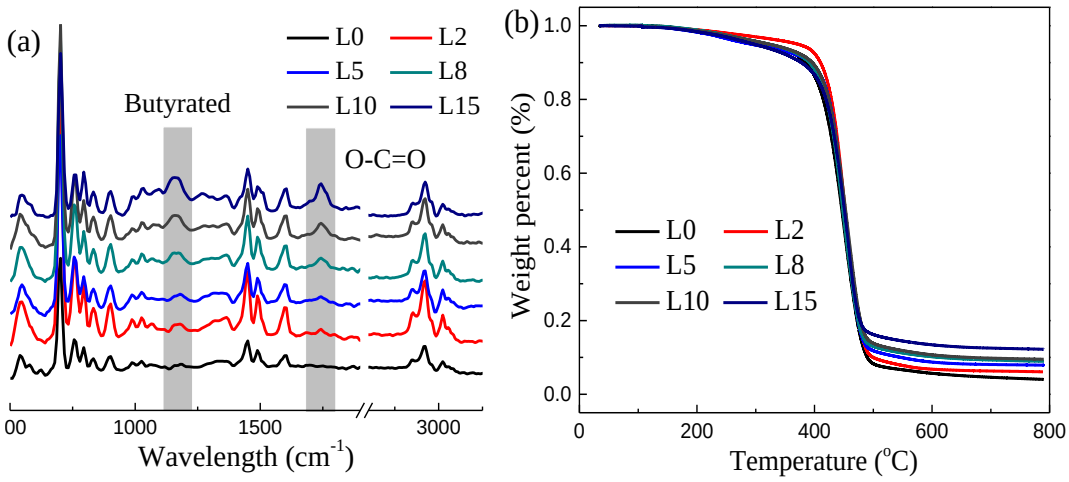

Figure 5.4 FTIR (a) and TGA (b) for lignin/polymer foams with different lignin contents

The effect of lignin concentration on the morphology and properties of polyHIPE composites was evaluated, as shown in Figure 5.5. The SEM image of the polyHIPE composite with lignin content up to 10 wt% shows open porous bimodal morphology, a

typical polyHIPE porous structure. The SEM image analysis demonstrated pore sizes in the range of 15-30 µm and 2-6 µm, while the pore wall thickness of the porous structure varied between 1-2 µm. For 15 wt% lignin composition, the unstable morphology of the polyHIPE is observed, which indicated the presence of excessive lignin significantly increased the number of coalesced pore. The changes in surface area, however, have little effect on the bulk liquid absorption capacity. As the porosity and density of the polyHIPE composite remain relatively constant at 90% and 72 mg/mL, respectively, the liquid absorption capacities for all samples are relatively similar, as indicated in Figure 5.6 (a). For hexane with the liquid density of 0.65 g/mL, the average absorption capacity of the porous samples was 12.5 mL/g. In addition, a higher average absorption capacity of 13.5 mL/g was obtained for dioxane with the liquid density of 1.03 g/mL. In contrast to the liquid absorption capacity, the change in pore formation affected the mechanical properties of the polyHIPE samples. PS-lignin polyHIPE composites up to 10 wt% lignin content lead to the enhanced compression modulus. Up to 62% improvement in the modulus was obtained, as depicted by polyHIPE composite with 5 wt% lignin content in Figure 5.6 (b). It is expected that the combination of lower pore size (as well as pore wall thickness) and the reinforcement of lignin in the composites would lead to the optimal improvement in the compression modulus.

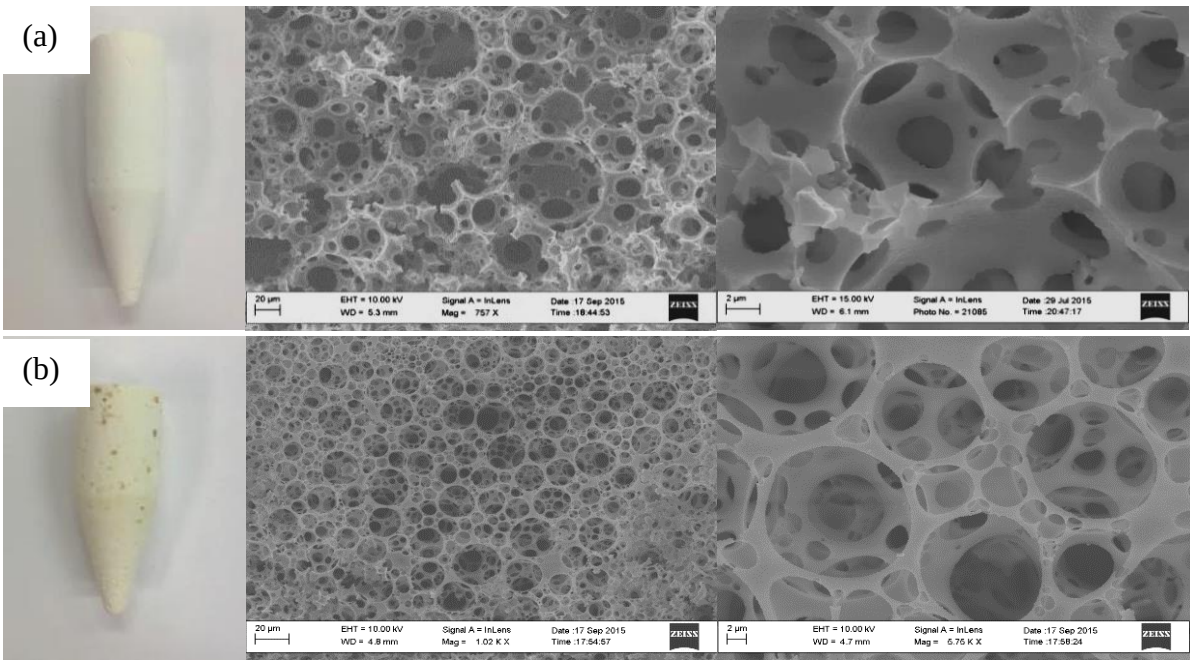

Figure5.5 Photos and SEM images for sample-L0 (a) and sample-L10 (b)

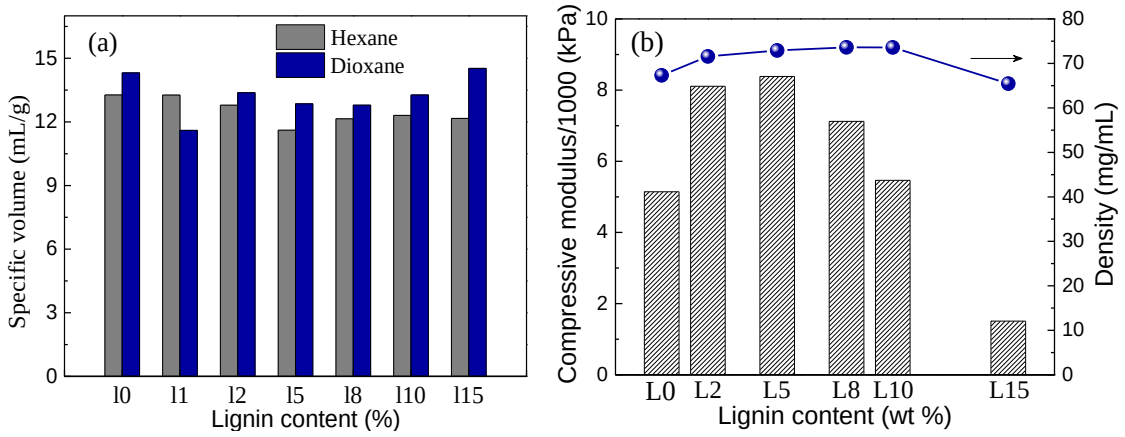

Figure5.6 (a) Absorption capabilities of lignin/polymer foams on hexane and dioxane; (b) compressive modulus and densities of lignin/polymer foams.

5.3.4 Preparation of lignin-PS composites through bulk polymerization

In order to investigate the mechanical properties of the bulk materials of the as-prepared foam, lignin-PS composites were prepared through direct bulk polymerization with

different lignin content, as shown in Figure 5.11 (appendix). The color of the composites became more yellow with the increasing of lignin content. The chemical structure and thermal properties of the as-prepared composites were confirmed by FTIR and TGA, as shown in Figure 5.12 (appendix), which are very similar as that of polyHIPE foams.

The thermomechanical performance of composites was tested with dynamic mechanical analysis (DMA). Three regions are observed in the storage modulus (E') curve as a function of temperature: glassy region where relatively stable E' is presented at a temperature below T_g, viscoelastic region where a noticeable decrease in E' is observed with increasing temperature, and rubbery region where a relatively slow decreasing E' is detected above T_g (Figure 5.13, appendix). Comparing to the neat PS, the composites shows more significant drop of E' in the viscoelastic region, which is associated with the addition of amorphous lignin content. The presence of lignin also caused a noticeable increase in the absolute value of glassy storage modulus. This increase can be related to the reinforcing effect of lignin.

The glass transition temperature (T_g) of the as-prepared composites is also determined by DMA. DMA results (Figure 5.7a) show that the T_g of sample-L0 is 116.8 ^oC and it decreases slightly as the lignin content increases. When the lignin content reaches 15 wt % (Sample-L15), the corresponding T_g is 101.5 ^oC. However, comparing with polystyrene composites, lignin has a higher T_g (~ 150 ^oC)[246] which is due to the restriction of molecular thermal mobility caused by the condensed rigid phenolic moieties and hydrogen bonding interactions.[128] The drop in T_g may be due to the enhanced free volume with lignin acting as polymeric plasticizers[128]. Moreover, in the polymer matrix, the addition of branched lignin component might also decrease the cross-linking

degree[247]. The latter reason plays the dominant role for the PS/lignin composites. Thus T_g show some decreases with lignin content for the composites. Despite of this, the incorporation of lignin into the polymer composites didn't affect T_g significantly.

Satoshi et al.[248] showed that lignin had Young's modulus of 4570 MPa, which is higher than that of polystyrene. It is noted that the polystyrene and composites here show relative lower modulus value partially due to incomplete reaction conversion. However, the result can still be useful for comparison analysis. From the experimental results of the tensile test, Young's modulus and tensile strength of the composites increased with the increasing of lignin content. For lignin content of 15 wt %, Young's modulus is 1391 MPa, which doubles that of Sample-L0 (Figure 5.7b). The experimental results of Young's modulus are compared with the calculated values by the rule of mixture, as shown in Table 3. For all the lignin-polymer composites, the experimental modulus values are positively derived from the calculated modulus by around 100 MPa, suggesting a synergistic effect on the composites toughness reinforcement by lignin which may be resulted from the inherent stiffness of lignin as well as the interfacial interaction between lignin and polymer molecules.[128] From the results and discussion above, it wasdemonstrated that the addition of lignin into the polymer matrix will enhance the Young's modulus and tensile strength without significantly sacrifice the thermomechanical properties.

Table 5.3 Experimental and calculated Young's modulus of lignin/polymer composites

	L0	L2	L5	L8	L10	L15
Experimental	697	911	976	1106	1193	1391

Calculated	697	773	887	1001	1077	1267
Δ	0	138	89	105	116	124

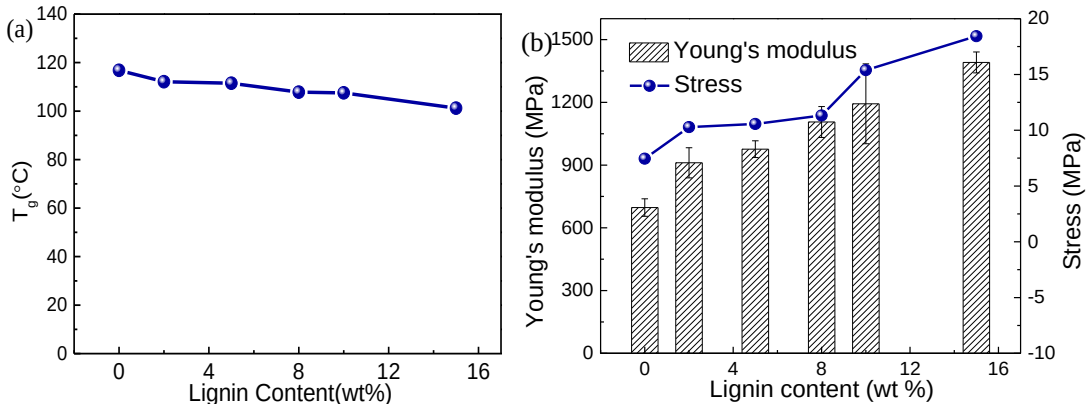

Figure 5.7 (a) Glass transition temperatures for lignin/polymer composites; (b) effects of lignin on Young's modulus and stress of lignin/polymer composites.

5.4 Conclusion

For the first time, the lignin-based emulsion-derived polymer composites foams were fabricated successfully. Lignin was demonstrated to be good substitution of traditional polymers in the form of both bulk composites and micro-sized porous foams. The miscibility of lignin with polymer was studied and predicted through Hansen solubility parameters model. The effects of lignin on the mechanical, thermal and structural properties of the composites were investigated. It was discovered that the addition of a certain amount of lignin would improve the modulus of the composites in both bulk and porous status. With this process described herein, lignin shows great potential to prepare "green" and sustainable composites in different applications.

5.5 Appendix

O 1s scan for original lignin and modified lignin

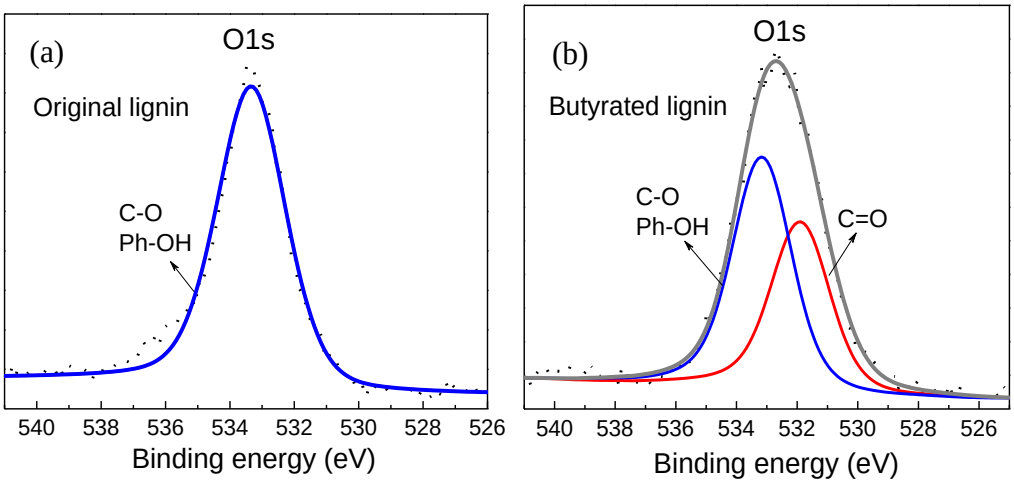

Figure 5.8 O 1s scan from XPS for original lignin and modified lignin

Photos of lignin in styrene

Original lignin cannot dissolve in styrene monomer. The modified lignin has a relatively large solubility in styrene monomer.

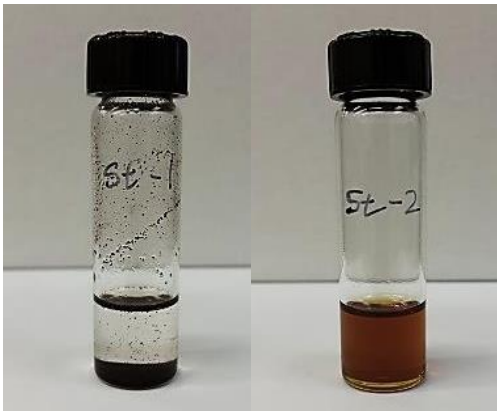

Figure 5.9 Photos of lignin in styrene: original lignin (left) and modified lignin (right)

SEM images for L15

L15

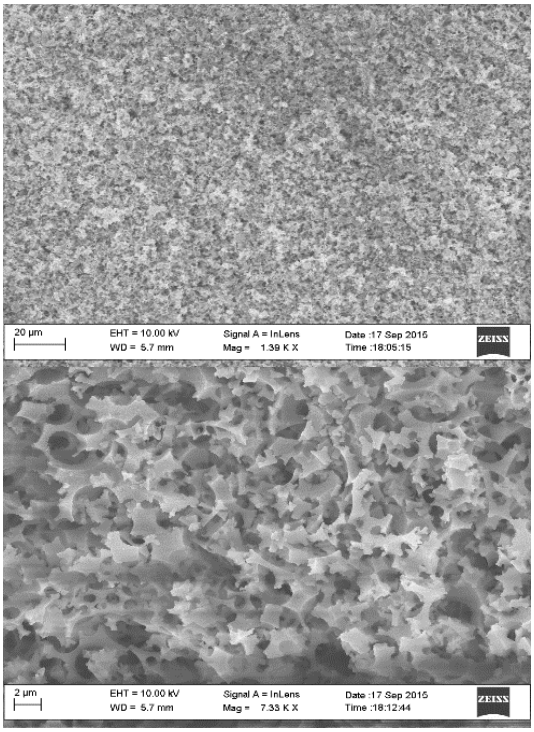

Figure 5.10 SEM images for sample L15

Lignin/polymer composites through bulk polymerization

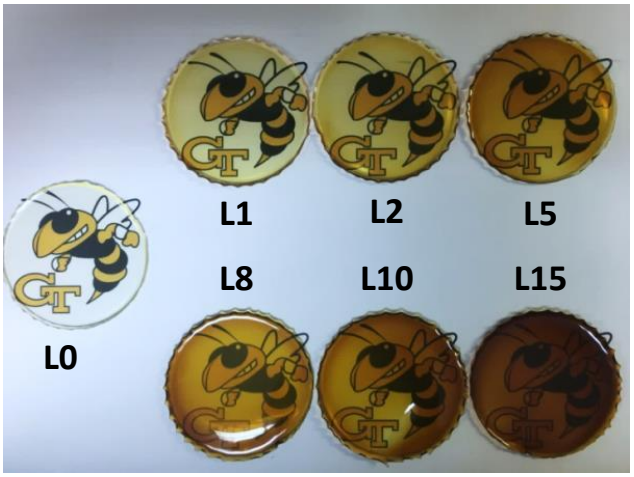

Figure 5.11 Photos of lignin/polymer composites through bulk polymerization with different lignin content, eg. L0-pure polymer without lignin; L1-lignin content is 1 wt %.

Characterizations of lignin/polymer composites prepared through bulk polymerization

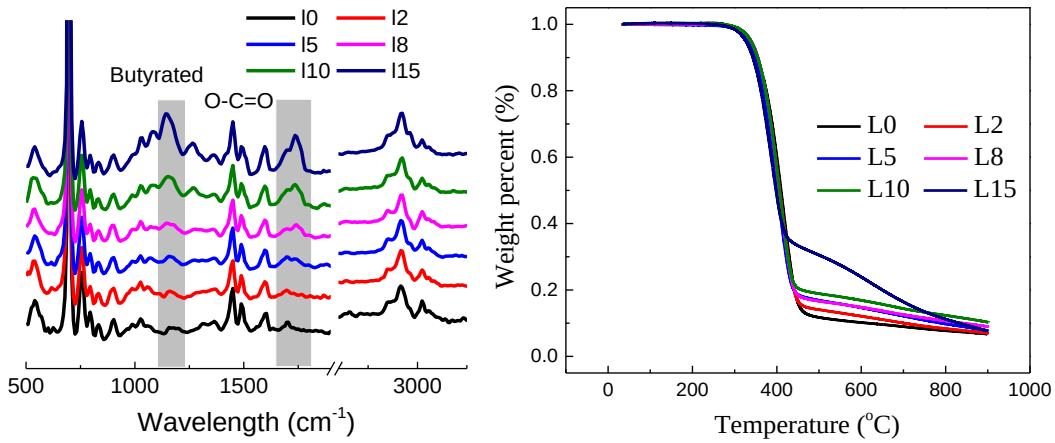

Figure 5.12 FTIR (left) and TGA (right) for lignin/polymer composites

Mechanical tests of lignin/polymer composites through bulk polymerization

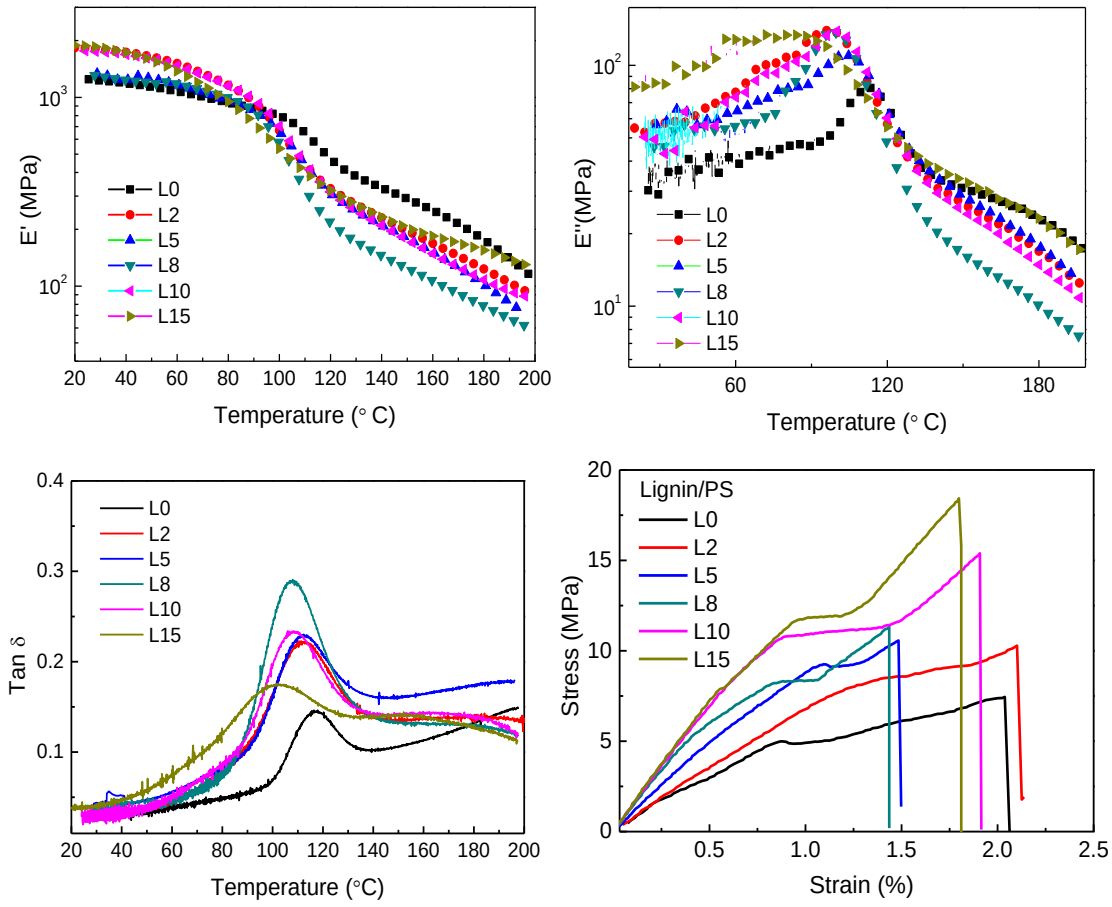

Figure 5.13 Mechanical tests results of lignin/polymer composites through bulk polymerization: (a) storage modulus by DMA; (b) loss modulus by DMA; (c) Tan δ by DMA; (d) Stress-strain curve by tensile test

Rule of mixture:

$Ec = E_{polymer} * V_{polymer} + E_{lignin} * V_{lignin}$

Where, Ec is the modulus of the composites, $E_{polymer}$ and E_{lignin} are the modulus of neat polymer and lignin , respectively. $V_{polymer}$ and V_{lignin} are the volume fractions of polymer and lignin in the composites samples.

CHAPTER VI

NOVEL LOW TEMPERATURE LIGNIN DEGRADATION TO AROMATIC COMPOUNDS WITH A REDOX COUPLE CATALYST

6.1 Introduction

Lignin, a heterogeneous alkyl-aromatic biopolymer has received great consideration as a sustainable source for bio-based chemicals which are presently obtained from fossil-based feedstock.[61, 249, 250] It is found in cell walls of plants with a weight content of 15 to 40%. In plant cell walls lignin plays role for defense, structure, and water transport. The high aromatic nature makes lignin as one of the few natural large-scale sources for production of aromatic compounds and its extraction from lignin is recognized as crucial aspect to the economic sustainability of integrated biorefineries. Among the lignocellulose components cellulose and hemicellulose are converted to fuels and chemicals whereas, lignin treated as waste product and used to produce heat and power in paper and pulp industries. Lignin into value added products has yet to get its goal to successful valorization of lignin.

Several methods have been reported for lignin depolymerization, such as hydrolysis, reduction and oxidation. In hydrolysis alkali hydroxides and carbonates in water are used as a catalyst to break C-O-C bonds to give phenols. Depolymerization occurs in hydrothermal conditions at high temperature (453-673K) and forms different products or intermediates and chars as by-product which makes the process more complicated for further processing.[251-254] In contrast to hydrolysis, reductive and oxidative depolymerization are more attractive since it can depolymerize lignin at

relatively mild reaction conditions.[255] In presence of H_2 (hydrogenation) or hydrogen sources (hydrogenolysis) lignin converts to aromatics by selective cleavage of C-O-C bonds. Homogeneous mild hydrogenolysis to break C-O bonds using Ni, Fe, and Ru complex as been reported in literature. Heterogeneous reductive processes have also been investigated for lignin depolymerization. *Qi et al.* recently reported catalytic hydrogenolysis of kraft lignin in alkali water by Ni on ZSM-5 zeolite with 91% yield to nine monomers.[256] Addition of noble metals such as Au and Ru to Ni enhances the ability to break C–O bonds in lignin.[257] Other metal catalysts like Cu,[258] Mo,[259, 260] Pt,[261] and Pd[262] also reported to have efficiency in catalytic hydrogenolysis of lignin into phenols. Despite the promising effects of catalytic systems for reductive depolymerization of lignin, the yields of monomeric phenols are still low. Moreover, the use of hydrogen or hydrogen sources is expensive and the process is complicated.

Selective oxidative depolymerization is also a good choice to achieve the goal of aromatics from lignin at mild reaction conditions. In general, the goal of oxidative lignin depolymerization is to produce polyfunctional aromatic compounds using metal oxides, molecular oxygen, or hydrogen peroxide as the oxidant. Rare earth metal oxides like CeO_2 and $LaFe_{1-x}Cu_xO_3$ (x = 0, 0.1 and 0.2) oxidative catalysts were used to convert alkaline lignin to vanillin and syringaldehyde.[156, 263] Synthesis of vanillin from lignin by oxidation is one of the dominated factors to venture oxidative depolymerization strategies[264]. Different salts of Fe, V, Co, Cu and Au, as a homogeneous oxidative catalyst were used by *Cui et al.* for oxidation of lignin and model compounds to aromatics.[265] Homogeneous and metal free oxidation methods using TEMPO/HNO_3based

lignin depolymerization to low molecular mass aromatics from aspen lignin with C-C bond cleavage was reported by Rahimi *et al*.[58]

Fe^{3+} has been reported to be effective to interrupt the ether and ester bonds in lignin and carbohydrate and to promote the biomass pretreatment process in the biorefinery area.[266-268] Therefore, we propose that redox couple of $Fe^{3+}/Fe^{2+}$is promising for the selective lignin degradation. The challenge is the re-oxidation of $Fe^{3+}$from $Fe^{2+}$with oxygen due to the low oxygen solubility in water and the poor overall reaction kinetics. To overcome this challenge, $NaNO_3$ is added as the oxygen vehicle, where NO^{3+} ions oxidizes the Fe^{2+} into Fe^{3+} in the aqueous phase and the as-reduced product NO is easily re-oxidized in the gas phase by oxygen. Thus the overall degradation rate will be promoted. To the best of our knowledge, this concept has not been used till now for oxidative lignin degradation to produce low molecular weight phenolic compounds.

6.2 Materials and Methods

6.2.1 Materials

Kraft lignin for the study was purchased from Sigma Aldrich. Ferric chloride and sodium nitrate for pretreatment were purchased form Sigma Aldrich, Chemicals used for all the studies were of analytical reagent grade.

6.2.2 Depolymerization of kraft lignin

The depolymerization experiments were carried out by using the redox couple in a laboratory scale Parr reactor with a total volume of 50 ml. The lignin mixed with 20 ml deionized water with 1-4 wt% of $FeCl_3/NaNO_3$ at 700-150 ^oC in 10 bar of O_2atmospheres

with constant stirring (200 rpm) for 30-120 min. The reaction mixtures were initially heated with a heating rate of ~5^{o}C/min to set the temperature and kept stirring until completion of the reaction time. After the reaction, cooled the reactor in tap water immediately and filtered to separate the sold part. Washed solids were analyzed for different changes after depolymerization by SEM, FTIR, XPS, ^{13}C-NMR and TG analysis. The lignin fragments in liquid were collected for further analysis in HPLC. The monomers formed during depolymerization were identified by GC-MS-FID. The quantification of monomers was determined with HPLC. In addition, GPC analysis was performed to confirm lignin depolymerization by determining molecular weights.

The residual solid after the depolymerization consists of the catalyst, unconverted/repolymerized lignin and the char (solid residue). The amount of individual products (wt%) were calculated on the basis of the calculation of peak areas of HPLC chromatogram comparing with the authentic standards using calibration curves. The lignin conversion, product yield, residue and mass balances were calculated on the basis of initial kraft lignin taken as equations[50]:

$$Soluble\ fraction\ (\%) = \frac{w_0 - w_1}{w_0} \times 100$$

$$Productyield(\%) = \frac{productweight}{w_0} \times 100$$

$$Residue(\%) = \frac{w_1}{w_0} \times 100$$

where w_0 is the weight of lignin substrate before reaction;

w_1 is the weight of solid residue.

6.2.3 Characterization of lignin samples

Analytical HPLC was performed with a Zorbax 300SB-C18 column, 150 mm x 4.6 mm, 5 μm; flow = 0.4 mL/min; eluents H_2O (A) (0.1% TFA), MeCN (B) (0.1% TFA). A gradient method was used in which the percentage of B was allowed to increase from 0 % to 10 % in 1 minute, from 10 % to 20 % over 20 minutes, then 20 % to 100 % over next 14 minutes. The column was finally equilibrated back to 0 % B and washed thoroughly between sample injections. Peaks in the range of 15-27.4 min represent the mono-aromatic compounds and peaks in the ranges of 32.5-37.5 are the dimeric and trimeric aromatic compounds.[60]

FTIR and TGA were carried out as described in Chapter IV.

To analyze the chemical elements of the depolymerized lignin surfaces and their binding energies X-ray photoelectron spectroscopy (XPS) was used. The analysis was carried out in a Thermo K-Alpha instrument equipped with a monochromatic AlKα radiation at 1486.6 eV X-ray source. The charge neutralization was performed by using a low energy flood gun and Cu substrates were used to support the samples. All binding energies for the spectra were calibrated with a binding energy of 284.8 eV of C 1s.

6.3 Results and discussions

6.3.1 Mechanism of lignin degradation by $FeCl_3/NaNO_3/O_2$

$FeCl_3$ is a commonly used oxidative agent, which is demonstrated to be effective for biomass degradation.[269] However, when Fe^{3+} is reduced into Fe^{2+} in the aqueous media, it is very difficult to re-oxidize Fe^{2+} back to Fe^{3+} by oxygen gas due to the low oxygen solubility in water and slow reaction kinetics at the gas-liquid interface. To overcome this

problem, $NaNO_3$was added into the catalyst system. It is well known that NO^{3-} ion is in the aqueous solution which can oxidize Fe^{2+} into Fe^{3+} easily and quickly. More importantly, when reduced, NO^{3-} ions are converted into NO gas which can be miscible with oxygen in the gaseous phase and be-oxidized by oxygen more fast. So the addition of $NaNO_3$ is supposed to increase the re-oxidation rate of Fe^{2+} and then increase the overall lignin degradation rate.

As shown in Figure 6.1, briefly, in the lignin degradation process, Fe^{3+} oxidizes lignin at 100 ^{o}C in presence of O_2 while Fe^{3+} is reduced to Fe^{2+} as shown in equation 1. Electrons of lignin transferred to Fe^{3+}. The NO_3^- ion from $NaNO_3$ oxidizes Fe^{2+} in presence of proton to $Fe^{3+}$with the formation of NO gas as shown in equation 2. Further NO is oxidized to NO_2 and then to $NO_3^-$by O_2 as shown in equation 3 & 4. NO_3^- ions can dissolve back to the aqueous solution quickly to oxidize newly formed Fe^{2+}. Therefore, the overall reaction of the depolymerization process is the oxidation of kraft lignin by oxygen to produce aromatic monomers.

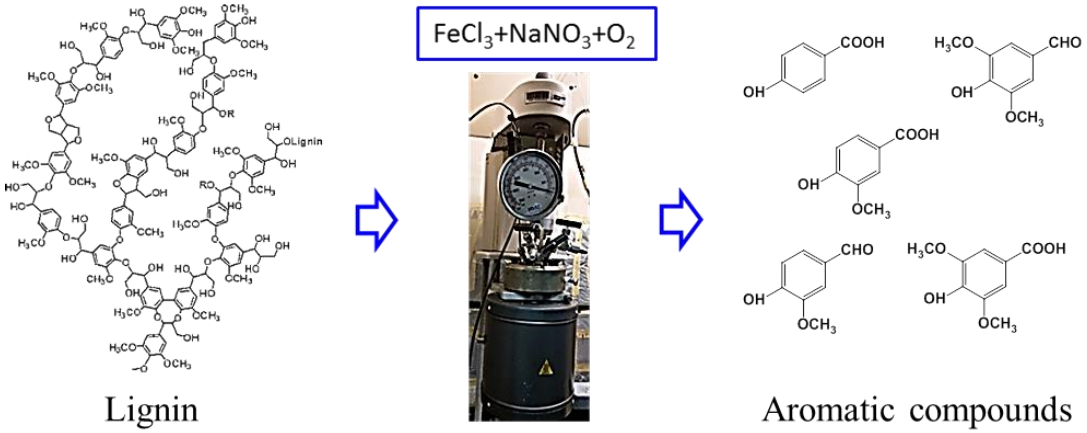

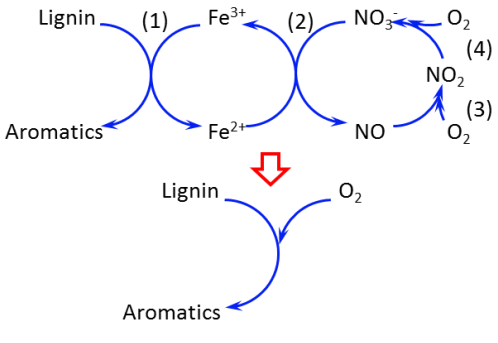

(1) $Lignin + Fe^{3+} \rightarrow Aromatics + Fe^{2+}$

(2) $3Fe^{2+} + NO_3^- + 4H^+ \rightarrow 3Fe^{3+} + NO + 2H_2O$

(3) $2NO + O_2 \rightarrow 2NO_2$

(4) $4NO_2 + O_2 + 2H_2O \rightarrow 4H^+ + 4NO_3^-$

$$Lignin + O_2 \rightarrow Aromatics$$

Figure 6.1 Schematic of lignin degradation into aromatics (above) and the mechanism of $FeCl_3/NaNO_3/O_2$catalyst

6.3.2 Monomer yield and analysis after lignin degradation

The catalytic depolymerization reactions were carried out using the $FeCl_3/NaNO_3/O_2$ system and the results are presented in Table 6.1. In G1, the effects of different catalytic system were compared and it clearly shows the advantage of the combination of $FeCl_3/NaNO_3/O_2$ on the reaction rate. The lignin soluble fraction was much higher when $FeCl_3/NaNO_3/O_2$ was used as catalyst compared with other catalytic system, including $FeCl_3/O_2$, $NaNO_3/O_2$and $FeCl_3/NaNO_3$. Besides, the soluble fraction increased as the reaction time extended. Specifically, the soluble fraction of lignin based on the amount of substrate weight left after filtration was from 25.3 % to 100% based on the varying experimental conditions. The soluble fraction for the system having water as solvent was maximum (89.5%) as compared to methanol as solvent (82.3%) at 100 ^oC for 4h. Complete dissolving of lignin was observed for the system for 4h at 160 ^oC.

The formation of individual compounds during lignin depolymerization can be seen from the HPLC chromatogram as shown in Figure 6.2. The standard chromatograms for six standards are shown in Figure 6.7 of appendix. The overall quantification for the

major compound obtained during the depolymerization is summarized in Table 6.2. In the case of methanol mediated depolymerization the major product obtained was vanillic acid along with syringic acid and vanillin upto 120 min of the reaction. For a longer time of reaction at 240 min only vanillic acid was observed with 5.2 wt% of initial amount of lignin. In water mediated depolymerization the conversion based on the lignin residue was more but the formation of monomers is less as compared to the methanol mediated depolymerization. This may be explained with the concept that methanol resists the re-condensation of monomers formed during the reaction. In case of water mediated reaction, two major peaks at 18 min and 20 min confirms the formation of vanillic acid and syringic acid at specified conditions. The broad peaks at around 35-40 min range are due to the dimeric or trimeric compounds during depolymerization. These peaks are very negligible when water was the solvent.

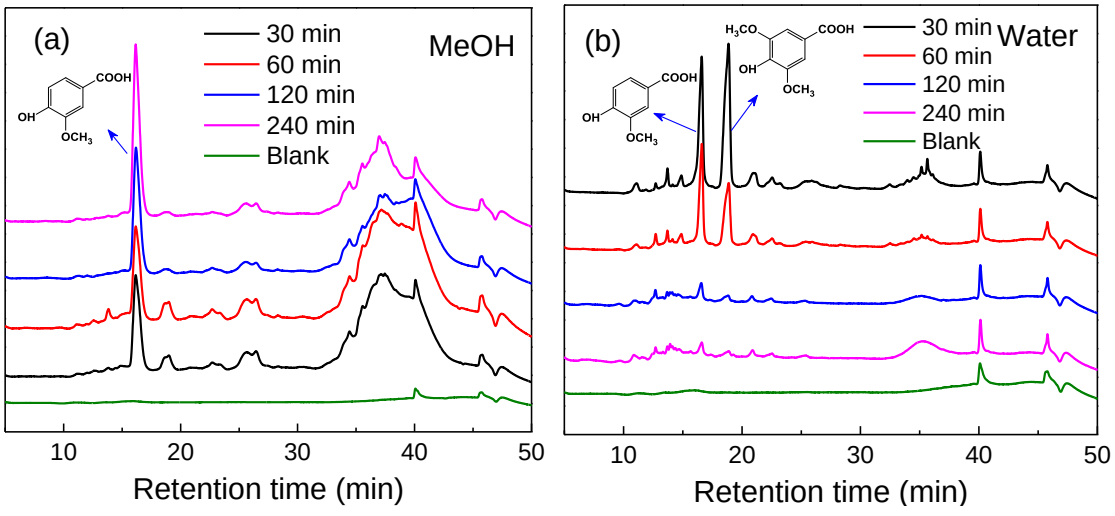

Figure 6.2 HPLC chromatograms of the compounds in the solutions after degradation: (a) in methanol; (b) in water.

Table 6.1 Lignin conversion by using $FeCl_3/NaNO_3/O_2$system

	Catalysts	Solvent	Time (hours)	Temperature (^oC)	Conversion (%)
G 1:	**$NaNO_3/O_2$**	DI water	2	100	40.13
	$FeCl_3/O_2$	DI water	2	100	59.75
	$FeCl_3/NaNO_3$	DI water	2	100	54.46
	$FeCl_3/NaNO_3/O_2$	DI water	2	100	79.15
G 2:	$FeCl_3/NaNO_3/O_2$	DI water	**0.5**	100	26.7
	$FeCl_3/NaNO_3/O_2$	DI water	**1**	100	31.4
	$FeCl_3/NaNO_3/O_2$	DI water	**2**	100	79.15
	$FeCl_3/NaNO_3/O_2$	DI water	**4**	100	89.5
G 3:	$FeCl_3/NaNO_3/O_2$	Methanol	**0.5**	100	25.25
	$FeCl_3/NaNO_3/O_3$	Methanol	**1**	100	38.15
	$FeCl_3/NaNO_3/O_4$	Methanol	**2**	100	70.55
	$FeCl_3/NaNO_3/O_5$	Methanol	**4**	100	82.3

Table 6.2 Catalytic conversion of kraft lignin by using $FeCl_3/NaNO_3/O_2$system at 100 ^oC

Compound	Methanol				Water			
(mg/20mL)	30 min	60 min	120 min	240 min	30 min	60 min	120 min	240 min
Vanillic acid	5.11	5.25	7.26	10.47	2.32	1.41	0.44	0.26
Syringic acid	1.24	1.25	0.62	-	2.95	1.45	0.43	0.41
Vanillin	0.23	0.33	0.25	-	0.38	0.31	0.22	0.27
Total	6.58	6.82	8.12	10.47	5.65	3.17	1.08	0.94
Yield (%)	3.3	3.4	4.1	5.2	2.8	1.5	0.5	0.5

6.3.3 Characterization of solid residue after reaction

Lignin and residue obtained after the reaction was characterized to evaluate the factors contributing to the depolymerization. The lignin residue was analyzed for molecular weight by dissolving it in dimethylformamide by using GPC. Figure 6.3 shows the GPC for raw lignin and solid residue and solution part after depolymerization at 100^{o}C for 240 min using $FeCl_3/NaNO_3$ catalyst. In both solid and solution fractions the number average molecular weight, M_n, decreases from 4774 to 2895 for solid residue and 2396 for liquid fractions respectively, indicating the depolymerization of lignin to lower fractions. Moreover, the retention time for the fractions after the reaction was increased as compared to raw lignin and more peaks were observed in case of solution part which may be attributed to the presence of more compounds formed from depolymerization reaction. Table 6.3 shows the molecular weights of raw lignin and lignin residue after depolymerization at different times in methanol and water mediated reactions. As the time increase the values of M_n, M_w and PDI value decrease, which is a clear indication of depolymerization with the reported catalyst system. The molecular weights of lignin are closely related to structural units present and their number of aryl ether bonds and C-C bonds between them.[28] During the reaction, depolymerization of lignin breaks the α-O-4and β-O-4 bonds, which is demonstrated by the relatively low molecular weight of these fractions.[270]

Table 6.3Molecular weights of raw lignin and lignin residue after depolymerization

Solvent	Sample	M_n	M_w	PDI
	Raw lignin	4792	8907	1.86

MeOH	30 min	3562	8027	2.25
	60 min	3596	7594	2.11
	120 min	3018	6449	2.14
	240 min	2895	5988	2.07
Water	30 min	3931	5530	1.41
	60 min	3274	3990	1.22
	120 min	3529	4250	1.20
	240 min	3208	4047	1.26

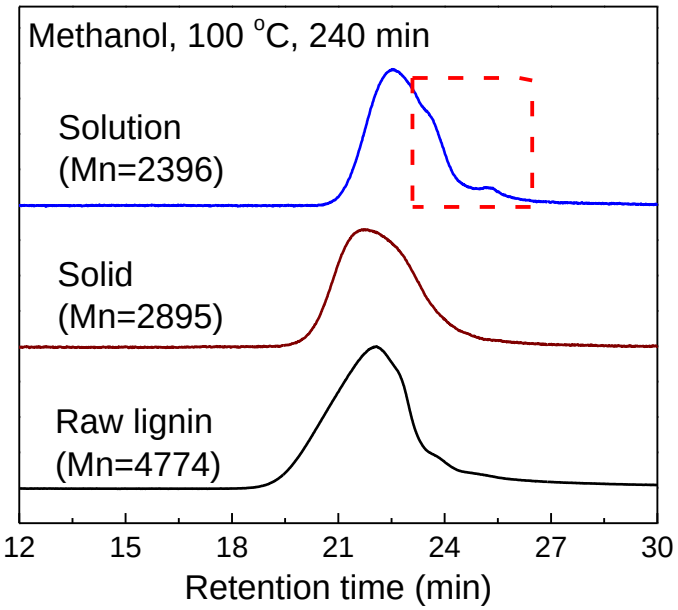

Figure6.3 Gel permeation chromatogram for raw lignin and solid residue and solution part after depolymerization.

The insight of molecular transformations can be visualized from FTIR spectra after depolymerization of kraft lignin as shown in Figure 6.4. The characteristics peaks for lignin in the range of 1100-1350 cm^{-1} for stretching vibrations of C-O and C-O-C bonds indicate the presence of $–OCH_3$ and C-O-C bonds. The peaks for C–H deformation vibrations at 1454 cm^{-1} ($–CH_{2–}$) and 1367 cm^{-1} ($–CH_3$) were observed. The C–H stretching vibrations of aromatic rings were also observed at 1593, 1514, and 1420 cm^{-1}.[271] A prominent peak around 1726 cm^{-1} arises after depolymerization in methanol mediated depolymerization due to the formation of C=O bonds (ketone, aldehyde or carboxylic acid etc.) from –OH in α-carbon. The peaks at 1366 cm^{-1} due to –OH deformation vibration decreases in both methanol and water mediated depolymerization. The peaks ranges from 1030-1120 cm^{-1} are almost vanishes in both water and methanol mediated depolymerization at a specified conditions indicating the cleavage of C-O (methoxyl) and C-O-C (ether) bonds during the reaction. The removal of guiacol units from the kraft lignin was evident from the decrease in peak intensities of C-O and C-H at 1265 and 1030 cm^{-1} respectively.[50]

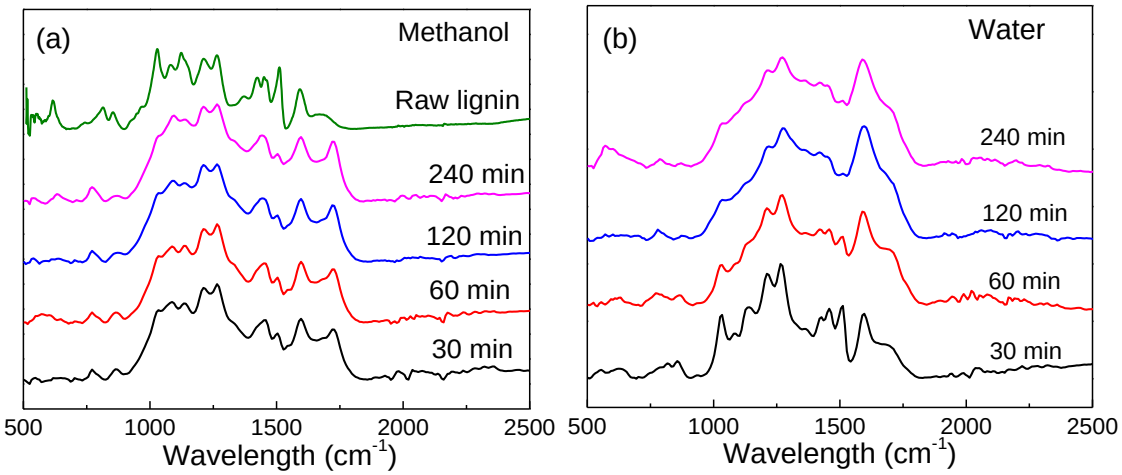

Figure 6.4 FTIR spectra of solid residue after lignin degradation: (a) in methanol; (b) in water

The surface chemistry of the kraft lignin during depolymerization was observed by XPS analysis as shown in Figure 6.5. The XPS data obtained consist of elemental surface composition and O/C ratios. From the elemental analysis, only O and C were detected and there were no residual Fe left on the surface of lignin samples after depolymerization. Table 6.3 shows the elemental compositions at the surface of the original kraft lignin and lignin residue after the reaction. The elemental C decreases with the increase in reaction time while the elemental O increases with time. The C/O ratios of the original kraft lignin and lignin residue after reaction decrease from 3.32 to 1.73 and 2.04 for water and methanol mediated reactions. This decrease in O/C ratios may be due to the inputs of more oxygen in the oxidation reaction during depolymerization.

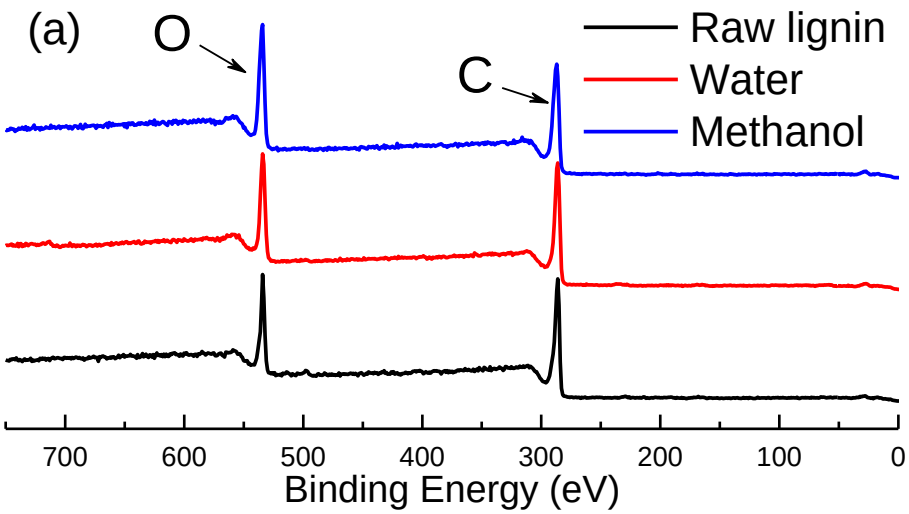

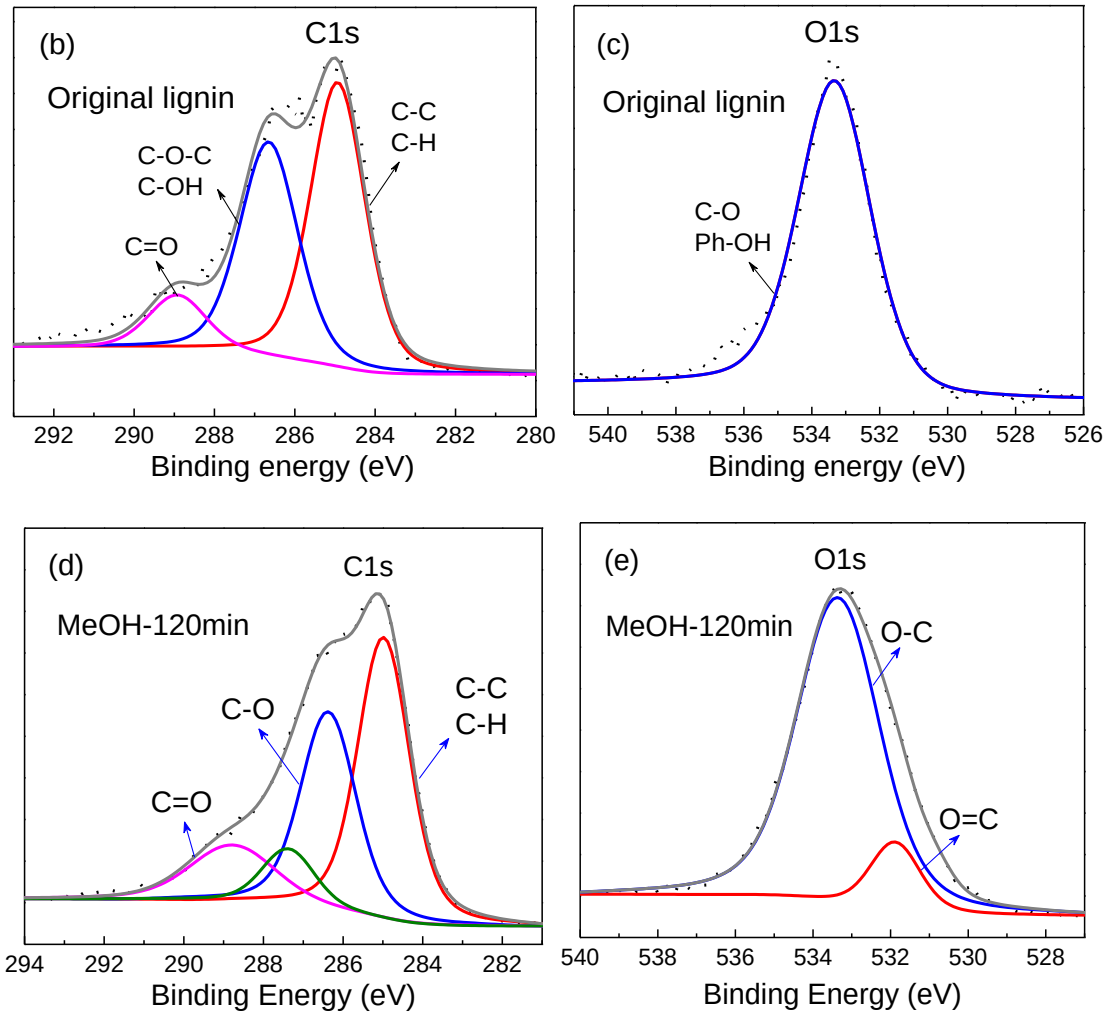

Figure 6.5 XPS spectra of raw lignin and residues of water and methanol mediated depolymerization (a) XPS survey of lignin before and after depolymerization in water and methanol mediated system; (b) C 1s scan of raw lignin; (c) O 1s scan of raw lignin; (d) C1 scan of lignin residue of methanol mediated depolymerization for 120 min at 100 ^{o}C; (e) O 1s scan of lignin residue methanol mediated depolymerization or 120 min at 100 ^{o}C.

Table 6.4.Comparison of the ratios of Carbon/oxygen of the raw kraft lignin and lignin residue after depolymerization

	Raw lignin	Water			Methanol		
		30 min	60 min	120 min	30 min	60 min	240 min
C	76.83	73.76	64.46	63.41	70.18	70.14	67.06
O	23.17	26.24	35.54	36.59	29.82	29.86	32.94
C/O	3.32	2.81	1.81	1.73	2.35	2.35	2.04

The Gaussian peaks were obtained through deconvolution of the C 1s and O 1s peaks and are shown in Figure 6.5 for original kraft lignin and lignin residue after the reaction. The chemical shifts for C ls in original kraft lignin into four categories C 1 (C–C/C–H), C2 (C–O-C and C-OH) and C3 (C=O) whereas, for lignin residue one additional peak C4 (O-C=O) was seen. The binding energy around 284 eV centers for C1s peak and gradually increases from C1 to C4. The O1s peak for lignin residue after depolymerization splits into two categories as O 1(C=O), O2 (C–O). The O1 is mainly due to oxygen in lignin while O_1 and O_2 were present in the pseudo lignin. After depolymerization, a general decreasing of C1 and an increasing of C2 to C3 along with new C4 were observed. The increase in C=O bonds and decrease in C-O bonds after depolymerization partially ascribed to -OH oxidation and cleavage of the β-O-4 linkages in lignin structure**.** The C-O and C=O bonds increased and C=C bond (or C-C) decreased after the depolymerization may also be assumed due to the oxidation of C-C (or C=C) bonds on the surface to C-O and C=O bonds by $FeCl_3/NaNO_3$. These formation of C=O from C-O during the reaction are inconformity with the results of FTIR spectra.

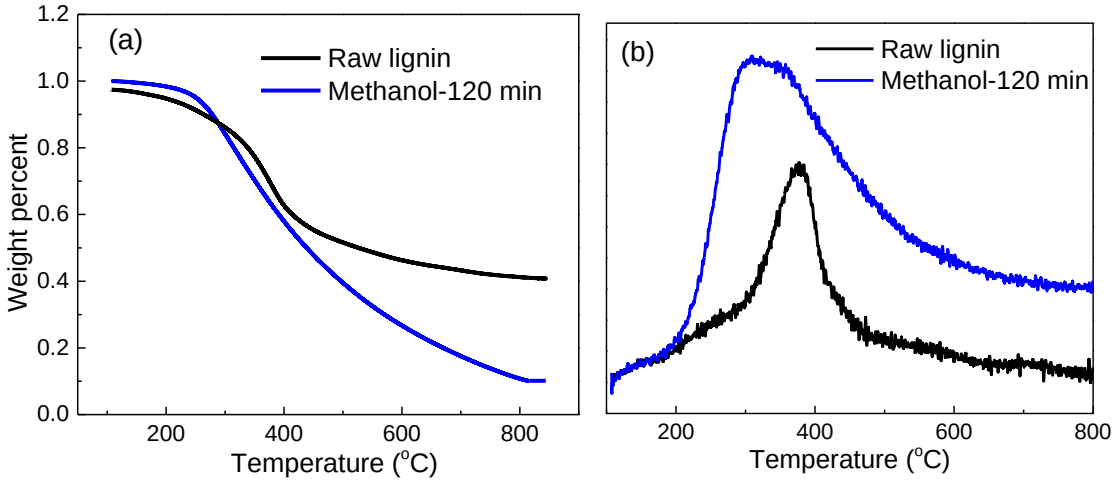

Figure 6.6(a) TGA curves of raw kraft lignin and lignin residue after degradation in methanol for 120 min at 100 °C; (b)(DTG) curves of raw kraft lignin and lignin residue in methanol for 120 min at 100 °C.

In order to study the thermal properties of lignin before and after degradation by $FeCl_3/NaNO_3/O_2$, TGA was carried out to examine lignin decomposition behavior in the temperature range upto 800 °C. The derivative thermogravimetry (DTG) curves of raw kraft lignin and lignin residue at a heating rate of 10 °C min^{-1} are shown in Figure 6.6. From the thermogram, it is clear that the thermal stability of the residue and the solid residue content decreased after the degradation. This is attributed to the formation of low molecular weight compounds during the reaction. For raw kraft lignin a strong peak around 400 °C was obtained which is ascribed to primary pyrolysis as similar to earlier reports in literature[272, 273]. Lignin residue after methanol mediated depolymerization had broader shoulders and the decomposition temperature ranges shifted to a lower temperature (200 to 350 °C). Moreover, the disappearance of strong peak at 400 °C

implies lower thermal stability of depolymerized lignin residue than the raw kraft lignin. The alteration in degradation temperature indicates that molecular weight affects the thermal stability and chemical composition since some functional groups have been transformed in comparison to raw kraft lignin as explained in appropriate analytical section.[274]

6.4 Conclusion

Lignin depolymerization with $FeCl_3/NaNO_3/O_2$catalyst system in presence of molecular oxygen (10 bar, 100 ^oC) could effectively depolymerize kraft lignin into organic liquid monomers specially. The conversion yield of monomers are of (5 wt %) which is significantly higher than typical yields reported in the literature. Based on the results of this study, we demonstrated that the catalyst system effectively depolymerize lignin at a lower temperature as compared to the methods reported till now.

6.5 Appendix

Calibration curves for standard samples:

Standard samples were dissolved in water and solutions with certain concentrations were prepared. Then Analytical HPLC was performed with a Zorbax 300SB-C18 column, 150 mm x 4.6 mm, 5 μm; flow = 0.4 mL/min; eluents H_2O (A) (0.1% TFA), MeCN (B) (0.1% TFA). A gradient method was used in which the percentage of B was allowed to increase from 0 % to 10 % in 1 minute, from 10 % to 20 % over 20 minutes, then 20 % to 100 % over next 14 minutes. The column was finally equilibrated back to 0 % B and washed

thoroughly between sample injections. Then the peak areas of different concentrations were calculated based on the HPLC chromatograms.

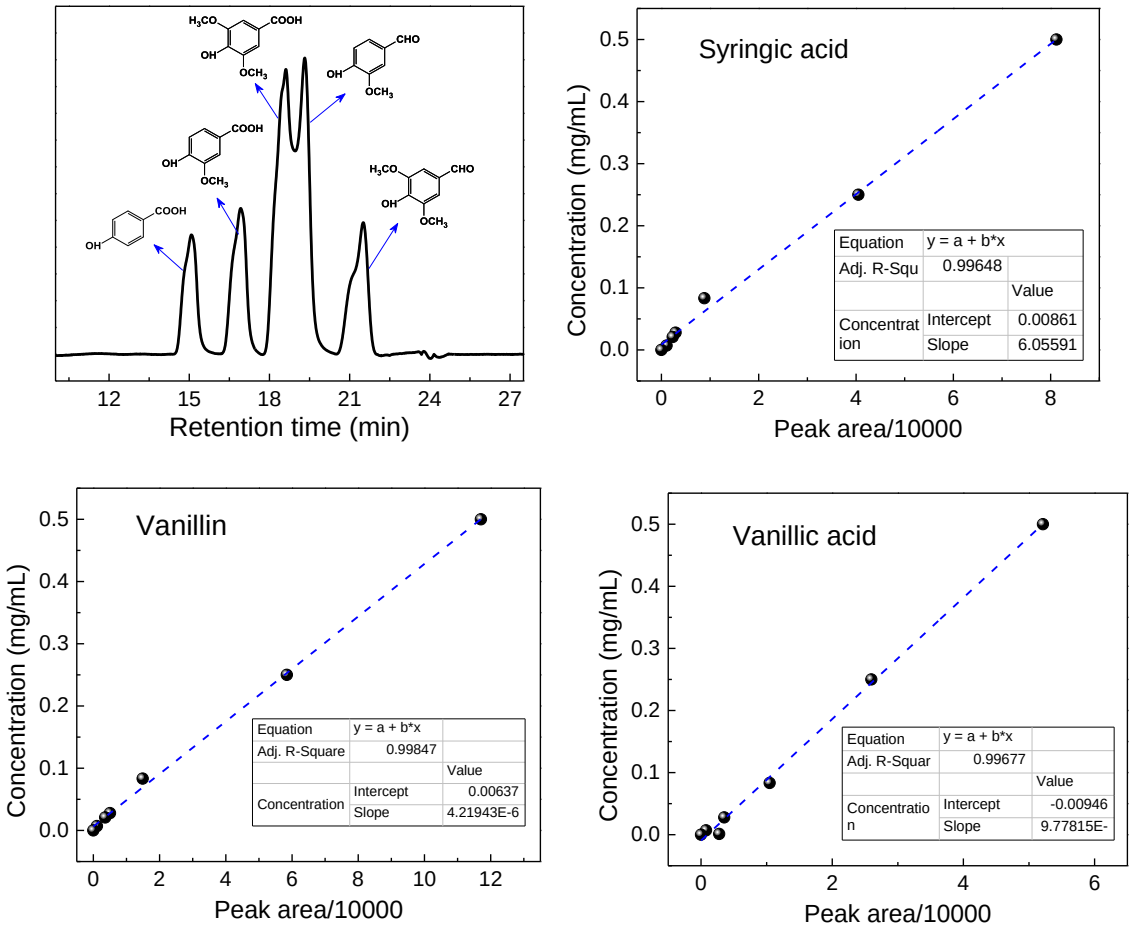

Figure 6.7 Calibration curves for different compounds

CHAPTER VII

NOVEL LOW TEMPERATURE, LOW ENERGY AND HIGH EFFICIENCY PRETREATMENT TECHNOLOGY FOR LARGE WOOD CHIPS WITH A REDOX COUPLE CATALYST

7.1 Introduction

The diminution of fossil fuel, environmental issues of it and higher requirement for worldwide energy enhances the demand for alternative sustainable bioresources for liquid fuels and chemicals.[11] Lignocellulosic biomass is one among the suitable and abundant feedstock recognized for producing mixed sugars for fermentation to biofuels and other biomaterials.[275] Wood pellets are one of the commonly available lignocellulosic renewable energy materials for fuel. The production of second generation biofuels from lignocellulosic sources is a major concern to industry and academia from the technology development perspectives. A typical lignocellulosic biomass has a rigid plant cell contains carbohydrate polymers called cellulose and hemicellulose with tightly bind aromatic polymer lignin. The polysaccharides present in wood which is a dominant lignocellulosic biomass depolymerized to produce corresponding monosaccharides such as glucose, xylose, mannose, etc by mild enzymatic hydrolysis than acid hydrolysis which further fermented to bioethanol.[276-279] One of the major components of lignocellulose is cellulose and can be hydrolyzed enzymatically to glucose and then fermented to bioethanol. However, due to the complex structure of lignocellulosic materials cellulose is protected by lignin and hemicelluloses and enzymatic hydrolysis of native lignocelluloses is difficult. Biomass pretreatment is an important step towards the

accessibility of hydrolytic enzymes to cellulose for glucose conversion. An efficient pretreatment process disrupts the cell wall matrix and reduces the recalcitrance by reducing the size of the biomass, increasing the surface area, modifying the structure of biomass, removal of lignin, partial depolymerization of hemicellulose, and reduction of cellulose crystallinity, eliminates the inhibitory components and etc can be accomplished. These changes in the biomass improve the hydrolysis process to recover higher amounts of fermentable sugars.[280, 281] The lignin present in the biomass specially in hard and softwoods determines the effectiveness of pretreatment since it presents in varying amounts with inter unit linkages. Lignin in softwood mainly contains G units with more C-C linkages and fewer C-O-C linkages than hardwood lignin which contains both S and G units. The sugar recovery is more challenging in softwood than hardwood as reported in many earlier works though the exact reasons for which are still not fully understood.[281-283]

In the recent past, several pretreatment methods have been reported for biomass using steam explosion,[284] microwave pretreatment,[285] ultrasonic pretreatment,[286] hot-compressed water pretreatment,[287] dilute acid,[288] ammonia,[282, 289] inorganic salt[290] and lime[291] etc. to remove or alter lignin and hemicellulose and to improve the enzymatic accessibility of the substrate. All physical and chemical methods reported so far suffers from low efficiency, high energy consumption and specially environmental hazards etc. Besides, the effectiveness of biomass pretreatment is dependent on several factors including the size of biomass and reduction in size thereby increases the surface area of biomass for enzymatic digestion and disruption of crystalline structure of cellulose. Most of the pretreatment methods reported for different biomass, uses raw material in grinded

form which consumes sustainable amount of energy thereby affects pretreatment economy. However, optimum particle size for pretreatment depends on the nature of biomass and methods used for it.[292-296] It is highly desirable to pretreat large size biomass directly instead of grinding one to digestible residues by enzymes.

As the most abundant oxidative agents, oxygen is proposed to be one of the ideal candidates to pretreat biomass. However, without a catalyst, the low rate kinetics of overall reactions at low temperature in aqueous and the poor selectivity of the as-obtained products hinder the practical application of oxygen.[147, 148] $FeCl_3$ has been previously used by some researchers for pretreatment of lignocellulosic materials including rice straw, bagasse and wood fiber.[297] $FeCl_3$ is effective in extracting hemicellulose and capable of interrupting ether and ester linkages between lignin and carbohydrate to enable biomass for enzyme accessible for sugar production with recyclability and less corrosion to equipment's than acids.[266-268] Most of the pretreatment process takes place at higher temperature, high catalyst concentration and uses grinded fractions of biomass. However, to use $FeCl_3$ as catalyst without consumption, the challenge is the re-oxidation of Fe^{2+} back to Fe^{3+} with oxygen due to the low oxygen solubility in water and overall reaction kinetics. Therefore, finding a chemical which can be used as a bridge between oxygen and iron salts to improve the re-oxidation rate of Fe^{2+} is highly expected.

The main objective of this study was to elucidate the redox system for pretreatment of hard and softwoods for improvement of enzymatic hydrolysis. Here we mainly focused on low temperature and energy consumption for maximum sugar production. The $FeCl_3/NaNO_3/O_2$ catalytic system was designed to pretreat both softwood and hardwood successfully. The addition of $NaNO_3$ can serve as the oxygen

vehicle, where NO^{3+} ions oxidizes the Fe^{2+} into Fe^{3+} in the aqueous phase and the as-reduced product NO is easily re-oxidized in the gas phase by oxygen. Thus, the barrier between different phases is broken and the overall pretreatment rate is significantly improved. To the best of our knowledge, this is the first report where wood chips are used in the pretreatment process at low temperature with $FeCl_3/NaNO_3/O_2$ as catalytic system. The effectiveness of the reported pretreatment of softwood and hardwood was evaluated and compared by soluble sugar production after enzymatic hydrolysis. The outcome of the study will provide implication for better design of biorefinery concept and for commodity chemicals from lignin at an environmental friendly condition.

7.2 Materials and Methods

7.2.1 Materials

HW and SW chips were purchased from Walmart and used without any other treatment for pretreatment studies. The sizes of the woods were around 25 × 21 × 3 mm in length, width, and thickness, respectively. Ferric chloride and sodium nitrate for pretreatment were purchased form Sigma Aldrich, USA. 3,5-Dintrosalicylic acid, Rochelle salt, phenol, Sodium metabisulfite and sodium hydroxide used for the sugar analysis were procured from Sigma-Aldrich Chemicals, USA. Chemicals used for all the studies were of analytical reagent grade. The chemical analysis of the hard and softwood samples was done by standard methods and the detailed procedure is given in supporting information. The wood extractives were determined by the standard procedure of Tappi T204 cm^{-97} in which extractives from dried wood samples were extracted using ethanol/benzene, acetone and dichloromethane (5 cycle each) in a soxhlet apparatus. The hollocellulose

(cellulose + hemicellulose) content was determined by using the standard sodium chlorite method.[298, 299] The cellulose content was determined by the modified gravimetric method using 65% nitric acid and ethyl alcohol as reported in literature.[300-302]

The hemicellulose contents were determined by difference of hollocellulose and cellulose. The hardwood contains 5.08% extractives, 68.7% hollocellulose, 42.4% cellulose and 26.3% hemicellulose. The softwood contains 6.01% extractives, 67.3% holocellulose, 40.9 % cellulose, and 26.4% hemicellulose.

7.2.2 Pretreatment of SW and HW

The pretreatment experiments by using the redox couple were carried out in a laboratory scale Parr reactor with a total volume of 50 ml. The biomass solid mixed with 40 ml deionized water with 1-4 wt% of $FeCl_3/NaNO_3$ at 80-150 ^oC in 10 bar of O_2 atmospheres with constant stirring (200 rpm) for 30-120 min. The heating rate for all the experiments was ~5^oC/min. The reaction mixtures were initially heated to set the temperature and kept stirring until completion of the reaction time. After the reaction, the reactor immediately cooled in tap water taking out from the heating jacket and filtered to separate the sold biomass. Washed the pretreated biomass with deionized water and used for enzymatic hydrolysis. Washed solids were analyzed for different changes after pretreatment by SEM, FTIR, XRD, XPS and TG analysis. The dissolved lignin fragments in pretreatment liquid were collected at pH 2-3 followed by water washing and drying for further analysis. The total experimental plan is given in Scheme S1.

7.2.3 Enzymatic Hydrolysis

After pretreated the hard and softwood samples were hydrolyzed by *cellulase* with an enzyme loading of 0.3g/g substrate in a 100 mL flask. The enzymatic hydrolysis reactions were performed in a 0.05 M HAc/NaAc buffer (pH 4.8) at 50 °C on a rotary shaker at 150 rpm. The samples for sugar analysis (0.5 mL) were withdrawn at intervals of 1, 4, 18 and 24 h and kept in boiling water to inactivate enzymes and filtered through a porous membrane of 0.2 μm diameter to remove water insoluble solids. Then the filtered samples were analyzed by DNS method for glucose concentration. In a typical analysis, 0.5 ml of sample is added to 1 ml of buffer solution and 3 ml of DNS reagent. Boil the mixture vigorously for 5 min and then cooled in ice cold water. Under these conditions, 3, 5-dinitrosalicylic acid (DNS) reduces to 3-amino, 5-nitrosalicylic acid. The absorbance was measured at 540 nm (Shimadzu) and the reducing sugars concentration was determined by using a standard calibration curve of glucose as shown in Figure 7.14 of appendix.[303-305]

7.2.4 Characterization of pretreated wood chips and liquids

SEM analysis was conducted to analyze the surface morphology of untreated and pretreated wood samples. All samples were sputtered by gold for 60 s prior to imaging with SEM (LEO 1530 SEM, Carl Zeiss) operating at an accelerating voltage of 10 kV.

The X-ray diffraction (XRD) patterns of the untreated and pretreated HW and SW samples were analyzed by X'Pert PRO diffractometer. The instrument is equipped with a Cu Kα radiation source(λ=0.154 nm) with a 2θ range of 10–60^{o} and the operation voltage

and current was maintained at 40 kV and 40 mA respectively. The crystallinity index (C.I) was determined as

$$C.I = (I_{002}-I_{amorphous}) / I_{002} \times 100\ \%$$

where, I_{002} is the intensity of (002) peak at $2\theta = 22.5^{o}$ and $I_{amorphous}$ is the intensity of the background at $2\theta = 18.3^{o}$.[306]

TGA, FTIR and XPS of untreated and pretreated wood samples were carried out as described in Chapter IV and Chapter VI, respectively.

The lignin samples recovered from the solution under acidic conditions after pretreatment were acetylated to soluble in tetrahydrofuran (THF) for GPC analysis. The acetylation of lignin samples was done by using 2 ml of acetic anhydride –pyridine (1/1, v/v) at room temperature for 24 hours under vigorous stirring. Ethanol was added to the reaction mixture and removed it by vacuum drying. The addition of ethanol and removal was continued until complete removal of traces of acetic acid and pyridine from the sample. The acetylated lignin samples were dissolved in THF for GPC analysis. The GPC analysis was performed in THF with a flow rate of 1 mL/min at 40 ^{o}C using a diode array detector (SPD - M20A) and RI detector (RID - 10A). The instrument was calibrated before analysis with EasiVial polystyrene standards (Agilent).

7.3 Results and Discussion

7.3.1 Pretreatment of HW and SW chips

The biological means for ethanol production from biomass involves pretreatment, hydrolysis and fermentation. Glucose to ethanol by fermentation is matured optimized technology and due to the recalcitrance offered by lignocellulosic biomass hydrolysis is

difficult. For this reason, pretreatment is essential to breakdown the linkages among components to make it favorable for hydrolysis of polysaccharides. In our system, wood chips became almost powder after pretreatment for 2h at 100 ^{o}C. The control experiment shows that there were almost no changes in the wood structure up to 60 ^{o}C with the same catalyst concentration and O_2 pressure. Similarly, without catalyst, keeping O_2 pressure the same and temperature constant at 100 ^{o}C also leaded to tiny changes in the wood structure. The overall process and the mechanism of pretreatment are as shown in Figure 7.16 of appendix.

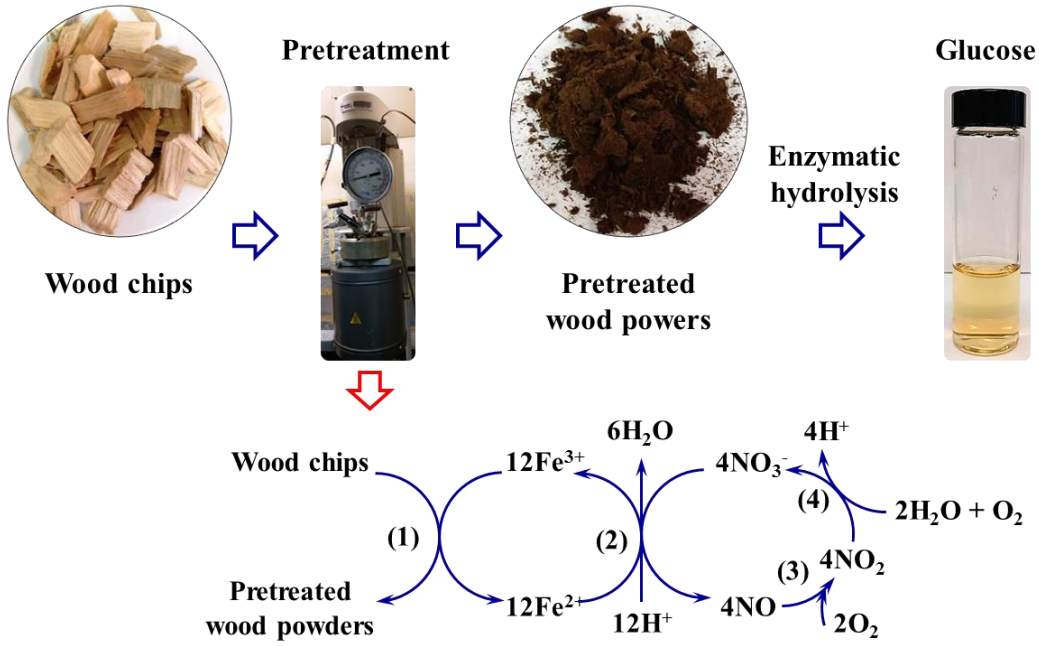

Figure 7.1 Schematic of the overall process of wood chip pretreatment and hydrolysis (up) and the catalytic process during the pretreatment (bottom)

(1) $Wood\ chips + Fe^{3+} \rightarrow Pretreated\ wood\ powders + Fe^{2+}$

(2) $3Fe^{2+} + NO_3^- + 4H^+ \rightarrow 3Fe^{3+} + NO + 2H_2O$

(3) $2NO + O_2 \rightarrow 2NO_2$

(4) $4NO_2 + O_2 + 2H_2O \rightarrow 4H^+ + 4NO_3^-$

Overall reaction: $Wood\ chips + O_2 \rightarrow$ Pretreated wood powders

Briefly, in the pretreatment process, Fe^{3+} from $FeCl_3$ oxidizes wood chips at 100 ^oC in presence of O_2 while Fe^{3+} is reduced to Fe^{2+} as shown in equation 1. Electrons are transferred to Fe^{3+} from biomass and protons are released into the solution. The NO_3^- ion from $NaNO_3$ oxidizes Fe^{2+} in presence of proton to Fe^{3+} with the formation of NO gas as shown in equation 2. NO is miscible with O_2 in the gas phase. Further NO is oxidized to NO_2 and then to NO_3^- in presence of O_2 as shown in equation 3 & 4. NO_3^- ions can dissolve back to the aqueous solution quickly to oxidize newly formed Fe^{2+}. Therefore, the overall reaction of the pretreatment process is the oxidation of wood chips by oxygen. The advantage of using the Fe^{3+}/ NO_3^- redox couple catalyst is that it can increase the re-oxidation kinetics of Fe^{2+} and thus improve the overall pretreatment rate at lower temperature and without any mechanical grinding of wood chips.

The wood samples were analyzed for cellulose and hemicellulose before and after pretreatment. The composition of the hard and softwood before and after pretreatment is shown in Table 7.1. From the table it can be clearly seen that after the pretreatment the cellulose percentage were increased in softwood (40.9 to 64.2 %) and hardwood (42.4 to 67.8 %) due to the removal of hemicellulose, lignin, and other components which is one of the essential criteria for the successful process. The total weight loss after pretreatment was about 30.3 % for softwood and 32.1% for hardwood respectively at optimum conditions. The hemicellulose removal for hardwood (26.3 to 19.1 %) was more as

compared to softwood (26.3 to 64.2 %) after pretreatment. The results of total weight loss, removal and hemicellulose and cellulose contents are consistent with each other after pretreatment and depends on the biomass composition and structure of lignin and hemicellulose.[307]

Table 7.1 Compositions of softwood and hardwood before and after pretreatment

	Before pretreatment		After pretreatment	
	Cellulose	Hemicellulose	Cellulose	Hemicellulose
Softwood	40.9%	26.4%	64.2%	24.3%
Hardwood	42.4%	26.3%	67.8%	19.1%

The effect of pretreatment on the surface morphology and physical characteristics of the wood samples can be seen in the photographs, optical microscopic images (Figure 7.2 for hardwood and Figure 7.10 of appendix for softwood) and SEM images (Figure 7.3). The optical microscopic images show that pretreated woods exhibited smaller or irregular fragments of fiber (Figure 7.2 (d) and 7.10 (d) of appendix). The colour of the samples after the pretreatment was dark brown as clearly seen in the photographs (Figure 7.2 (c) for hardwood and Figure 7.10 (c) of appendix for softwood) which might be due to the formation of chromophores from lignin. In the SEM images, deposition of nearly spherical droplets of re-condensed lignins or pseudolignins is clearly shown. In both cases, the destruction of microfibers is seen. In general, high temperature pretreatment has degrading effects while low temperature pretreatment initiated structural swelling.[308]

These depositions are more for hardwood (Figure 7.3 (b)) and negligible in the case of softwood (Figure 7.3 (d)) samples pretreated at the 100 ^{o}C for 2h. In the case of softwood, however, the surface remains free of droplet formation even at the most severe pretreatment conditions. This may be attributed to the more resistant nature of softwood lignin as compared to the lignin of hardwoods due to their different composition. The lignins in softwood are mostly of guaiacyl units (phenolic ring with one methoxyl group), whereas lignins in hardwood have both guaiacyl and syringyl groups (phenolic ring with two methoxyl groups). Therefore, hardwood lignins having aromatic ring with more methoxyl are less condensed and able to be controlled by pretreatment for enzymatic hydrolysis. However, for both the hard and softwood samples the color after pretreatment was brown which may be due to the relocation of lignin particles on the surface of the surface as well as formation of pseudolignin.[309-311]

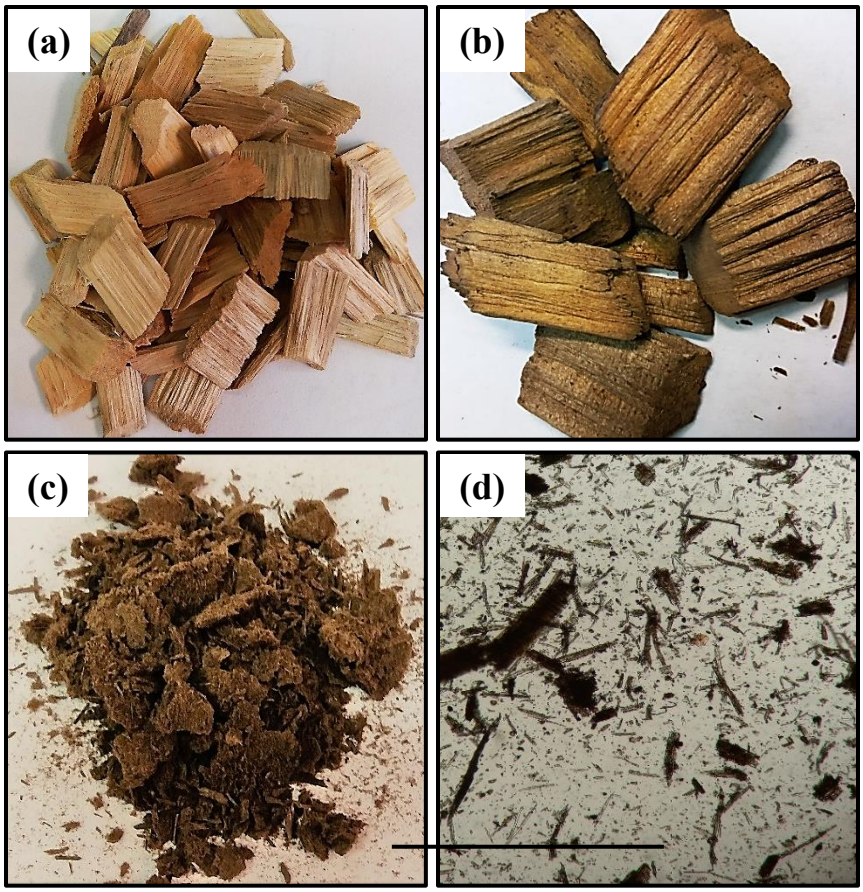

Figure 7.2 Photos of hardwood: (a) untreated hardwood; (b) hardwood treated in pure water at 100 ^{o}C for 2 hours; (c) hardwood treated in $FeCl_3/NaNO_3/O_2$ at 100 ^{o}C for 2 hours; (d) optical microscopic image of pretreated hardwood in $FeCl_3/NaNO_3/O_2$. The scale bar of microscopic view is 0.1 mm.

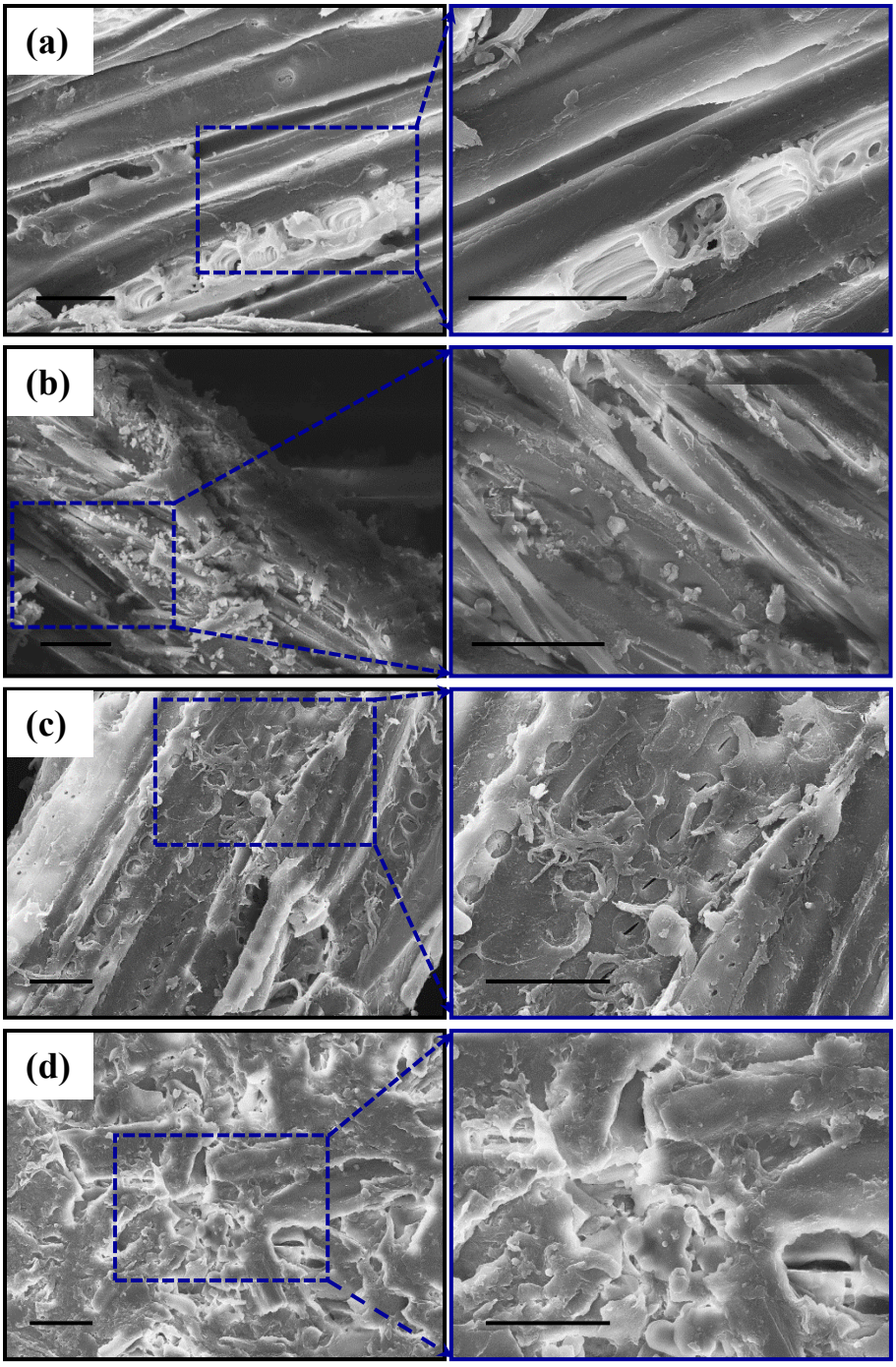

Figure 7.3 SEM of hardwood and softwood samples: (a) raw hardwood; (b) pretreated hardwood; (c) raw softwood; (d) pretreated softwood. The scale bar is 20 μm.

7.3.2 Enzymatic hydrolysis of pretreated woods

The increased enzymatic accessibility to biomass is the goal of pretreatment. Pretreatment by $FeCl_3$ degrades hemicellulose in biomass materials, the bonds holding the biomass component removed by catalytic attack and carbohydrates can be accessed by enzymes in presence of decreased lignin[312, 313] The FCSNRC pretreated hard and softwood samples were hydrolyzed to fermentable sugars by enzymatic hydrolysis. In hydrolysis process the polymer chains of cellulose and hemicellulose breaks into its monomers. Furthermore, degradation of hemicellulose takes place in hydrolysis to glucose, arabinose, mannose and dextrose to increase total sugar yield.[314] The optimum pretreatment conditions for enzymatic hydrolysis in terms of pretreatment temperature, time and catalyst loading and substrate concentrations are explained to make the process viable. The yield of enzymatic hydrolysis was determined as

Yield (%)= (soluble glucose) / (Cellulose in raw wood) x 100

The effect of pretreatment temperature on hydrolysis was investigated from 80-150 ^oC for HW and SW samples at 2 wt% and 3 wt% of $FeCl_3/NaNO_3$ respectively for 2h at 150 psig O_2 pressure. Figure 7.4 shows the dependence of pretreatment temperature of HW and SW at the specified conditions. Enzymatic hydrolysis reactions were monitored at regular interval of time up to 24h. The conversion profiles with time are of same pattern for all the hydrolysis reactions wherein up to 4h time the sugar release from the biomass samples under investigation is faster as compared to the later part of hydrolysis. For both SW and HW, the percentage of sugar yield increases from 80 to 100 ^oC and

decreases afterwards. The yield of sugar was more in case of HW as compared to the SW chips. The reason may be due to the degradation of cellulose above 100 ^{o}C or degradation of lignins to monomers which inhibits the hydrolysis. The yields of enzymatic hydrolysis of FCSNRC pretreated HW and SW samples were higher than the of pure cellulose (23.9%) samples at the same hydrolysis conditions.

In order to understand the effect of catalyst concentration in pretreatment the concentration range varied from 1-3 wt % based on the amount of SW and HW chips. Figure 7.5 (a) demonstrated the influence of $FeCl_3$/ $NaNO_3$ concentration on the yield of HW and SW samples. Control experiments of pretreatment without catalyst, with $FeCl_3$ without $NaNO_3$ and with $NaNO_3$ without $FeCl_3$ shows below 10% yield in hydrolysis. When $FeCl_3$/ $NaNO_3$ concentrations were increased from 1 wt % to 3 wt % the hydrolysis yield increases from 24.87 % to 70.66 % and 40.0% to 71.53 % for SW and HW respectively. For SW the hydrolysis yield was maximum for samples pretreated at 3 wt % catalyst concentration while for hardwood it was 2 wt%. However, once the $FeCl_3$/ $NaNO_3$ concentration was raised to 4 wt %, the hydrolysis yield was almost same. Pretreatment of biomass using higher $FeCl_3$ concentrations gives higher cellulose conversion for eucalyptus mechanical pulp fiber after *cellulase* hydrolysis suggesting that ferric chloride destroys the tight structure by decomposing hemicellulose.[266, 315] Higher concentration of $FeCl_3$ lowers the pH value which negatively affected the gucan recovery and finally to the overall sugar and equipments.[313]

Figure 7.15 (appendix) and Figure 7.5 (b) depicts the cellulose conversion of SW and HW for different pretreatment time under the same enzymatic hydrolysis parameters. The experiments were conducted for 30-120 min and it is evident from the figure that

increase in time increases the hydrolysis yield up to 120 min and after that no substantial increase in hydrolysis yield was observed. This drift suggests the degradation of hemicellulose with time as similar to the temperature effects of pretreatment. Moreover, longer pretreatment time may degrade cellulose which could decrease the overall viability of the process.

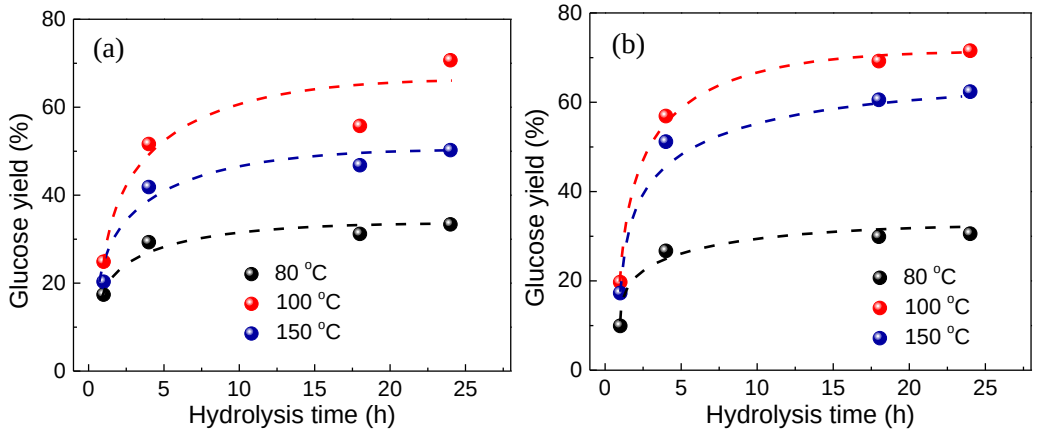

Figure 7.4 Effect of pretreatment temperature on glucose yield: (a) softwood; (b) hardwood. Pretreatment was carried out at 80-150 °C and150 psig O_2 pressure with 3 wt% (softwood) and 2 wt% (hardwood) of $FeCl_3/NaNO_3$ for 2h. Enzymatic hydrolysis was carried out with *cellulase* loading of 0.3g/g substrate in 0.05 M HAc/NaAc buffer (pH 4.8) at 50 °C.

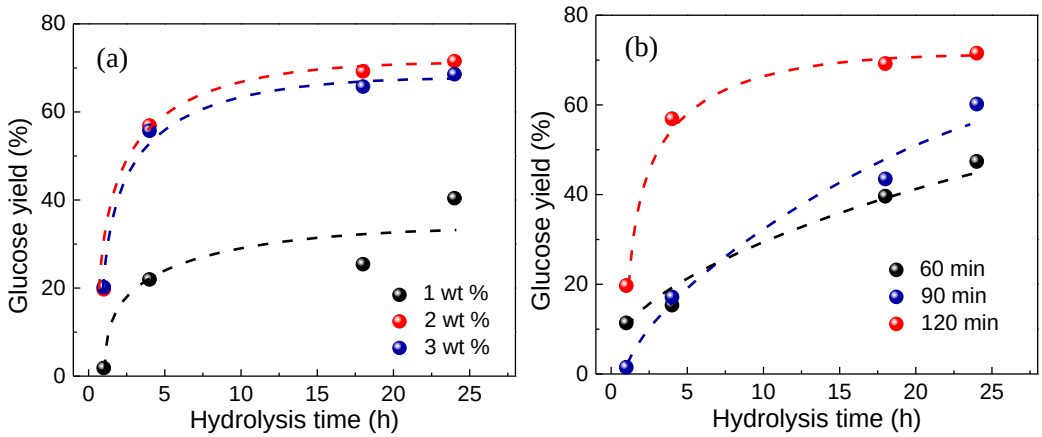

Figure 7.5 Effect of catalyst amount (a) and pretreatment time (b) on glucose yield (hardwood). Pretreatment was carried out at 100 ^{o}C and150 psig O_2 pressure with $FeCl_3/NaNO_3$ (1-3 wt%, Fig (a)) and (2 wt%, Fig. (b)) for time (120 min for (a) and 60-120 min, Fig. (b)). Enzymatic hydrolysis was carried out with *cellulase* loading of 0.3g/g substrate in 0.05 M HAc/NaAc buffer (pH 4.8) at 50 °C.

In summary, a novel and energy-saving pretreatment process was designed successfully, where un-grinded hardwood and softwood chips were pretreated directly by $FeCl_3/NaNO_3/O_2$ at low temperature. $NaNO_3$ serves, herein, as a bridge between gaseous phase and liquid phase, which increases the overall reaction kinetics under mild conditions. This technology is promising to break the wood chip complex to make the carbohydrates more accessible to the enzymes, which is further demonstrated by the high glucose yield after the following enzymatic hydrolysis process.

7.2.3 Investigation on properties of untreated and pretreated woods

The high glucose yield obtained in the hydrolysis is mainly resulted from the effective pretreatment by $FeCl_3/NaNO_3/O_2$ as described. To further understand the effects of the

pretreatment, the properties of untreated and pretreated woods were investigated by different characterization techniques.

The effective pretreatment may change the crystalline nature of biomass along with the chemical composition. To understand the relative cellulose crystallinity XRD analysis is useful and in general lower value in pretreated samples gives higher enzymatic digestibility.[316] In lignocellulosic biomass, cellulose only contributes to the overall crystallinity of the materials. The cellulose structure includes the highly ordered regions as long range crystallinity along with the short range regions of amorphous and short range less ordered regions. The long range crystallinity contributes more to the recalcitrance of lignocellulosic materials than the sort range crystallinity, thereby short range crystalline regions can be easily disrupted or even removed.

Highly rigorous pretreatment methods remove both the sort and long range crystallinity from the biomass to break the strong inter and intramolecular bonds. The relative crystallinity of biomass can be evaluated with crystallinity index which is a measure of severity of pretreatment.[317] The crystallinity index is the height ratio between a major crystalline peak (I_{002}-$I_{amorphous}$) and 002 plane of peak. The calculation of C.I gives the indication of severity of pretreatment, if the pretreatment removes the crystallinity of short range crystallinity regions the intensity of the peaks will increase whereas the decrease in peak intensity signifies the removal of highly ordered long range crystalline regions.[306, 317] The XRD patterns of soft and hardwood samples before and after the pretreatment are not much different since the cellulose content in pretreated samples were nearly same, thereby giving the similar cellulose for XRD analysis. The XRD patterns of untreated and pretreated hard and softwood samples are shown in Figure

7.6. The peaks at specific 2θ angles of 22.6°, 21.7°, 18.9° and 16.3° corresponds to the lattice planes of 002, $10\bar{1}$ and 101 for cellulose I and cellulose II respectively. After pretreatment of both soft and hardwood samples at 100 ^{o}C the peaks at 2θ angles 18.9° and 16.3° appear which may be attributed to the change in crystalline states from Cellulose II to cellulose I. In general deformation of crystalline cellulose I structure in pretreated materials subject to a higher enzymatic hydrolysis yield than untreated substrates. The increase in peak intensity is due to the removal of amorphous hemicellulose after pretreatment. The XRD analysis of untreated and pretreated hardwood and softwoods samples, as shown in Figure 7.6, represents the difference in cellulose crystallinity. The increase in the sharpness and intensity of peaks due to the cellulose indicates the effectiveness of pretreatment process at different conditions as specified. The crystallinity index (CrI) of soft and hardwood before and after pretreatment was increased from 55.42 to 63.32 % and 53.65 to 79.33 % respectively. The increase in CrI after pretreatment for hardwood was more prominent than softwood as expected. The lower value of CrI for softwood after pretreatment than hardwood indicates that the easy accessibility of enzymes to hardwood cellulose for hydrolysis than the softwood cellulose respectively.[317]

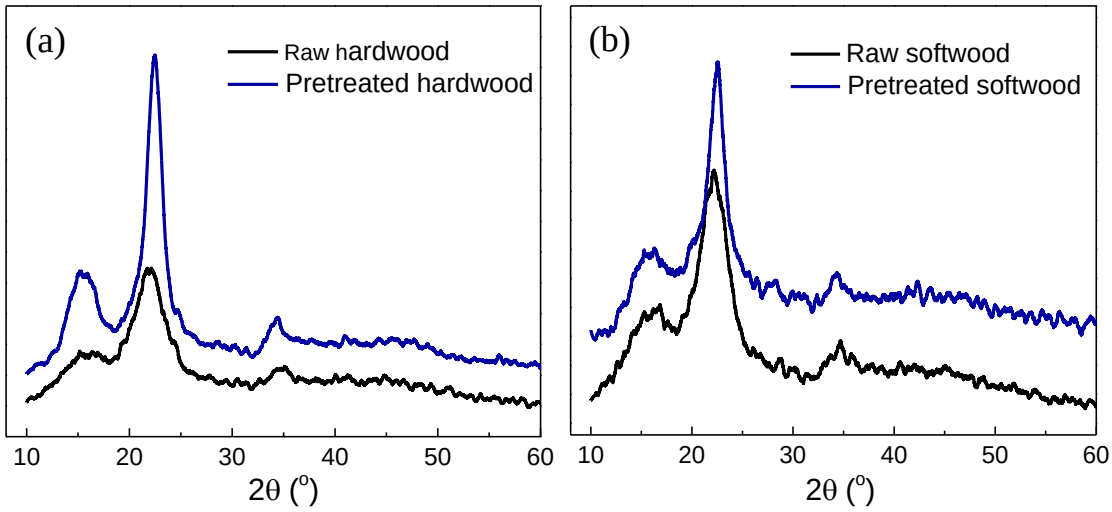

Figure 7.6 XRD pattern of hardwood (a) and softwood (b) samples before and after pretreatment. Pretreatment was carried out at 100 ^{o}C and150 psig O_2 pressure with $FeCl_3/NaNO_3$ (2 wt%, Fig (a)) and (3 wt%, Fig. (b)) for 120 min.

To evaluate the changes in thermal properties of SW and HW samples before and after FCSNRC pretreatment weight loss (thermogravimetry, TG) and weight loss rate (differential thermogravimetry, DTG) curves were drawn as shown in Figure 7.7. It is presumed that there is no interaction between the extractives, hemicellulose, cellulose, and lignin. The contributions of different components can be exemplified by DTG profile with separate peaks. In all SW and HW samples, a small weight loss (about 3 wt%) in the range of 30 °C to 130 °C was observed due to evaporation of water in the biomass or due to low molecular weight compounds left over in the samples. From the figure of TGA, the signals centered at 286−216 and 298−355 °C were assigned to the mass loss rates of extractives and hemicellulose. The signals centered at 334−384 and 360−389 °C were mainly associated to the mass loss rates of cellulose and lignin, respectively.[318, 319] As shown in Figure 7.7, the weight loss fractions of raw and pretreated SW and HW samples

were significantly influenced by FCSNRC pretreatment. The prominent differences in their weight loss fractions for both HW and SW samples were primarily due to their different chemical compositions. During FCSNRC pretreatment, the weight loss fractions for hemicellulose and lignin dropped significantly indicating the removal of it from the samples after pretreatment. However, the weight loss fraction for cellulose is very limited for both HW and SW samples. The change in weight loss fractions was more for SW than HW samples.

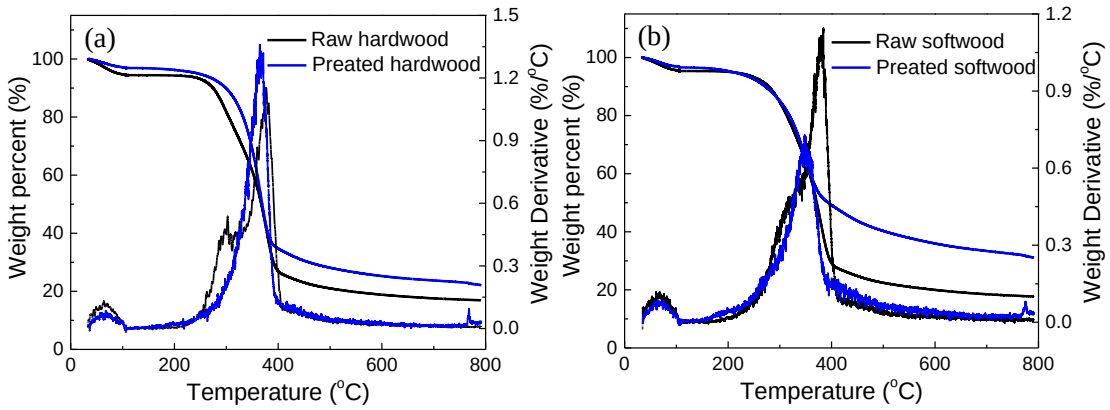

Figure 7.7 TGA/DTA of hardwood (a) and softwood (b) samples before and after pretreatment. Pretreatment was carried out at 100 ^{o}C and150 psig O_2 pressure with $FeCl_3/NaNO_3$ (2 wt%, Fig (a)) and (3 wt%, Fig. (b)) for 120 min.

The probable changes in molecular structure of major hard and softwood compounds were assessed by the total Fourier transform infrared reflectance (FTIR). The FTIR spectra of untreated and pretreated hard and softwood samples are shown in Figure 7.8(a) & (b). The spectral differences between soft and hardwoods are due to the hemicellulose and lignin. No spectral differences connected to cellulose compounds. In

softwood lignin guaiacyl units predominates over small amount of p-hydroxyphenyl and syringyl units while in hardwood lignin syringyl and guaiacyl units predominates over p-hydroxyl units.[320] The bands correspond to syringil units at 1595, 1326, 1230 and 1422 cm^{-1} can be seen in hardwood while in softwoods these peaks are not prominent. For both hard and softwood samples before and after the pretreatment the wavenumber at 1735 cm^{-1} corresponding to $C=O_{str}$ vibrations of lignin is vanished after the pretreatment. Similarly, peaks at 1235 cm^{-1} corresponds to syringlyl nuclei of plane at 2, 5, 6 position of guaiacyl unit vanishes due to the removal of lignin after pretreatment. At 1057 cm^{-1} and 1316 cm^{-1} corresponds to the C-O deformation in aliphatic alcohol and ether and CH_2 wagging vibration respectively increases due to the ether bond breaking between and lignin and cellulose. The band at 897cm^{-1} assigned to $C\text{-}O\text{-}C_{str}$ of amorphous cellulose due to β-(1-4) glycosidic linkage shifted after pretreatment which may be due to the transformation of Cellulose I to Cellulose II. The decrease in intensity at 1235 cm^{-1} ($C\text{-}O_{str}$ of lignin and hemicellulose), 1375 cm^{-1}(deformation in cellulose, hemicellulose and lignin) 1735 cm^{-1} (carbonyl $C\text{-}O_{str}$) after pretreatment may be due to the cleavage of ester linkages in lignin and hemicellulose and cleavage of lignin side chain due to removal of lignin. A new peak at 1057 cm^{-1} after the pretreatment due to $C\text{-}O\text{-}H_{str}$ of primary and secondary alcohols suggests the removal of hemicellulose from the hardwood.[313] The other characteristic peak positions for both hard and softwood samples before and after are almost same but some decrease in peak intensities.

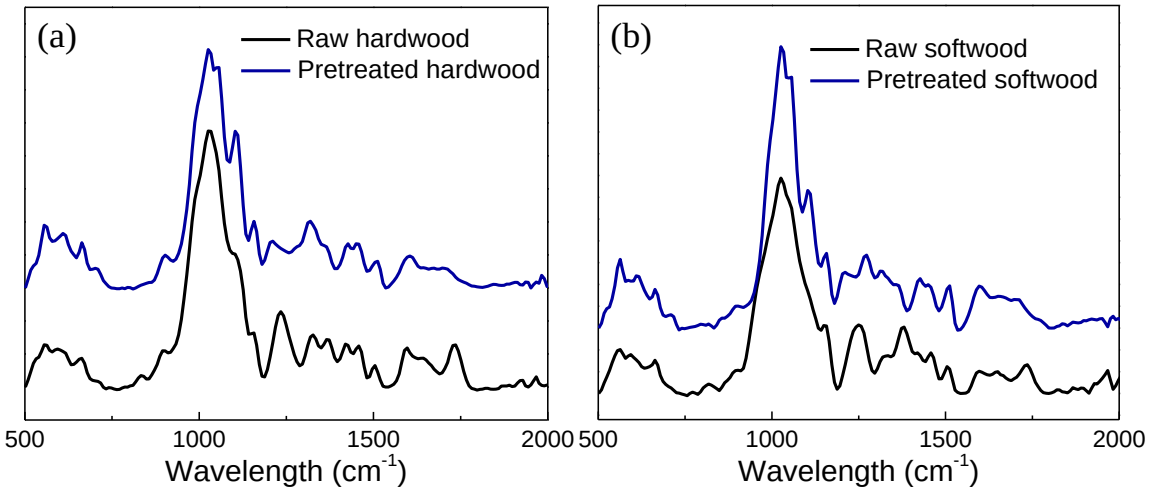

Figure 7.8 FTIR spectra of hardwood (a) and softwood (b) samples before and after pretreatment. Pretreatment was carried out at 100 ^{o}C and150 psig O_2 pressure with $FeCl_3/NaNO_3$ (2 wt%, Fig (a)) and (3 wt%, Fig. (b)) for 120 min.

The chemistry on the surface of the biomass before and after FCSNRC pretreatment was examined by XPS as shown in Figure 7.9. The obtained XPS data consisted of the elemental surface composition and O/C ratios. From the spectra, only elements detected were O and C, there were no residual Fe present on the surface of biomass after the pretreatment for both the soft and hardwood samples. In the cellulose hydrolysis, Fe^{3+} can form complexes with lignin which inhibit the process by deactivating the enzyme active sites.[321] For both soft and hardwoods the C 1s and O 1s spectrum peaks were observed at 284 eV and 531 eV respectively. The O/C ratios of the hard and softwood increase from 0.38 to 0.49 and 0.35 to 0.49 respectively. This change of O/C ratios may be attributed to the introduction of more oxygen in the oxidation reaction during pretreatment.

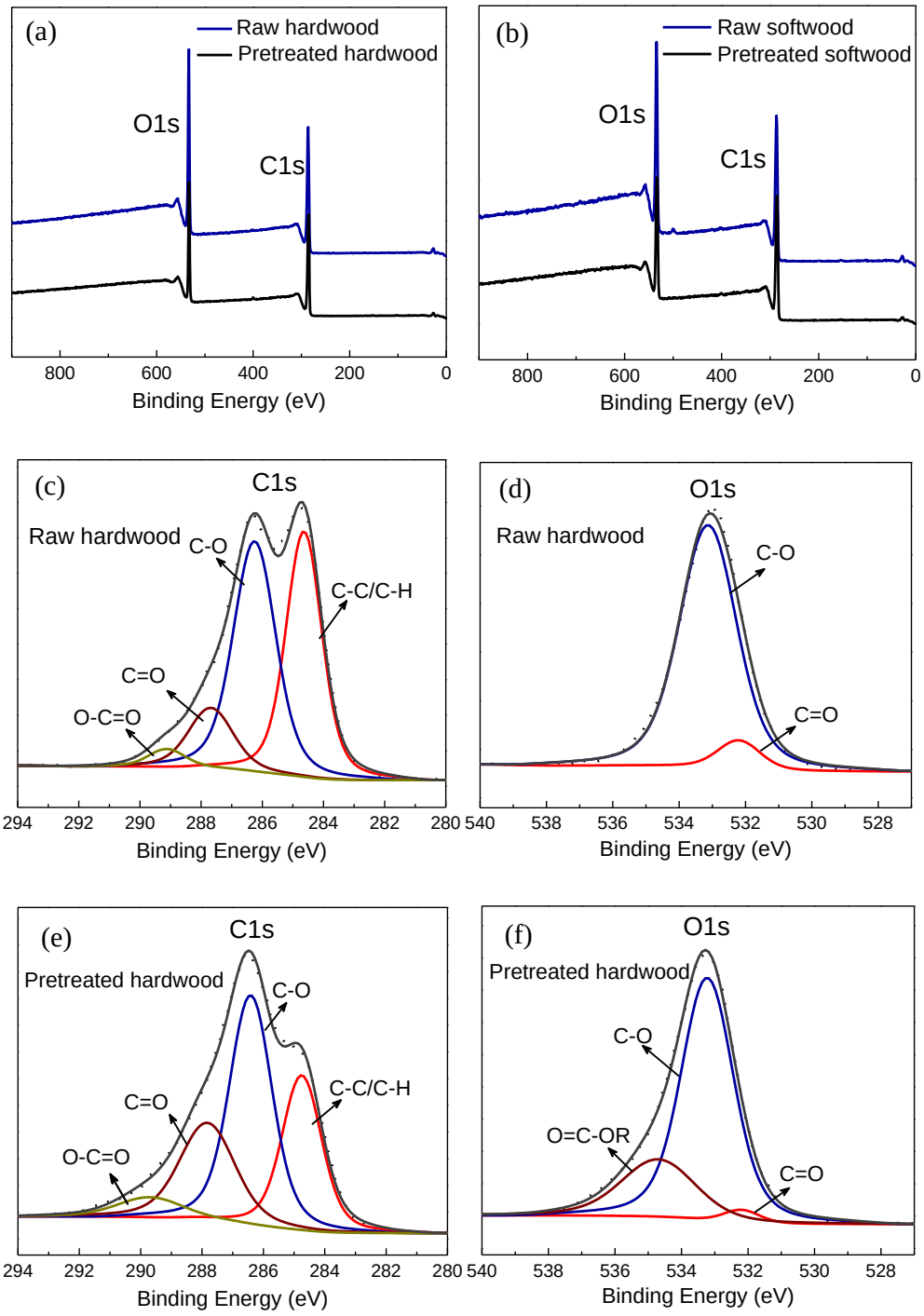
(a)
Raw hardwood
Pretreated hardwood
O1s
C1s
800
600
400
200
0
Binding Energy (eV)
(b)
Raw softwood
Pretreated softwood
O1s
C1s
800
600
400
200
0
Binding Energy (eV)
(c)
C1s
Raw hardwood
C-O
C-C/C-H
C=O
O-C=O
294
292
290
288
286
284
282
280
Binding Energy (eV)
(d)
O1s
Raw hardwood
C-O
C=O
540
538
536
534
532
530
528
Binding Energy (eV)
(e)
C1s
Pretreated hardwood
C-O
C-C/C-H
C=O
O-C=O
294
292
290
288
286
284
282
280
Binding Energy (eV)
(f)
O1s
Pretreated hardwood
C-O
O=C-OR
C=O
540
538
536
534
532
530
528
Binding Energy (eV)

Figure 7.9 XPS spectra of hardwood and softwood samples: (a) XPS survey of hardwood before and after pretreatment; (b) XPS survey of softwood before and after pretreatment; (c) C 1s scan of raw hardwood; (d) O 1s scan of raw hardwood; (e) C1 scan of pretreated hardwood; (d) O 1s scan of pretreated hardwood.

The Gaussian peaks obtained through deconvolution of the C 1s and O 1s peaks are shown in Figure 7.9 for hardwood and Figure 7.13 (appendix) for softwood before and after pretreatment. The chemical shifts for C ls in both hard and softwood deconvoluted into four categories C 1 (C–C/C–H), C2 (C–O), C3 (C=O) and C4 (O–C=O). The C1(C–C or C–H) arises mainly due to lignin and extractives while C 2 (C–O) and C 3(C=O) are the predominant linkage in cellulose and holocellulose was rich in C 2 and O 2.[322-324] The binding energy for C1s peak centers around 284 eV and gradually decreases from C4 to C1. The O1s peaks for hard and softwoods also deconvoluted into three categories as O 1(C=O), O2 (C–O) and O3 (O=C-OR). The O1 is mainly due to oxygen in lignin, while O2 arises primarily from oxygen in carbohydrates. Also, both O_1 and O_2 were present in the pseudo lignin. Table S1 shows the chemical compositions at the surface of the soft and hardwoods before and after pretreatment. After pretreatment, a general decreasing of C1 and an increasing of C2 to C4 were observed. The O/C ratio and C 1 has been shown to be proportional to each other. A high O/C ratio reflects higher cellulose content, while a lower value suggests the presence of more lignin.[325] Both soft and hardwood the decrease in C 1 and increase in O/C after pretreatment clearly indicated the removal of lignin after pretreatment. The decrease in O 2 in both hard and softwoods indicates the removal of hemicellulose after pretreatment which are inconformity with the

IR results discussed in the appropriate section. The increase in C=O bonds and decrease in C-O bonds after pretreatment partially ascribed to -OH oxidation and cleavage of the β-O-4 linkages in lignin structure.[62] The C-O and C=O bonds increased and C=C bond (or C-C) decreased after the pretreatment may also be assumed due to the oxidation of C-C (or C=C) bonds on the surface to C-O and C=O bonds by $FeCl_3/NaNO_3$.

During the pretreatment lignin was removed from the wood samples. The monomers formed during the pretreatment can be seen from the HPLC chromatogram for hard and softwood samples as shown in Figure 7.12of appendix. For both hard and softwoods at 100 ^oC the formation of phenolic monomers is prominent but as the temperature increased to 150 ^oC the intensity of the peaks decreases which may be due to further degradation of phenolics to CO_2 gases.

The lignin removed after pretreatment was also analyzed for molecular weight by using a derivatization method to form acetylated lignin after recovered by precipitation from the pretreated liquor as described in the materials section. The molecular weight of lignin present in hard and softwoods influence the recalcitrance and the valorization of lignin for biorefinery concept. The molecular weight of lignin after pretreatment depends on the source and isolation and purification procedures employed. Pretreatment alters the molecular weight of lignin in the biomass which contribute to the reduction of recalcitrance.[326, 327]

Table 7.2 Molecular weights of hard and softwood recovered lignins after pretreatment

	Peak 1			Peak 2		
	M_n (Da)	M_w (Da)	PDI	M_n (Da)	M_w (Da)	PDI
Softwood	644	688	1.04	185	197	1.06
Hardwood	925	945	1.03	228	250	1.10
Spruce alkali lignin[328]	3301	12007	3.64	-	-	-
Birch alkali lignin[328]	3086	12274	3.98	-	-	-
Spruce organosolv lignin[328]	846	2226	2.6	-	-	-
Birch organosolv lignin[328]	937	2150	2.3	-	-	-
*Eucalyptus pellita*Kraft-AQ pulping lignin[329]	492	493	1.0	-	-	-
Softwood kraft lignin[330]	1100	1680	1.5	-	-	-
Oil palm lignin[331]	1263	874	1.44	-	-	-

The GPC chromatogram for recovered hard and softwood lignins after pretreatment are shown in Figure 7.10 in appendix. The number average molecular weight (Mn), weight average molecular weight (Mw), and polydispersity index (D) of two peaks for pretreated hard and softwood recovered lignin samples along with comparisons of lignin from different sources are shown in Table 2. The molecular weights of softwood lignin (M_n=644 Da, 185 Da, M_w=688 Da, 197 Da) were low as compared to the hardwood (M_n=925 Da, 228 Da, M_w=945 Da, 250 Da). From the table we can see that for both hard and softwood lignin samples have relatively small molecular weight lignin with limited polydispersity. The low polydispersity index indicates relatively narrow molecular weight distributions.[331] The low molecular weight compounds in the pretreated liquor clearly show the effectiveness of the pretreatment process which depolymerizes high molecular weight lignins into monomeric, dimeric and or oligomeric lignin species. During the pretreatment, the solvent could contact into the plant cell wall and break the linkages between them. This caused lignin to separate from cellulose and hemicelluloses. Moreover, due to the partial cleavage of β-O-4 linkages of lignin contributed to the production of low molecular weight lignin fractions[332] The association of carbohydrate with lignin contributes to a high molar mass of the extracted lignins whereas low molecular weight indicates small molecules of lignin[333]

The properties analysis of untreated and pretreated woods demonstrated the catalytic effectiveness of the proposed $FeCl_3/NaNO_3/O_2$ system on wood chips pretreatment. Consequently, it further promoted the hydrolysis process to get a high glucose yield.

7.4Conclusion

A novel low temperature pretreatment method for hard and softwoods by $FeCl_3/NaNO_3$ in presence of O_2 was presented. The structural changes and functional groups during pretreatment for hard and softwoods were well characterized by FTIR, XRD, SEM, and XPS. The $FeCl_3/NaNO_3$ catalyst system showed the ability to pretreat hardwoods and softwoods chips directly and effectively at low temperature by reducing the cellulose degree of polymerization, removing lignin and reducing recalcitrance offered by biomass which resulted in cellulose that easily assimilated by enzymes. Though it is very difficult to estimate all the factors responsible for better sugar recovery due to the modification of complex biomass structures after pretreatment by reported ion pairs it provides the working mechanism and understanding the structural changes of hard and softwoods during the process at a glance.

7.5Appendix

Photographs and microscopic image of untreated and pretreated softwood samples

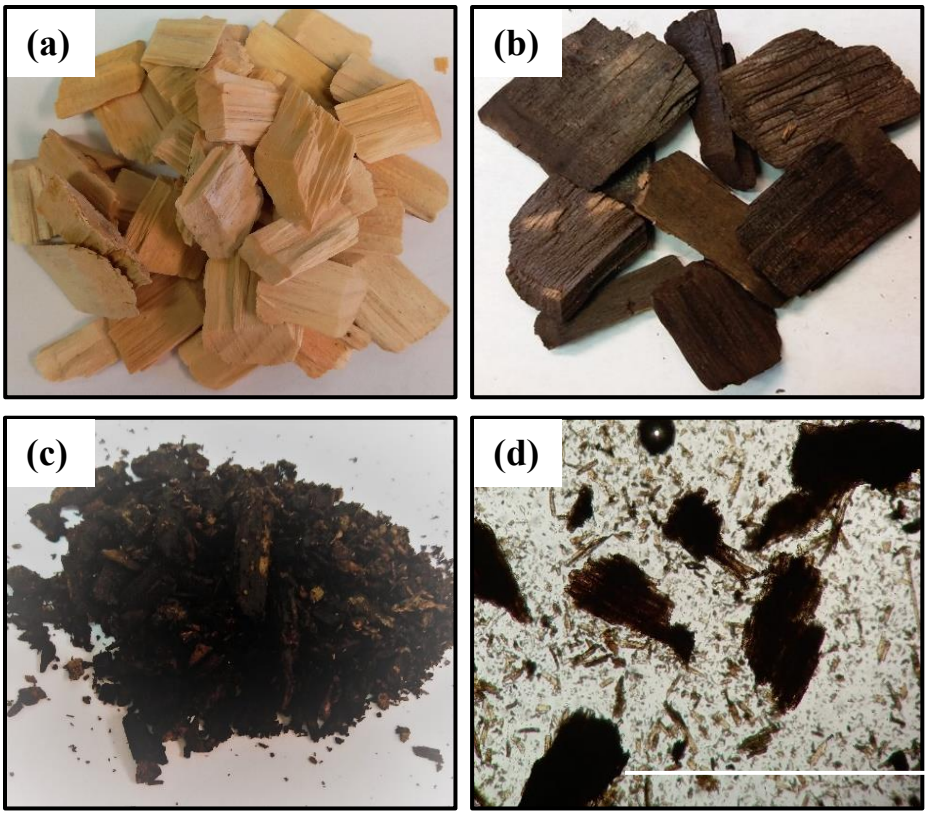

Figure 7.10 Photos of softwood: (a) untreated softwood; (b) softwood treated in water at 100 ^{o}C for 2 hours; (c) pretreated softwood in $FeCl_3/NaNO_3/O_2$ at 100 ^{o}C for 2 hours; (d) optical microscopic image of pretreated softwood in $FeCl_3/NaNO_3/O_2$. The scale bar of microscopic view is 0.1 mm.

Components analysis of the pretreatment solutions of softwood and hardwood by HPLC

Analytical HPLC was performed with a Zorbax 300SB-C18 column, 150 mm x 4.6 mm, 5 μm; flow = 0.4 mL/min; eluents H_2O (A) (0.1% TFA), MeCN (B) (0.1% TFA). A gradient method was used in which the percentage of B was allowed to increase from 0 % to 10 % in 1 minute, from 10 % to 20 % over 20 minutes, then 20 % to 100 % over next 14 minutes. The column was finally equilibrated back to 0 % B and washed thoroughly

between sample injections. Peaks in the range of 15-27.4 min represent the mono-aromatic compounds and peaks in the ranges of 32.5-37.5 are the dimeric and trimeric aromatic compounds.[60]

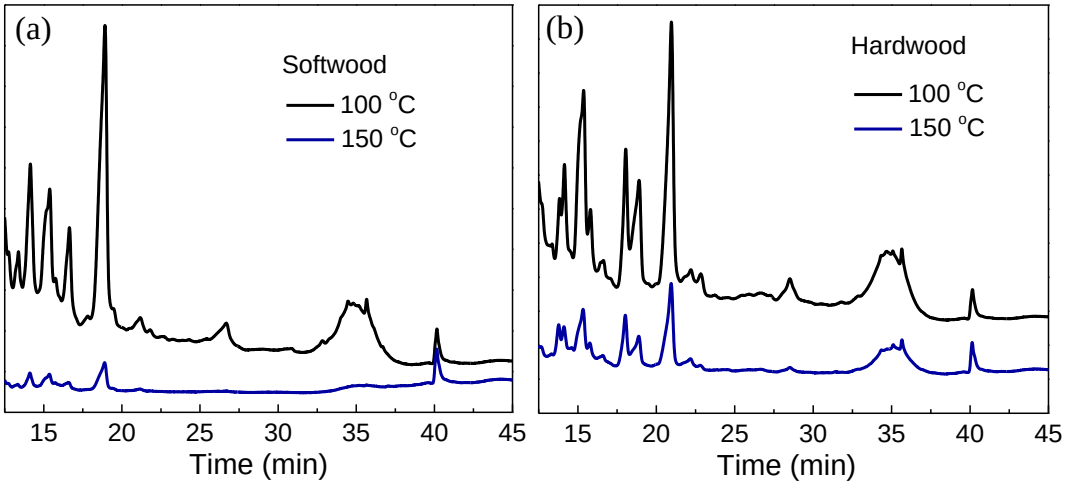

Figure7.11 HPLC of the pretreatment solutions of softwood (a) and hardwood (b) under 100 °C and 150 °C

Molecular weights of hard and soft wood recovered lignins after pretreatment

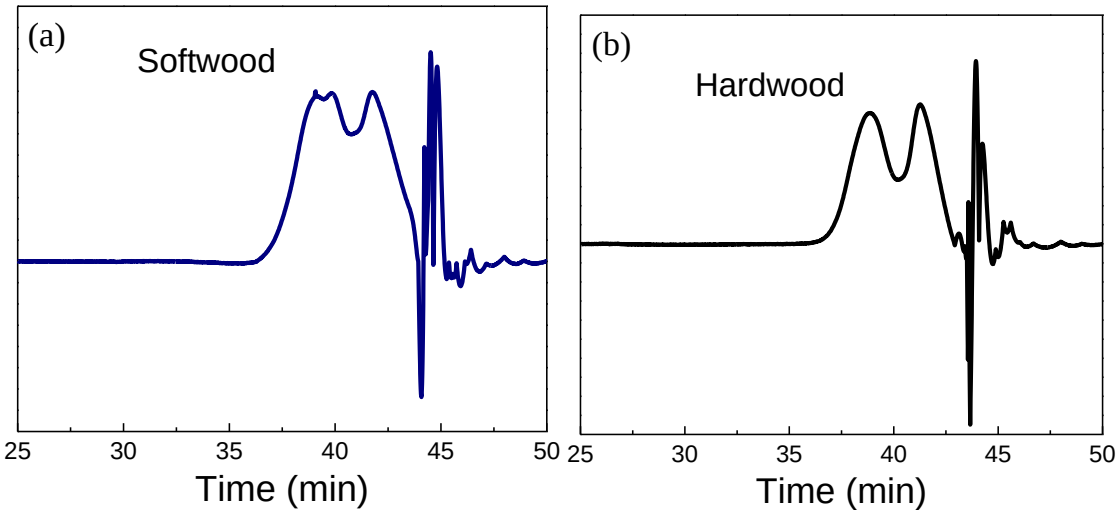

Figure 7.12 GPC chromatogram of lignin segments from softwood (a) and hardwood (b) pretreatment process

XPS for softwood

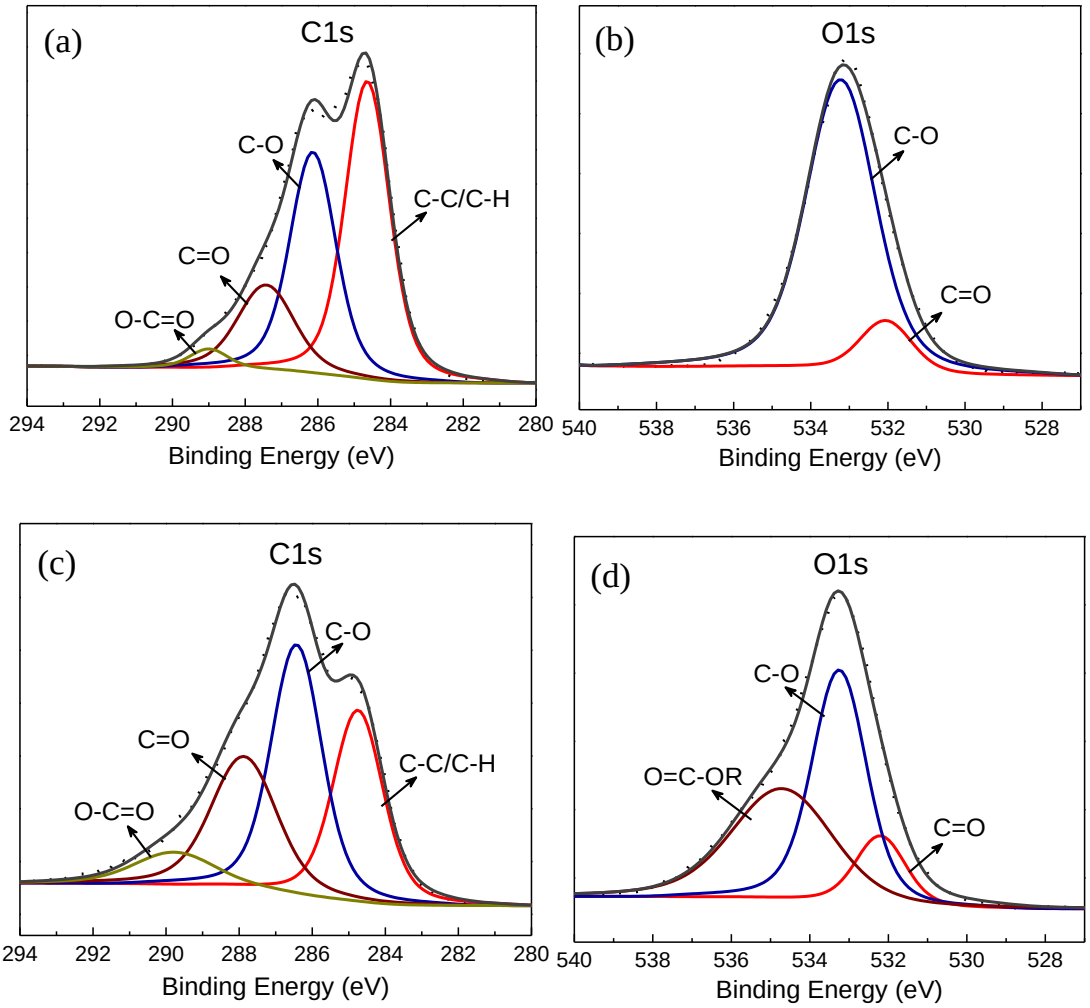

Figure 7.13 XPS spectra of softwood samples before and after pretreatment: (a) C 1s scan for raw softwood; (b) O 1s scan for raw softwood; (c) C 1s scan for pretreated softwood; (d) O 1s for pretreated softwood

Table 7.3 Comparison of chemical compositions at the surface of the soft and hardwoods before and after pretreatment

Samples	C1 (C–C/C–H)	C2 (C–O)	C3 (C=O)	C4 (O–C=O)	O1 (C=O)	O2 (C-O)	O3 (O=C-O)	O/C
Softwood	46	35	16	3	12	88	--	0.35
Pretreated softwood	28	38	26	8	13	46	41	0.49
Hardwood	40	45	12	3	9	91	--	0.38
Pretreated hardwood	27	43	24	6	3	73	24	0.49

Calibration curve of glucose concentration

The calibration curve was made based on the NREL standard method.[334] Precisely, from a stock solution of anhydrous glucose (10mg/ml) four different solutions concentration ranging from 0.3 mg/ml to 6.7 mg/ml were made by diluting with citrate buffer of pH 4.8. Incubate all the solutions at 50 ^{o}C with blank for 60 min and added 3 ml of DNS solution to each. Boil the solutions vigorously in water bath for 5 mins and cooled to room temperature. The absorbance of the solutions was measured at 540 nm in a UV-Vis spectrophotometer.

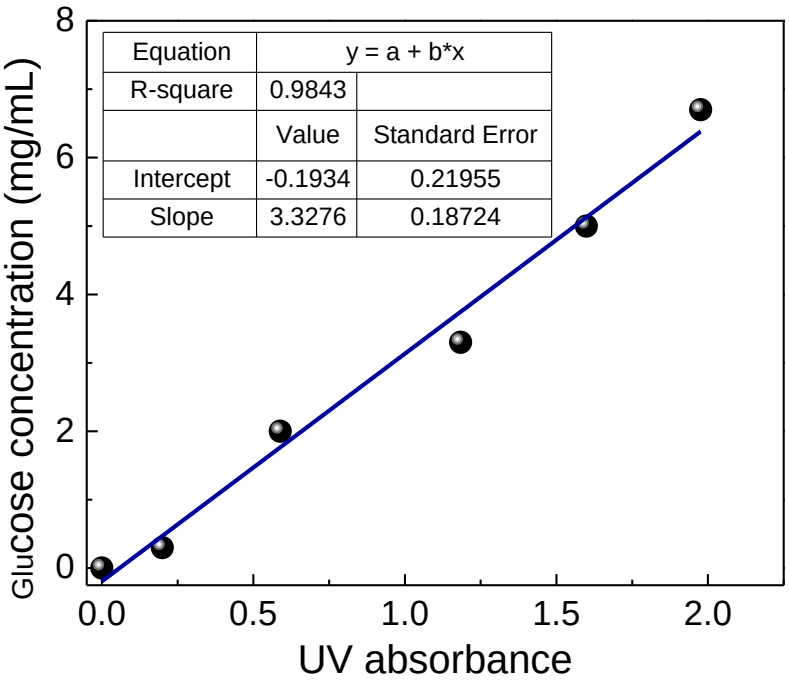

Figure 7.14 Calibration curve of glucose concentration

Effect of catalyst amount and pretreatment time on glucose yield (softwood)

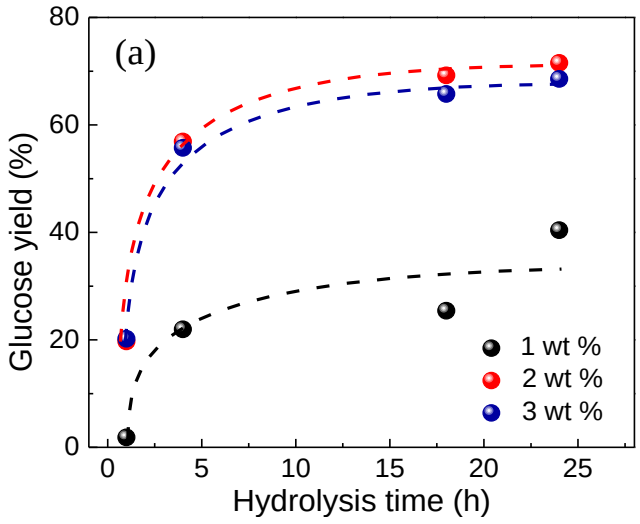

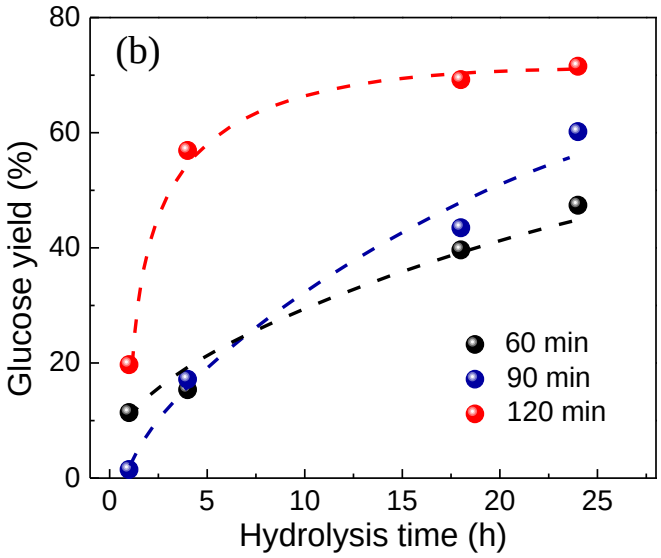

Figure 7.15 Effect of catalyst amount (a) and pretreatment time (b) on glucose yield (softwood)

Experimental diagram for pretreatment and hydrolysis of wood chips

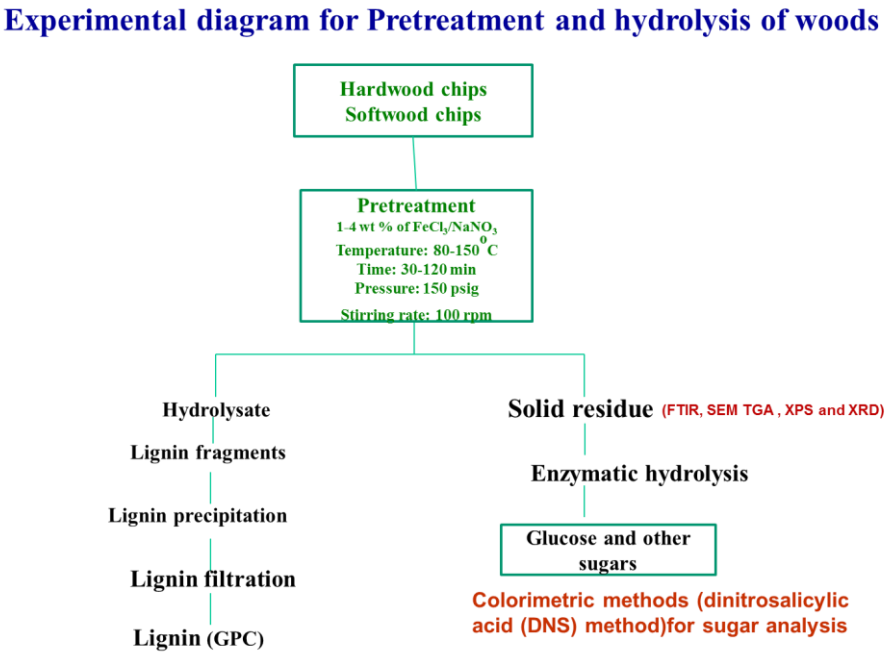

Figure 7.16 Total experimental plan

CHAPTER VIII

OVERALL CONCLUSIONS AND RECOMMENDATIONS

8.1 Conclusions

With the increasing attention toward “green”, the utilization of renewable compounds has attracted strong interest to promote sustainability for the existing current industry and to save the limited reserves of fossil fuel resources. Burning lignin directly for heating without further utilization is a great waste of natural sources due to its huge annual production and extensive potential applications. In this dissertation, the lignin valorization through modification and degradation into composites and chemicals is explored. We modified lignin to overcome the challenge of structure uncertainty to prepare lignin-based surfactant and more sustainable composites. Besides, we designed a new catalytic system to degrade lignin in order to obtain aromatic compounds. Briefly, some conclusions could be summarized as below:

In the first part of this research, a bio-based surfactant was prepared by chemical modification of kraft lignin. Grafting of BA, MPS and BIBB onto kraft lignin were conducted to change its amphiphilicity. The lignin modified with MPS and BIBB was only partially dissolved in organic monomers due to the low grafting ratio. In contrast, over 95% of the hydroxyl group conversion was achieved when BA was used. The BA modified lignin (lignin-B) was found to be completely soluble in the monomers. The interfacial tension measurement indicated the capability of lignin-B to decrease the interface energy between water and styrene dramatically. As the result, a stable water-in-oil emulsion was achieved using lignin-B as the emulsifier and was kept stable over 30

days. These results suggest that lignin has a promising potential to be used as a bio-based surfactant.

The concept of "green" composites has drawn great attentions due to the global environmental issues and the attempt to reduce dependency on fossil fuels resources. In the second part of this research, the composites of lignin and polymer are prepared successfully through bulk polymerization and high internal phase emulsions (HIPEs) polymerization, where lignin serves both as one composite component to substitute traditional polymers and also as fillers to enhance the mechanical properties. The kraft lignin is modified first to increase the compatibility with both monomer and polymer, which is further studied and verified through Hassan Solubility Parameter model. Furthermore, the thermal, mechanical and structural properties of the lignin/polymer composites are studied in detail. The addition of lignin in the composites will increase its modulus and won't affect its glass transition temperature much. The lignin content in the foams can reach 10 wt % of the total substrate to maintain good porous structure and mechanical properties.

Lignin is the only natural aromatic macromolecular feedstock of large production and therefore, is supposed to be good sources of sustainable aromatic chemicals. However, most of the degradation processes suffer from low reactions kinetics and harsh conditions. In this part, a low temperature oxidative degradation of lignin to form vanillic compounds by using $FeCl_3/NaNO_3/O_2$ as catalyst under mild conditions was offered. The addition of $NaNO_3$ serves as a bridge between oxygen (gaseous phase) and iron salts (liquid phase) to improve the re-oxidation rate of Fe^{2+} and thus promote the overall degradation rate. Besides, we found this catalyst system was also effective in the biomass

pretreatment. Pretreatment of lignocellulosic biomass especially for softwoods and hardwoods play the vital role to remove the recalcitrance offered by lignin and hemicellulose for conversion of cellulose to soluble sugar. The pretreatment experiments were systematically conducted to identify optimum conditions for effective enzymatic hydrolysis of soft and hard wood chips. A conversion of 71.53% and 70.66% of cellulose was obtained for hard and softwood samples; pretreated by using 2wt% and 3 wt% of the catalyst respectively. The results of our study make the conclusion that $FeCl_3/NaNO_3$ can be used for pretreatment in the production of soluble sugar for successive production of ethanol.

8.2 Recommendations for future work

In the research of lignin-based surfactant, reaction conditions can be optimized via experimental parameters, like water content, PH value and temperature to increase the grafting extents of MPS and BIBB onto lignin. Besides, future attentions could focus on developing new modification approaches by grafting different chemicals. To the best of our knowledge, most of the lignin-based surfactants are water soluble and very few researches focused on dissolving lignin in organic phase. Therefore, exploring new chemicals to modify lignin should be a promising direction.

In the part of lignin-polymer composites, it is meaningful to study the styrene polymerization kinetics when lignin is added into the system. Lignin contains various kinds of functional groups, including aromatic –OH groups, which may serve as the inhibitor of free radicals. While most of the phenolic –OH groups are converted into ester groups during the modification process, there are still some parts left. Thus it is necessary

to investigate the effect of lignin on polymerization kinetics. Besides, the lignin content in the porous foam was 10 wt %, which might be improved by finding new modification approach to further enhance the compatibility between lignin and polymers.

In the part of lignin degradation, $FeCl_3/NaNO_3/O_2$was demonstrated to be effective to degrade lignin into aromatics under mild conditions; however, the mechanism and catalyst recyclability should be further studied in detail. The compounds in the solutions after degradation are supposed to be investigated and analyzed through NMR and GC-MS.

Besides, as mentioned in Chapter 2, the most desired products from lignin degradation are supposed to be benzene, toluene and xylene, which are the building blocks of other aromatic compounds. However, most chemicals from lignin oxidation process possess some extent of oxygenation. Therefore, it is meaningful to seek the catalyst system that can degrade lignin effectively by reduction. Anthroquinone (AQ) has been demonstrated to be effective to promote the delignification in the traditional pulp and paper industry. Thus lignin degradation into aromatics by reduction reaction with AQ/formaldehyde is proposed to be a good direction in the following steps.

REFERENCES

1. Mu, W.; Ben, H.; Ragauskas, A.; Deng, Y., Lignin Pyrolysis Components and Upgrading—Technology Review. *BioEnergy Research* **2013,** 6, (4), 1183-1204.

2. Ragauskas, A. J.; Williams, C. K.; Davison, B. H.; Britovsek, G.; Cairney, J.; Eckert, C. A.; Frederick, W. J.; Hallett, J. P.; Leak, D. J.; Liotta, C. L.; Mielenz, J. R.; Murphy, R.; Templer, R.; Tschaplinski, T., The Path Forward for Biofuels and Biomaterials. *Science* **2006,** 311, (5760), 484-489.

3. Beer, C.; Reichstein, M.; Tomelleri, E.; Ciais, P.; Jung, M.; Carvalhais, N.; Rödenbeck, C.; Arain, M. A.; Baldocchi, D.; Bonan, G. B., Terrestrial gross carbon dioxide uptake: global distribution and covariation with climate. *Science* **2010,** 329, (5993), 834-838.

4. Graham-Rowe, D., Agriculture: Beyond food versus fuel. *Nature* **2011,** 474, (7352), S6-S8.

5. Robbins, M., Policy: fuelling politics. *Nature* **2011,** 474, (7352), S22-S24.

6. Lanzafame, P.; Centi, G.; Perathoner, S., Catalysis for biomass and CO 2 use through solar energy: opening new scenarios for a sustainable and low-carbon chemical production. *Chemical Society Reviews* **2014,** 43, (22), 7562-7580.

7. Luterbacher, J.; Alonso, D. M.; Dumesic, J., Targeted chemical upgrading of lignocellulosic biomass to platform molecules. *Green Chemistry* **2014,** 16, (12), 4816-4838.

8. Perlack, R. D.; Eaton, L. M.; Turhollow Jr, A. F.; Langholtz, M. H.; Brandt, C. C.; Downing, M. E.; Graham, R. L.; Wright, L. L.; Kavkewitz, J. M.; Shamey, A. M., US billion-ton update: biomass supply for a bioenergy and bioproducts industry. **2011**.

9. Nonhebel, S., Renewable energy and food supply: will there be enough land? *Renewable and Sustainable Energy Reviews* **2005,** 9, (2), 191-201.

10. Ragauskas, A. J.; Beckham, G. T.; Biddy, M. J.; Chandra, R.; Chen, F.; Davis, M. F.; Davison, B. H.; Dixon, R. A.; Gilna, P.; Keller, M., Lignin valorization: improving lignin processing in the biorefinery. *Science* **2014,** 344, (6185), 1246843.

11. Faaij, A. P., Bio-energy in Europe: changing technology choices. *Energy policy* **2006,** 34, (3), 322-342.

12. Lane, J., Beta renewables: Biofuels digest's 2014 5-minute guide. *Biofuels Digest* **2014**.

13. Lovins, A. B.; Aranow, B., Winning the Oil Endgame-Innovation for Profits. *Jobs, and Security, Rocky Mountain Institute, Colorado* **2005**.

14. Auras, R.; Harte, B.; Selke, S., An overview of polylactides as packaging materials. *Macromolecular bioscience* **2004,** 4, (9), 835-864.

15. Perlack, R. D.; Wright, L. L.; Turhollow, A. F.; Graham, R. L.; Stokes, B. J.; Erbach, D. C. *Biomass as feedstock for a bioenergy and bioproducts industry: the technical feasibility of a billion-ton annual supply*; DTIC Document: 2005.

16. Sannigrahi, P.; Ragauskas, A. J., Characterization of fermentation residues from the production of bio-ethanol from lignocellulosic feedstocks. *Journal of Biobased Materials and Bioenergy* **2011,** 5, (4), 514-519.

17. Stewart, D., Lignin as a base material for materials applications: Chemistry, application and economics. *Ind. Crop. Prod.* **2008,** 27, (2), 202-207.

18. Langholtz, M.; Downing, M.; Graham, R.; Baker, F.; Compere, A.; Griffith, W.; Boeman, R.; Keller, M., Lignin-derived carbon fiber as a co-product of refining cellulosic

biomass. *SAE International Journal of Materials and Manufacturing* **2014,** 7, (2013-01-9092), 115-121.

19. Azadi, P.; Inderwildi, O. R.; Farnood, R.; King, D. A., Liquid fuels, hydrogen and chemicals from lignin: A critical review. *Renew. Sust. Energ. Rev.* **2013,** 21, 506-523.

20. Baker, D. A.; Rials, T. G., Recent advances in low-cost carbon fiber manufacture from lignin. *J. Appl. Polym. Sci.* **2013,** 130, (2), 713-728.

21. Peng, C.; Zhang, G.; Yue, J.; Xu, G., Pyrolysis of lignin for phenols with alkaline additive. *Fuel Processing Technology* **2014,** 124, 212-221.

22. Tuck, C. O.; Pérez, E.; Horváth, I. T.; Sheldon, R. A.; Poliakoff, M., Valorization of biomass: deriving more value from waste. *Science* **2012,** 337, (6095), 695-699.

23. van Haveren, J.; Scott, E. L.; Sanders, J., Bulk chemicals from biomass. *Biofuels Bioprod. Biorefining* **2008,** 2, (1), 41-57.

24. Gupta, C.; Washburn, N. R., Polymer-Grafted Lignin Surfactants Prepared via Reversible Addition–Fragmentation Chain-Transfer Polymerization. *Langmuir* **2014,** 30, (31), 9303-9312.

25. Zhang, Z.; Zhang, Y.; Lin, Z.; Mulyadi, A.; Mu, W.; Deng, Y., Butyric anhydride modified lignin and its oil-water interfacial properties. *Chemical Engineering Science* **2017,** 165, 55-64.

26. Upton, B. M.; Kasko, A. M., Strategies for the Conversion of Lignin to High-Value Polymeric Materials: Review and Perspective. *Chem. Rev.* **2016,** 116, (4), 2275-2306.

27. Rubin, E. M., Genomics of cellulosic biofuels. *Nature* **2008,** 454, (7206), 841-845.

28. Sjostrom, E., *Wood chemistry: fundamentals and applications*. Elsevier: 2013.

29. Zhang, X.; Lei, H.; Chen, S.; Wu, J., Catalytic co-pyrolysis of lignocellulosic biomass with polymers: a critical review. *Green Chemistry* **2016,** 18, (15), 4145-4169.

30. Habibi, Y.; Lucia, L. A.; Rojas, O. J., Cellulose nanocrystals: chemistry, self-assembly, and applications. *Chem. Rev.* **2010,** 110, (6), 3479-3500.

31. van Wyk, J. P. H., Biotechnology and the utilization of biowaste as a resource for bioproduct development. *Trends in Biotechnology* **2001,** 19, (5), 172-177.

32. de Souza Lima, M. M.; Borsali, R., Rodlike cellulose microcrystals: structure, properties, and applications. *Macromolecular Rapid Communications* **2004,** 25, (7), 771-787.

33. Zhu, H.; Luo, W.; Ciesielski, P. N.; Fang, Z.; Zhu, J.; Henriksson, G.; Himmel, M. E.; Hu, L., Wood-derived materials for green electronics, biological devices, and energy applications. *Chem. Rev.* **2016,** 116, (16), 9305-9374.

34. Payen, A., Mémoire sur la composition du tissu propre des plantes et du ligneux. *Comptes rendus* **1838,** 7, 1052-1056.

35. Gray, H. L.; Staud, C. J., Recent Advances in Cellulose and Starch Chemistry. *Chem. Rev.* **1928,** 4, (4), 355-373.

36. David, K.; Ragauskas, A. J., Switchgrass as an energy crop for biofuel production: a review of its ligno-cellulosic chemical properties. *Energy & Environmental Science* **2010,** 3, (9), 1182-1190.

37. Monomers, P., Composites from Renewable Resources, ed. MN Belgacem and A. Gandini. In Elsevier, Amsterdam: 2008.

38. Mäki-Arvela, P.; Salmi, T.; Holmbom, B.; Willför, S.; Murzin, D. Y., Synthesis of Sugars by Hydrolysis of Hemicelluloses- A Review. *Chem. Rev.* **2011,** 111, (9), 5638-5666.

39. Sjöström, E., Puukemia (Forest chemistry). In Otakustantamo: Espoo, Finland: 1978.

40. Laine, C., *Structures of hemicelluloses and pectins in wood and pulp*. Helsinki University of Technology: 2005.

41. Um, B.-H.; van Walsum, G. P., Acid hydrolysis of hemicellulose in green liquor pre-pulping extract of mixed northern hardwoods. *Applied biochemistry and biotechnology* **2009,** 153, (1-3), 127.

42. Weng, J. K.; Chapple, C., The origin and evolution of lignin biosynthesis. *New Phytologist* **2010,** 187, (2), 273-285.

43. Vanholme, R.; Demedts, B.; Morreel, K.; Ralph, J.; Boerjan, W., Lignin Biosynthesis and Structure. *Plant Physiology* **2010,** 153, (3), 895-905.

44. Davin, L. B.; Lewis, N. G., Lignin primary structures and dirigent sites. *Current opinion in biotechnology* **2005,** 16, (4), 407-415.

45. Dorrestijn, E.; Laarhoven, L. J.; Arends, I. W.; Mulder, P., The occurrence and reactivity of phenoxyl linkages in lignin and low rank coal. *Journal of Analytical and Applied Pyrolysis* **2000,** 54, (1), 153-192.

46. Lin, S. Y.; Dence, C. W., *Methods in lignin chemistry / Stephen Y. Lin, Carlton W. Dence (eds.)*. Berlin ; New York : Springer-Verlag, c1992.: 1992.

47. Chakar, F. S.; Ragauskas, A. J., Review of current and future softwood kraft lignin process chemistry. *Ind. Crop. Prod.* **2004,** 20, (2), 131-141.

48. Zakzeski, J.; Bruijnincx, P. C. A.; Jongerius, A. L.; Weckhuysen, B. M., The Catalytic Valorization of Lignin for the Production of Renewable Chemicals. *Chem. Rev.* **2010,** 110, (6), 3552-3599.

49. Lange, H.; Decina, S.; Crestini, C., Oxidative upgrade of lignin – Recent routes reviewed. *Eur. Polym. J.* **2013,** 49, (6), 1151-1173.

50. Kumar, C. R.; Anand, N.; Kloekhorst, A.; Cannilla, C.; Bonura, G.; Frusteri, F.; Barta, K.; Heeres, H. J., Solvent free depolymerization of Kraft lignin to alkyl-phenolics using supported NiMo and CoMo catalysts. *Green Chemistry* **2015,** 17, (11), 4921-4930.

51. Thielemans, W.; Wool, R. P., Lignin esters for use in unsaturated thermosets: Lignin modification and solubility modeling. *Biomacromolecules* **2005,** 6, (4), 1895-1905.

52. Saito, T.; Brown, R. H.; Hunt, M. A.; Pickel, D. L.; Pickel, J. M.; Messman, J. M.; Baker, F. S.; Keller, M.; Naskar, A. K., Turning renewable resources into value-added polymer: development of lignin-based thermoplastic. *Green Chemistry* **2012,** 14, (12), 3295-3303.

53. Bouxin, F. P.; McVeigh, A.; Tran, F.; Westwood, N. J.; Jarvis, M. C.; Jackson, S. D., Catalytic depolymerisation of isolated lignins to fine chemicals using a Pt/alumina catalyst: part 1—impact of the lignin structure. *Green Chemistry* **2015,** 17, (2), 1235-1242.

54. Chen, F.; Tobimatsu, Y.; Havkin-Frenkel, D.; Dixon, R. A.; Ralph, J., A polymer of caffeyl alcohol in plant seeds. *Proceedings of the National Academy of Sciences* **2012,** 109, (5), 1772-1777.

55. Wunderlich, B.; Bodily, D. M.; Kaplan, M. H., Theory and Measurements of the Glass-Transformation Interval of Polystyrene. *J Appl Phys* **1964,** 35, (1), 95-102.

56. Ujihara, M.; Nakatsubo, F.; Katahira, R., A novel selective cleavage method for β-O-4 substructure in lignins named TIZ method. I. Degradation of guaiacyl and syringyl models. *Journal of wood chemistry and technology* **2003,** 23, (1), 71-87.

57. Lee, R. A.; Bédard, C.; Berberi, V.; Beauchet, R.; Lavoie, J.-M., UV–Vis as quantification tool for solubilized lignin following a single-shot steam process. *Bioresource technology* **2013,** 144, 658-663.

58. Rahimi, A.; Azarpira, A.; Kim, H.; Ralph, J.; Stahl, S. S., Chemoselective metal-free aerobic alcohol oxidation in lignin. *Journal of the American Chemical Society* **2013,** 135, (17), 6415-6418.

59. Brebu, M.; Vasile, C., Thermal degradation of lignin—a review. *Cellulose Chemistry & Technology* **2010,** 44, (9), 353.

60. Rahimi, A.; Ulbrich, A.; Coon, J. J.; Stahl, S. S., Formic-acid-induced depolymerization of oxidized lignin to aromatics. *Nature* **2014,** 515, (7526), 249-252.

61. Shuai, L.; Amiri, M. T.; Questell-Santiago, Y. M.; Héroguel, F.; Li, Y.; Kim, H.; Meilan, R.; Chapple, C.; Ralph, J.; Luterbacher, J. S., Formaldehyde stabilization facilitates lignin monomer production during biomass depolymerization. *Science* **2016,** 354, (6310), 329-333.

62. Du, X.; Liu, W.; Zhang, Z.; Mulyadi, A.; Brittain, A.; Gong, J.; Deng, Y., Low-Energy Catalytic Electrolysis for Simultaneous Hydrogen Evolution and Lignin Depolymerization. *ChemSusChem* **2017,** 10, (5), 847-854.

63. Pu, Y.; Kosa, M.; Kalluri, U. C.; Tuskan, G. A.; Ragauskas, A. J., Challenges of the utilization of wood polymers: how can they be overcome? *Applied microbiology and biotechnology* **2011,** 91, (6), 1525.

64. Capanema, E. A.; Balakshin, M. Y.; Kadla, J. F., A comprehensive approach for quantitative lignin characterization by NMR spectroscopy. *Journal of agricultural and food chemistry* **2004,** 52, (7), 1850-1860.

65. Pu, Y.; Cao, S.; Ragauskas, A. J., Application of quantitative 31P NMR in biomass lignin and biofuel precursors characterization. *Energy & Environmental Science* **2011,** 4, (9), 3154-3166.

66. Mullen, C. A.; Strahan, G. D.; Boateng, A. A., Characterization of various fast-pyrolysis bio-oils by NMR spectroscopy. *Energy Fuels* **2009,** 23, (5), 2707-2718.

67. Özbay, N.; Uzun, B. B.; Varol, E. A.; Pütün, A. E., Comparative analysis of pyrolysis oils and its subfractions under different atmospheric conditions. *Fuel processing technology* **2006,** 87, (11), 1013-1019.

68. Froass, P. M.; Ragauskas, A. J.; Jiang, J. E., NMR studies Part 3: Analysis of lignins from modern kraft pulping technologies. *Holzforschung-International Journal of the Biology, Chemistry, Physics and Technology of Wood* **1998,** 52, (4), 385-390.

69. Baptista, C.; Robert, D.; Duarte, A., Relationship between lignin structure and delignification degree in Pinus pinaster kraft pulps. *Bioresource technology* **2008,** 99, (7), 2349-2356.

70. Ben, H. X.; Ragauskas, A. J., NMR Characterization of Pyrolysis Oils from Kraft Lignin. *Energy Fuels* **2011,** 25, (5), 2322-2332.

71. Pu, Y. Q.; Ragauskas, A. J., Structural analysis of acetylated hardwood lignins and their photoyellowing properties. *Can. J. Chem.-Rev. Can. Chim.* **2005,** 83, (12), 2132-2139.

72. Sannigrahi, P.; Ragauskas, A. J.; Miller, S. J., Lignin Structural Modifications Resulting from Ethanol Organosolv Treatment of Loblolly Pine. *Energy Fuels* **2010,** 24, 683-689.

73. Nagy, M.; Kosa, M.; Theliander, H.; Ragauskas, A. J., Characterization of CO2 precipitated Kraft lignin to promote its utilization. *Green Chemistry* **2010,** 12, (1), 31-34.

74. Ben, H.; Ragauskas, A. J., NMR characterization of pyrolysis oils from kraft lignin. *Energy Fuels* **2011,** 25, (5), 2322-2332.

75. Heikkinen, S.; Toikka, M. M.; Karhunen, P. T.; Kilpeläinen, I. A., Quantitative 2D HSQC (Q-HSQC) via suppression of J-dependence of polarization transfer in NMR spectroscopy: application to wood lignin. *Journal of the American Chemical Society* **2003,** 125, (14), 4362-4367.

76. Liitiä, T. M.; Maunu, S. L.; Hortling, B.; Toikka, M.; Kilpeläinen, I., Analysis of technical lignins by two-and three-dimensional NMR spectroscopy. *Journal of agricultural and food chemistry* **2003,** 51, (8), 2136-2143.

77. Capanema, E. A.; Balakshin, M. Y.; Chen, C.-L.; Gratzl, J. S.; Gracz, H., Structural analysis of residual and technical lignins by 1H-13C correlation 2D NMR-spectroscopy. *Holzforschung* **2001,** 55, (3), 302-308.

78. Phillips, M., The Chemistry of Lignin. *Chem. Rev.* **1934,** 14, (1), 103-170.

79. Kai, D.; Tan, M. J.; Chee, P. L.; Chua, Y. K.; Yap, Y. L.; Loh, X. J., Towards lignin-based functional materials in a sustainable world. *Green Chemistry* **2016,** 18, (5), 1175-1200.

80. Gellerstedt, G.; Lindfors, E.-L., Structural changes in lignin during kraft pulping. *Holzforschung-International Journal of the Biology, Chemistry, Physics and Technology of Wood* **1984,** 38, (3), 151-158.

81. Smook, G. A.; Kocurek, M. J., *Handbook for pulp & paper technologists*. TAPPI; Canadian Pulp and Paper Association: 1982.

82. Sen, S.; Patil, S.; Argyropoulos, D. S., Thermal properties of lignin in copolymers, blends, and composites: a review. *Green Chemistry* **2015,** 17, (11), 4862-4887.

83. Aniceto, J. P. S.; Portugal, I.; Silva, C. M., Biomass-Based Polyols through Oxypropylation Reaction. *ChemSusChem* **2012,** 5, (8), 1358-1368.

84. Gonçalves, A. R.; Benar, P., Hydroxymethylation and oxidation of Organosolv lignins and utilization of the products. *Bioresource Technology* **2001,** 79, (2), 103-111.

85. Zhang, L.; Huang, J., Effects of hard-segment compositions on properties of polyurethane–nitrolignin films. *J. Appl. Polym. Sci.* **2001,** 81, (13), 3251-3259.

86. Huang, J.; Zhang, L., Effects of NCO/OH molar ratio on structure and properties of graft-interpenetrating polymer networks from polyurethane and nitrolignin. *Polymer* **2002,** 43, (8), 2287-2294.

87. Arend, M.; Westermann, B.; Risch, N., Modern variants of the Mannich reaction. *Angewandte Chemie International Edition* **1998,** 37, (8), 1044-1070.

88. Yue, X.; Chen, F.; Zhou, X., Improved interfacial bonding of PVC/wood-flour composites by lignin amine modification. *BioResources* **2011,** 6, (2), 2022-2044.

89. Du, X.; Li, J.; Lindström, M. E., Modification of industrial softwood kraft lignin using Mannich reaction with and without phenolation pretreatment. *Ind. Crop. Prod.* **2014,** 52, 729-735.

90. Thielemans, W.; Wool, R. P., Lignin Esters for Use in Unsaturated Thermosets: Lignin Modification and Solubility Modeling. *Biomacromolecules* **2005,** 6, (4), 1895-1905.

91. Xiao, B.; Sun, X. F.; Sun, R., The chemical modification of lignins with succinic anhydride in aqueous systems. *Polymer Degradation and Stability* **2001,** 71, (2), 223-231.

92. Thiebaud, S.; Borredon, M. E., Solvent-free wood esterification with fatty acid chlorides. *Bioresource Technology* **1995,** 52, (2), 169-173.

93. Sailaja, R. R. N.; Deepthi, M. V., Mechanical and thermal properties of compatibilized composites of polyethylene and esterified lignin. *Materials & Design* **2010,** 31, (9), 4369-4379.

94. Sadeghifar, H.; Cui, C.; Argyropoulos, D. S., Toward Thermoplastic Lignin Polymers. Part 1. Selective Masking of Phenolic Hydroxyl Groups in Kraft Lignins via Methylation and Oxypropylation Chemistries. *Ind. Eng. Chem. Res.* **2012,** 51, (51), 16713-16720.

95. Wu, L. C. F.; Glasser, W. G., Engineering plastics from lignin. I. Synthesis of hydroxypropyl lignin. *J. Appl. Polym. Sci.* **1984,** 29, (4), 1111-1123.

96. Effendi, A.; Gerhauser, H.; Bridgwater, A. V., Production of renewable phenolic resins by thermochemical conversion of biomass: A review. *Renewable and Sustainable Energy Reviews* **2008,** 12, (8), 2092-2116.

97. Homma, H.; Kubo, S.; Yamada, T.; Koda, K.; Matsushita, Y.; Uraki, Y., Conversion of Technical Lignins to Amphiphilic Derivatives with High Surface Activity. *Journal of Wood Chemistry and Technology* **2010,** 30, (2), 164-174.

98. Zhou, B. W.; Ha, C. Y.; Deng, L. L.; Mo, J. Q.; Sun, C. N.; Shen, M. M., Preparation of Surfactant with the Aid of Ultrasonic Treatment Via Alkylation of Sodium Lignosulfonate. *Acta Polym Sin* **2013**, (11), 1363-1368.

99. Kong, F.; Wang, S.; T. Price, J.; Konduri, M. K. R.; Fatehi, P., Water soluble kraft lignin-acrylic acid copolymer: synthesis and characterization. *Green Chemistry* **2015**.

100. Zhou, M.; Wang, W.; Yang, D.; Qiu, X., Preparation of a new lignin-based anionic/cationic surfactant and its solution behaviour. *RSC Advances* **2015,** 5, (4), 2441-2448.

101. Telysheva, G.; Dizhbite, T.; Paegle, E.; Shapatin, A.; Demidov, I., Surface-active properties of hydrophobized derivatives of lignosulfonates: Effect of structure of organosilicon modifier. *J. Appl. Polym. Sci.* **2001,** 82, (4), 1013-1020.

102. Pang, Y.-X.; Qiu, X.-Q.; Yang, D.-J.; Lou, H.-M., Influence of oxidation, hydroxymethylation and sulfomethylation on the physicochemical properties of calcium lignosulfonate. *Colloids and Surfaces A: Physicochemical and Engineering Aspects* **2008,** 312, (2), 154-159.

103. Norgren, M.; Edlund, H., Lignin: Recent advances and emerging applications. *Current Opinion in Colloid & Interface Science* **2014,** 19, (5), 409-416.

104. Shulga, G.; Shakels, V.; Aniskevicha, O.; Bikova, T.; Treimanis, A., Effect of alkaline modification on viscometric and surface: Active properties of soluble lignin. *Cellulose chemistry and technology* **2006,** 40, (6), 383-392.

105. Aso, T.; Koda, K.; Kubo, S.; Yamada, T.; Nakajima, I.; Uraki, Y., Preparation of novel lignin-based cement dispersants from isolated lignins. *Journal of Wood Chemistry and Technology* **2013,** 33, (4), 286-298.

106. He, W.; Fatehi, P., Preparation of sulfomethylated softwood kraft lignin as a dispersant for cement admixture. *RSC Advances* **2015,** 5, (58), 47031-47039.

107. Wang, J.; Manley, R. S. J.; Feldman, D., Synthetic polymer-lignin copolymers and blends. *Prog. Polym. Sci.* **1992,** 17, (4), 611-646.

108. Reza Barzegari, M.; Alemdar, A.; Zhang, Y.; Rodrigue, D., Mechanical and rheological behavior of highly filled polystyrene with lignin. *Polymer Composites* **2012,** 33, (3), 353-361.

109. Canetti, M.; Bertini, F., Supermolecular structure and thermal properties of poly (ethylene terephthalate)/lignin composites. *Composites Science and Technology* **2007,** 67, (15), 3151-3157.

110. Kadla, J. F.; Kubo, S., Miscibility and hydrogen bonding in blends of poly (ethylene oxide) and kraft lignin. *Macromolecules* **2003,** 36, (20), 7803-7811.

111. Pouteau, C.; Baumberger, S.; Cathala, B.; Dole, P., Lignin–polymer blends: evaluation of compatibility by image analysis. *Comptes rendus biologies* **2004,** 327, (9), 935-943.

112. Maldhure, A. V.; Ekhe, J.; Deenadayalan, E., Mechanical properties of polypropylene blended with esterified and alkylated lignin. *J. Appl. Polym. Sci.* **2012,** 125, (3), 1701-1712.

113. Sailaja, R., Low density polyethylene and grafted lignin polyblends using epoxy-functionalized compatibilizer: mechanical and thermal properties. *Polym. Int.* **2005,** 54, (12), 1589-1598.

114. Sun, Y.; Yang, L.; Lu, X.; He, C., Biodegradable and renewable poly(lactide)-lignin composites: synthesis, interface and toughening mechanism. *Journal of Materials Chemistry A* **2015,** 3, (7), 3699-3709.

115. Teramoto, Y.; Lee, S.-H.; Endo, T., Phase Structure and Mechanical Property of Blends of Organosolv Lignin Alkyl Esters with Poly([epsi]-caprolactone). *Polym. J* **2009,** 41, (3), 219-227.

116. Xiao, S.; Feng, J.; Zhu, J.; Wang, X.; Yi, C.; Su, S., Preparation and characterization of lignin-layered double hydroxide/styrene-butadiene rubber composites. *J. Appl. Polym. Sci.* **2013,** 130, (2), 1308-1312.

117. Pouteau, C.; Dole, P.; Cathala, B.; Averous, L.; Boquillon, N., Antioxidant properties of lignin in polypropylene. *Polymer Degradation and Stability* **2003,** 81, (1), 9-18.

118. Domenek, S.; Louaifi, A.; Guinault, A.; Baumberger, S., Potential of lignins as antioxidant additive in active biodegradable packaging materials. *Journal of Polymers and the Environment* **2013,** 21, (3), 692-701.

119. Pucciariello, R.; Bonini, C.; D'Auria, M.; Villani, V.; Giammarino, G.; Gorrasi, G., Polymer blends of steam-explosion lignin and poly (ε-caprolactone) by high-energy ball milling. *J. Appl. Polym. Sci.* **2008,** 109, (1), 309-313.

120. Kai, D.; Jiang, S.; Low, Z. W.; Loh, X. J., Engineering highly stretchable lignin-based electrospun nanofibers for potential biomedical applications. *Journal of Materials Chemistry B* **2015,** 3, (30), 6194-6204.

121. Wang, S.-X.; Yang, L.; Stubbs, L. P.; Li, X.; He, C., Lignin-derived fused electrospun carbon fibrous mats as high performance anode materials for lithium ion batteries. *ACS applied materials & interfaces* **2013,** 5, (23), 12275-12282.

122. Vanderlaan, M.; Thring, R., Polyurethanes from Alcell® lignin fractions obtained by sequential solvent extraction. *Biomass and bioenergy* **1998,** 14, (5), 525-531.

123. Sarkar, S.; Adhikari, B., Synthesis and characterization of lignin–HTPB copolyurethane. *Eur. Polym. J.* **2001,** 37, (7), 1391-1401.

124. Nakamura, K.; Hatakeyama, T.; Hatakeyama, H., Thermal properties of solvolysis lignin-derived polyurethanes. *Polym. Adv. Technol.* **1992,** 3, (4), 151-155.

125. Saito, T.; Perkins, J. H.; Jackson, D. C.; Trammel, N. E.; Hunt, M. A.; Naskar, A. K., Development of lignin-based polyurethane thermoplastics. *RSC Advances* **2013,** 3, (44), 21832-21840.

126. Kim, Y. S.; Kadla, J. F., Preparation of a Thermoresponsive Lignin-Based Biomaterial through Atom Transfer Radical Polymerization. *Biomacromolecules* **2010,** 11, (4), 981-988.

127. Hilburg, S. L.; Elder, A. N.; Chung, H.; Ferebee, R. L.; Bockstaller, M. R.; Washburn, N. R., A universal route towards thermoplastic lignin composites with improved mechanical properties. *Polymer* **2014,** 55, (4), 995-1003.

128. Chung, Y.-L.; Olsson, J. V.; Li, R. J.; Frank, C. W.; Waymouth, R. M.; Billington, S. L.; Sattely, E. S., A renewable lignin–lactide copolymer and application in biobased composites. *ACS Sustainable Chemistry & Engineering* **2013,** 1, (10), 1231-1238.

129. Panesar, S. S.; Jacob, S.; Misra, M.; Mohanty, A. K., Functionalization of lignin: Fundamental studies on aqueous graft copolymerization with vinyl acetate. *Ind. Crop. Prod.* **2013,** 46, 191-196.

130. Alonso, D. M.; Bond, J. Q.; Dumesic, J. A., Catalytic conversion of biomass to biofuels. *Green Chemistry* **2010,** 12, (9), 1493-1513.

131. Besson, M. l.; Gallezot, P.; Pinel, C., Conversion of biomass into chemicals over metal catalysts. *Chem. Rev.* **2013,** 114, (3), 1827-1870.

132. Lee, S. H.; Doherty, T. V.; Linhardt, R. J.; Dordick, J. S., Ionic liquid-mediated selective extraction of lignin from wood leading to enhanced enzymatic cellulose hydrolysis. *Biotechnology and Bioengineering* **2009,** 102, (5), 1368-1376.

133. McMillan, J. D., Pretreatment of lignocellulosic biomass. In ACS Publications: 1994.

134. Faba, L.; Díaz, E.; Ordóñez, S., Recent developments on the catalytic technologies for the transformation of biomass into biofuels: A patent survey. *Renewable and Sustainable Energy Reviews* **2015,** 51, 273-287.

135. Wyman, C. E., Biomass ethanol: technical progress, opportunities, and commercial challenges. *Annual Review of Energy and the Environment* **1999,** 24, (1), 189-226.

136. Mosier, N.; Wyman, C.; Dale, B.; Elander, R.; Lee, Y.; Holtzapple, M.; Ladisch, M., Features of promising technologies for pretreatment of lignocellulosic biomass. *Bioresource technology* **2005,** 96, (6), 673-686.

137. Brandt, A.; Hallett, J. P.; Leak, D. J.; Murphy, R. J.; Welton, T., The effect of the ionic liquid anion in the pretreatment of pine wood chips. *Green Chemistry* **2010,** 12, (4), 672-679.

138. Ladisch, M. R.; Ladisch, C. M.; Tsao, G. T., Cellulose to sugars: new path gives quantitative yield. *Science* **1978,** 201, (4357), 743-745.

139. Sakakibara, A., A structural model of softwood lignin. *Wood Science and Technology* **1980,** 14, (2), 89-100.

140. Ralph, J.; Lundquist, K.; Brunow, G.; Lu, F.; Kim, H.; Schatz, P. F.; Marita, J. M.; Hatfield, R. D.; Ralph, S. A.; Christensen, J. H., Lignins: natural polymers from oxidative coupling of 4-hydroxyphenyl-propanoids. *Phytochemistry Reviews* **2004,** 3, (1-2), 29-60.

141. Boudet, A.; Lapierre, C.; Grima-Pettenati, J., Biochemistry and molecular biology of lignification. *New Phytologist* **1995,** 129, (2), 203-236.

142. Li, C.; Zhao, X.; Wang, A.; Huber, G. W.; Zhang, T., Catalytic Transformation of Lignin for the Production of Chemicals and Fuels. *Chem. Rev.* **2015,** 115, (21), 11559-11624.

143. Zhang, J.; Chen, Y.; Brook, M. A., Reductive Degradation of Lignin and Model Compounds by Hydrosilanes. *ACS Sustainable Chemistry & Engineering* **2014,** 2, (8), 1983-1991.

144. Kozliak, E. I.; Kubátová, A.; Artemyeva, A. A.; Nagel, E.; Zhang, C.; Rajappagowda, R. B.; Smirnova, A. L., Thermal Liquefaction of Lignin to Aromatics:

Efficiency, Selectivity, and Product Analysis. *ACS Sustainable Chemistry & Engineering* **2016,** 4, (10), 5106-5122.

145. Sarkanen, S., Enzymatic Lignin Degradation. In *Enzymes in Biomass Conversion*, American Chemical Society: 1991; Vol. 460, pp 247-269.

146. Holladay, J.; Bozell, J.; White, J.; Johnson, D., Top value-added chemicals from biomass. *DOE Report PNNL* **2007,** 16983.

147. Rodrigues Pinto, P. C.; Borges da Silva, E. A.; Rodrigues, A. r. E. d., Insights into oxidative conversion of lignin to high-added-value phenolic aldehydes. *Ind. Eng. Chem. Res.* **2010,** 50, (2), 741-748.

148. Villar, J.; Caperos, A.; Garcia-Ochoa, F., Oxidation of hardwood kraft-lignin to phenolic derivatives with oxygen as oxidant. *Wood Science and Technology* **2001,** 35, (3), 245-255.

149. Wu, G.; Heitz, M., Catalytic mechanism of Cu2+ and Fe3+ in alkaline O2 oxidation of lignin. *Journal of wood chemistry and technology* **1995,** 15, (2), 189-202.

150. DiCosimo, R.; Szabo, H. C., Oxidation of lignin model compounds using single-electron-transfer catalysts. *The Journal of Organic Chemistry* **1988,** 53, (8), 1673-1679.

151. Partenheimer, W., The aerobic oxidative cleavage of lignin to produce hydroxyaromatic benzaldehydes and carboxylic acids via metal/bromide catalysts in acetic acid/water mixtures. *Advanced Synthesis & Catalysis* **2009,** 351, (3), 456-466.

152. Wu, G.; Heitz, M.; Chornet, E., Improved alkaline oxidation process for the production of aldehydes (vanillin and syringaldehyde) from steam-explosion hardwood lignin. *Ind. Eng. Chem. Res.* **1994,** 33, (3), 718-723.

153. Deng, H.; Lin, L.; Sun, Y.; Pang, C.; Zhuang, J.; Ouyang, P.; Li, Z.; Liu, S., Perovskite-type oxide LaMnO3: An efficient and recyclable heterogeneous catalyst for the wet aerobic oxidation of lignin to aromatic aldehydes. *Catalysis letters* **2008,** 126, (1-2), 106.

154. Gao, P.; Li, C.; Wang, H.; Wang, X.; Wang, A., Perovskite hollow nanospheres for the catalytic wet air oxidation of lignin. *Chinese Journal of Catalysis* **2013,** 34, (10), 1811-1815.

155. Deng, H.; Lin, L.; Liu, S., Catalysis of Cu-doped Co-based perovskite-type oxide in wet oxidation of lignin to produce aromatic aldehydes. *Energy Fuels* **2010,** 24, (9), 4797-4802.

156. Zhang, J.; Deng, H.; Lin, L., Wet aerobic oxidation of lignin into aromatic aldehydes catalysed by a perovskite-type oxide: LaFe1-xCuxO3 (x= 0, 0.1, 0.2). *Molecules* **2009,** 14, (8), 2747-2757.

157. Pope, M. T.; Müller, A., Polyoxometalate Chemistry: An Old Field with New Dimensions in Several Disciplines. *Angewandte Chemie International Edition in English* **1991,** 30, (1), 34-48.

158. Pratt Iii, H. D.; Hudak, N. S.; Fang, X.; Anderson, T. M., A polyoxometalate flow battery. *Journal of Power Sources* **2013,** 236, 259-264.

159. Hartung, S.; Bucher, N.; Chen, H.-Y.; Al-Oweini, R.; Sreejith, S.; Borah, P.; Yanli, Z.; Kortz, U.; Stimming, U.; Hoster, H. E.; Srinivasan, M., Vanadium-based polyoxometalate as new material for sodium-ion battery anodes. *Journal of Power Sources* **2015,** 288, 270-277.

160. Voitl, T.; Rudolf von Rohr, P., Oxidation of lignin using aqueous polyoxometalates in the presence of alcohols. *ChemSusChem* **2008,** 1, (8-9), 763-769.

161. Khenkin, A. M.; Neumann, R., Oxidative C− C Bond Cleavage of Primary Alcohols and Vicinal Diols Catalyzed by H5PV2Mo10O40 by an Electron Transfer and Oxygen Transfer Reaction Mechanism. *Journal of the American Chemical Society* **2008,** 130, (44), 14474-14476.

162. Weinstock, I. A.; Hammel, K. E.; Moen, M. A.; Landucci, L. L.; Ralph, S.; Sullivan, C. E.; Reiner, R. S., Selective Transition-Metal Catalysis of Oxygen Delignification. Using Water-Soluble Salts of Polyoxometalate (POM) Anions. Part II. Reactions of α-[SiVW 11 O 40] 5-with Phenolic Lignin-Model Compounds. *Holzforschung-International Journal of the Biology, Chemistry, Physics and Technology of Wood* **1998,** 52, (3), 311-318.

163. Evtuguin, D. V.; Daniel, A. I.; Silvestre, A. J.; Amado, F. M.; Neto, C. P., Lignin aerobic oxidation promoted by molybdovanadophosphate polyanion [PMo 7 V 5 O 40] 8−. Study on the oxidative cleavage of β-O-4 aryl ether structures using model compounds. *Journal of Molecular Catalysis A: Chemical* **2000,** 154, (1), 217-224.

164. Zhu, Y.; Chuanzhao, L.; Sudarmadji, M.; Hui Min, N.; Biying, A. O.; Maguire, J. A.; Hosmane, N. S., An efficient and recyclable catalytic system comprising nanopalladium (0) and a pyridinium salt of iron bis (dicarbollide) for oxidation of substituted benzyl alcohol and lignin. *ChemistryOpen* **2012,** 1, (2), 67-70.

165. Chatel, G.; Rogers, R. D., Review: Oxidation of lignin using ionic liquids An innovative strategy to produce renewable chemicals. *ACS Sustainable Chemistry & Engineering* **2013,** 2, (3), 322-339.

166. Zakzeski, J.; Jongerius, A. L.; Weckhuysen, B. M., Transition metal catalyzed oxidation of Alcell lignin, soda lignin, and lignin model compounds in ionic liquids. *Green chemistry* **2010,** 12, (7), 1225-1236.

167. Shibata, I.; Isogai, A., Depolymerization of cellouronic acid during TEMPO-mediated oxidation. *Cellulose* **2003,** 10, (2), 151-158.

168. Nguyen, J. D.; Matsuura, B. S.; Stephenson, C. R., A photochemical strategy for lignin degradation at room temperature. *Journal of the American Chemical Society* **2014,** 136, (4), 1218-1221.

169. Marker, T.; Roberts, M.; Linck, M.; Felix, L.; Ortiz-Toral, P.; Wangerow, J.; Tan, E.; Gephart, J.; Shonnard, D. *Biomass to gasoline and diesel using integrated hydropyrolysis and hydroconversion*; Gas Technology Institute: 2013.

170. Pepper, J. M.; Hibbert, H., Studies on Lignin and Related Compounds. LXXXVII. High Pressure Hydrogenation of Maple Wood1. *Journal of the American Chemical Society* **1948,** 70, (1), 67-71.

171. Sergeev, A. G.; Hartwig, J. F., Selective, nickel-catalyzed hydrogenolysis of aryl ethers. *Science* **2011,** 332, (6028), 439-443.

172. He, J.; Zhao, C.; Lercher, J. A., Ni-catalyzed cleavage of aryl ethers in the aqueous phase. *Journal of the American Chemical Society* **2012,** 134, (51), 20768-20775.

173. Song, Q.; Wang, F.; Xu, J., Hydrogenolysis of lignosulfonate into phenols over heterogeneous nickel catalysts. *Chemical Communications* **2012,** 48, (56), 7019-7021.

174. Song, Q.; Wang, F.; Cai, J.; Wang, Y.; Zhang, J.; Yu, W.; Xu, J., Lignin depolymerization (LDP) in alcohol over nickel-based catalysts via a fragmentation–hydrogenolysis process. *Energy & Environmental Science* **2013,** 6, (3), 994-1007.

175. Toledano, A.; Serrano, L.; Pineda, A.; Romero, A. A.; Luque, R.; Labidi, J., Microwave-assisted depolymerisation of organosolv lignin via mild hydrogen-free hydrogenolysis: catalyst screening. *Applied Catalysis B: Environmental* **2014,** 145, 43-55.

176. Parsell, T. H.; Owen, B. C.; Klein, I.; Jarrell, T. M.; Marcum, C. L.; Haupert, L. J.; Amundson, L. M.; Kenttämaa, H. I.; Ribeiro, F.; Miller, J. T., Cleavage and hydrodeoxygenation (HDO) of C–O bonds relevant to lignin conversion using Pd/Zn synergistic catalysis. *Chemical Science* **2013,** 4, (2), 806-813.

177. Whiffen, V. M.; Smith, K. J., Hydrodeoxygenation of 4-methylphenol over unsupported MoP, MoS2, and MoO x catalysts. *Energy Fuels* **2010,** 24, (9), 4728-4737.

178. Zhao, H.; Li, D.; Bui, P.; Oyama, S., Hydrodeoxygenation of guaiacol as model compound for pyrolysis oil on transition metal phosphide hydroprocessing catalysts. *Applied Catalysis A: General* **2011,** 391, (1), 305-310.

179. Ma, X.; Tian, Y.; Hao, W.; Ma, R.; Li, Y., Production of phenols from catalytic conversion of lignin over a tungsten phosphide catalyst. *Applied Catalysis A: General* **2014,** 481, 64-70.

180. Lin, Y.-C.; Li, C.-L.; Wan, H.-P.; Lee, H.-T.; Liu, C.-F., Catalytic hydrodeoxygenation of guaiacol on Rh-based and sulfided CoMo and NiMo catalysts. *Energy Fuels* **2011,** 25, (3), 890-896.

181. González-Borja, M. Á.; Resasco, D. E., Anisole and guaiacol hydrodeoxygenation over monolithic Pt–Sn catalysts. *Energy Fuels* **2011,** 25, (9), 4155-4162.

182. Ohta, H.; Feng, B.; Kobayashi, H.; Hara, K.; Fukuoka, A., Selective hydrodeoxygenation of lignin-related 4-propylphenol into n-propylbenzene in water by Pt-Re/ZrO 2 catalysts. *Catalysis Today* **2014,** 234, 139-144.

183. Feng, B.; Kobayashi, H.; Ohta, H.; Fukuoka, A., Aqueous-phase hydrodeoxygenation of 4-propylphenol as a lignin model to n-propylbenzene over Re-Ni/ZrO 2 catalysts. *Journal of Molecular Catalysis A: Chemical* **2014,** 388, 41-46.

184. Zhao, C.; Kou, Y.; Lemonidou, A. A.; Li, X.; Lercher, J. A., Highly Selective Catalytic Conversion of Phenolic Bio-Oil to Alkanes. *Angewandte Chemie* **2009,** 121, (22), 4047-4050.

185. Oasmaa, A.; Alén, R.; Meier, D., Catalytic hydrotreatment of some technical lignins. *Bioresource Technology* **1993,** 45, (3), 189-194.

186. Okuda, K.; Umetsu, M.; Takami, S.; Adschiri, T., Disassembly of lignin and chemical recovery—rapid depolymerization of lignin without char formation in water–phenol mixtures. *Fuel processing technology* **2004,** 85, (8), 803-813.

187. Yokoyama, C.; Nishi, K.; Nakajima, A.; Seino, K., Thermolysis of organosolv lignin in supercritical water and supercritical methanol. *Journal of The Japan Petroleum Institute* **1998,** 41, (4), 243-250.

188. Huang, X.; Korányi, T. I.; Boot, M. D.; Hensen, E. J., Catalytic depolymerization of lignin in supercritical ethanol. *ChemSusChem* **2014,** 7, (8), 2276-2288.

189. Binder, J. B.; Gray, M. J.; White, J. F.; Zhang, Z. C.; Holladay, J. E., Reactions of lignin model compounds in ionic liquids. *Biomass and Bioenergy* **2009,** 33, (9), 1122-1130.

190. Fatehi, P.; Catalan, L.; Cave, G., Simulation analysis of producing xylitol from hemicelluloses of pre-hydrolysis liquor. *Chemical Engineering Research and Design* **2014,** 92, (8), 1563-1570.

191. Xie, Y. J.; Hill, C. A. S.; Xiao, Z. F.; Militz, H.; Mai, C., Silane coupling agents used for natural fiber/polymer composites: A review. *Compos. Pt. A-Appl. Sci. Manuf.* **2010,** 41, (7), 806-819.

192. Morandi, G.; Heath, L.; Thielemans, W., Cellulose Nanocrystals Grafted with Polystyrene Chains through Surface-Initiated Atom Transfer Radical Polymerization (SI-ATRP). *Langmuir* **2009,** 25, (14), 8280-8286.

193. El Mansouri, N. E.; Yuan, Q. L.; Huang, F. R., SYNTHESIS AND CHARACTERIZATION OF KRAFT LIGNIN-BASED EPOXY RESINS. *BioResources* **2011,** 6, (3), 2492-2503.

194. Braun, J. L.; Holtman, K. M.; Kadla, J. F., Lignin-based carbon fibers: Oxidative thermostabilization of kraft lignin. *Carbon* **2005,** 43, (2), 385-394.

195. Faix, O., Investigation of Lignin Polymer Models (DHP's) by FTIR Spectroscopy. In *Holzforschung - International Journal of the Biology, Chemistry, Physics and Technology of Wood*, 1986; Vol. 40, p 273.

196. Kong, T.; Ye, L.; Zhang, A. Y.; Feng, Z. G., Loose-fit polypseudorotaxanes constructed from gamma-CDs and PHEMA-PPG-PEG-PPG-PHEMA. *Beilstein Journal of Organic Chemistry* **2014,** 10, 2461-2469.

197. Lin, J.; Kong, T.; Ye, L.; Zhang, A.-y.; Feng, Z.-g., Self-assemblies of γ-CDs with pentablock copolymers PMA-PPO-PEO-PPO-PMA and endcapping via atom transfer radical polymerization of 2-methacryloyloxyethyl phosphorylcholine. *Beilstein Journal of Organic Chemistry* **2015,** 11, 2267-2277.

198. Li, S.; Lundquist, K., A new method for the analysis of phenolic groups in lignins by 1H NMR spectroscopy. *Nordic Pulp & Paper Research Journal* **1994,** 9, (3), 191-195.

199. Lundquist, K., NMR studies of lignins. 5. Investigation of non-derivatized spruce and birch lignin by 1HNMR spectroscopy. *Acta Chem. Scand. B* **1981,** 35, 497-501.

200. Lundquist, K., On the occurrence of β-1 structures in lignins. *Journal of wood chemistry and technology* **1987,** 7, (2), 179-185.

201. Brochier Salon, M.-C.; Abdelmouleh, M.; Boufi, S.; Belgacem, M. N.; Gandini, A., Silane adsorption onto cellulose fibers: Hydrolysis and condensation reactions. *Journal of Colloid and Interface Science* **2005,** 289, (1), 249-261.

202. Guo, S.; Zhang, C.; Wang, W.; Liu, T., Preparation and characterization of organic-inorganic hybrid nanomaterials using polyurethane-b-poly [3-(trimethoxysilyl) propyl methacrylate] via RAFT polymerization. *Polym. Lett* **2010,** 4, 17-25.

203. Kanhakeaw, P.; Rutnakornpituk, B.; Wichai, U.; Rutnakornpituk, M., Surface-Initiated Atom Transfer Radical Polymerization of Magnetite Nanoparticles with Statistical Poly(tert-butyl acrylate)-poly(poly(ethylene glycol) methyl ether methacrylate) Copolymers. *Journal of Nanomaterials* **2015,** 2015, 10.

204. Gundersen, S. A.; Sjöblom, J., High- and low-molecular-weight lignosulfonates and Kraft lignins as oil/water-emulsion stabilizers studied by means of electrical conductivity. *Colloid Polym Sci* **1999,** 277, (5), 462-468.

205. Lawson, J., J; Doughty, J., Viscosities of Solutions of Pine Wood Lignin from Kraft Black Liquor. *Industrial & Engineering Chemistry Chemical and Engineering Data Series* **1958,** 3, (1), 128-131.

206. Kar, F.; Arslan, N., Effect of temperature and concentration on viscosity of orange peel pectin solutions and intrinsic viscosity–molecular weight relationship. *Carbohydrate Polymers* **1999,** 40, (4), 277-284.

207. Binks, B.; Lumsdon, S., Catastrophic phase inversion of water-in-oil emulsions stabilized by hydrophobic silica. *Langmuir* **2000,** 16, (6), 2539-2547.

208. Shotton, P. G.; Hewlett, P. C.; James, A. N., POLYDISPERSE NATURE OF LIGNOSULFONATES. *Tappi* **1972,** 55, (3), 407-&.

209. Gardon, J. L.; Mason, S. G., PHYSICOCHEMICAL STUDIES OF LIGNINSULPHONATES .2. BEHAVIOR AS POLYELECTROLYTES. *Can. J. Chem.-Rev. Can. Chim.* **1955,** 33, (10), 1491-1501.

210. Doherty, W. O.; Mousavioun, P.; Fellows, C. M., Value-adding to cellulosic ethanol: Lignin polymers. *Ind. Crop. Prod.* **2011,** 33, (2), 259-276.

211. Calvo-Flores, F. G.; Dobado, J. A., Lignin as renewable raw material. *ChemSusChem* **2010,** 3, (11), 1227-1235.

212. Sun, Y.; Yang, L.; Lu, X.; He, C., Biodegradable and renewable poly (lactide)–lignin composites: synthesis, interface and toughening mechanism. *Journal of Materials Chemistry A* **2015,** 3, (7), 3699-3709.

213. Kumar, S.; Mohanty, A.; Erickson, L.; Misra, M., Lignin and its applications with polymers. *Journal of Biobased Materials and Bioenergy* **2009,** 3, (1), 1-24.

214. Sena-Martins, G.; Almeida-Vara, E.; Duarte, J., Eco-friendly new products from enzymatically modified industrial lignins. *Ind. Crop. Prod.* **2008,** 27, (2), 189-195.

215. de Oliveira, W.; Glasser, W. G., Multiphase materials with lignin. 11. Starlike copolymers with caprolactone. *Macromolecules* **1994,** 27, (1), 5-11.

216. Deng, Y.; Feng, X.; Zhou, M.; Qian, Y.; Yu, H.; Qiu, X., Investigation of aggregation and assembly of alkali lignin using iodine as a probe. *Biomacromolecules* **2011,** 12, (4), 1116-1125.

217. Xing, W.; Yuan, H.; Yang, H.; Song, L.; Hu, Y., Functionalized lignin for halogen-free flame retardant rigid polyurethane foam: preparation, thermal stability, fire performance and mechanical properties. *Journal of Polymer Research* **2013,** 20, (9), 234.

218. Canetti, M.; Bertini, F.; De Chirico, A.; Audisio, G., Thermal degradation behaviour of isotactic polypropylene blended with lignin. *Polymer degradation and stability* **2006,** 91, (3), 494-498.

219. Song, P.; Cao, Z.; Fu, S.; Fang, Z.; Wu, Q.; Ye, J., Thermal degradation and flame retardancy properties of ABS/lignin: Effects of lignin content and reactive compatibilization. *Thermochimica acta* **2011,** 518, (1), 59-65.

220. Liu, L.; Qian, M.; Song, P. a.; Huang, G.; Yu, Y.; Fu, S., Fabrication of green lignin-based flame retardants for enhancing the thermal and fire retardancy properties of polypropylene/wood composites. *ACS Sustainable Chemistry & Engineering* **2016,** 4, (4), 2422-2431.

221. Nadji, H.; Bruzzese, C.; Belgacem, M. N.; Benaboura, A.; Gandini, A., Oxypropylation of lignins and preparation of rigid polyurethane foams from the ensuing polyols. *Macromol. Mater. Eng.* **2005,** 290, (10), 1009-1016.

222. Li, Y.; Ragauskas, A. J., Kraft lignin-based rigid polyurethane foam. *Journal of Wood Chemistry and Technology* **2012,** 32, (3), 210-224.

223. Zhang, T.; Xu, Z.; Wu, Y.; Guo, Q., Assembled block copolymer stabilized high internal phase emulsion hydrogels for enhancing oil safety. *Ind. Eng. Chem. Res.* **2016,** 55, (16), 4499-4505.

224. Cameron, N. R., High internal phase emulsion templating as a route to well-defined porous polymers. *Polymer* **2005,** 46, (5), 1439-1449.

225. Williams, J. M., High internal phase water-in-oil emulsions: influence of surfactants and cosurfactants on emulsion stability and foam quality. *Langmuir* **1991,** 7, (7), 1370-1377.

226. Cameron, N. R.; Sherrington, D. C., High internal phase emulsions (HIPEs) — Structure, properties and use in polymer preparation. In *Biopolymers Liquid Crystalline Polymers Phase Emulsion*, Springer Berlin Heidelberg: Berlin, Heidelberg, 1996; pp 163-214.

227. Bhumgara, Z., Polyhipe foam materials as filtration media. *Filtration & Separation* **1995,** 32, (3), 245-251.

228. Wakeman, R. J.; Bhumgara, Z. G.; Akay, G., Ion exchange modules formed from polyhipe foam precursors. *Chem. Eng. J.* **1998,** 70, (2), 133-141.

229. Krajnc, P.; Štefanec, D.; Brown, J. F.; Cameron, N. R., Aryl acrylate based high-internal-phase emulsions as precursors for reactive monolithic polymer supports. *Journal of Polymer Science Part A: Polymer Chemistry* **2005,** 43, (2), 296-303.

230. Hansen, C. M., *Hansen solubility parameters: a user's handbook*. CRC press: 2007.

231. Hansen, C. M.; Smith, A. L., Using Hansen solubility parameters to correlate solubility of C60 fullerene in organic solvents and in polymers. *Carbon* **2004,** 42, (8–9), 1591-1597.

232. Redelius, P., Bitumen Solubility Model Using Hansen Solubility Parameter. *Energy Fuels* **2004,** 18, (4), 1087-1092.

233. Deepa, A. K.; Dhepe, P. L., Lignin Depolymerization into Aromatic Monomers over Solid Acid Catalysts. *ACS Catalysis* **2015,** 5, (1), 365-379.

234. Barta, K.; Warner, G. R.; Beach, E. S.; Anastas, P. T., Depolymerization of organosolv lignin to aromatic compounds over Cu-doped porous metal oxides. *Green Chemistry* **2014,** 16, (1), 191-196.

235. Wang, Q.; Liu, S.; Yang, G.; Chen, J., Characterization of high-boiling-solvent lignin from hot-water-extracted bagasse. *Energy Fuels* **2014,** 28, (5), 3167-3171.

236. Myint, A. A.; Lee, H. W.; Seo, B.; Son, W.-S.; Yoon, J.; Yoon, T. J.; Park, H. J.; Yu, J.; Yoon, J.; Lee, Y.-W., One pot synthesis of environmentally friendly lignin nanoparticles with compressed liquid carbon dioxide as an antisolvent. *Green Chemistry* **2016,** 18, (7), 2129-2146.

237. Ge, Y.; Xiao, D.; Li, Z.; Cui, X., Dithiocarbamate functionalized lignin for efficient removal of metallic ions and the usage of the metal-loaded bio-sorbents as potential free radical scavengers. *Journal of Materials Chemistry A* **2014,** 2, (7), 2136-2145.

238. Jia, Z.; Lu, C.; Zhou, P.; Wang, L., Preparation and characterization of high boiling solvent lignin-based polyurethane film with lignin as the only hydroxyl group provider. *RSC Advances* **2015,** 5, (66), 53949-53955.

239. Mulyadi, A.; Zhang, Z.; Dutzer, M.; Liu, W.; Deng, Y., Facile approach for synthesis of doped carbon electrocatalyst from cellulose nanofibrils toward high-performance metal-free oxygen reduction and hydrogen evolution. *Nano Energy* **2017,** 32, 336-346.

240. Hansen, C. M., Polymer additives and solubility parameters. *Progress in Organic Coatings* **2004,** 51, (2), 109-112.

241. Hansen, C.; Björkman, A., The ultrastructure of wood from a solubility parameter point of view. *Holzforschung-International Journal of the Biology, Chemistry, Physics and Technology of Wood* **1998,** 52, (4), 335-344.

242. Floury, J.; Desrumaux, A.; Lardieres, J., Effect of high-pressure homogenization on droplet size distributions and rheological properties of model oil-in-water emulsions. *Innovative Food Science & Emerging Technologies* **2000,** 1, (2), 127-134.

243. Pal, R., Effect of droplet size on the rheology of emulsions. *AIChE Journal* **1996,** 42, (11), 3181-3190.

244. Ratvijitvech, T.; Barrow, M.; Cooper, A. I.; Adams, D. J., The effect of molecular weight on the porosity of hypercrosslinked polystyrene. *Polym. Chem.* **2015,** 6, (41), 7280-7285.

245. Marti, M.; Fabregat, G.; Estrany, F.; Aleman, C.; Armelin, E., Nanostructured conducting polymer for dopamine detection. *Journal of Materials Chemistry* **2010,** 20, (47), 10652-10660.

246. Youssefian, S.; Rahbar, N., Molecular origin of strength and stiffness in bamboo fibrils. *Scientific reports* **2015,** 5, 11116.

247. Liu, W.; Zhou, R.; Goh, H. L. S.; Huang, S.; Lu, X., From waste to functional additive: toughening epoxy resin with lignin. *ACS applied materials & interfaces* **2014,** 6, (8), 5810-5817.

248. Kubo, S.; Kadla, J. F., Poly (ethylene oxide)/organosolv lignin blends: Relationship between thermal properties, chemical structure, and blend behavior. *Macromolecules* **2004,** 37, (18), 6904-6911.

249. Rahimi, A.; Ulbrich, A.; Coon, J. J.; Stahl, S. S., Formic-acid-induced depolymerization of oxidized lignin to aromatics. *Nature* **2014,** 515, (7526), 249.

250. Linger, J. G.; Vardon, D. R.; Guarnieri, M. T.; Karp, E. M.; Hunsinger, G. B.; Franden, M. A.; Johnson, C. W.; Chupka, G.; Strathmann, T. J.; Pienkos, P. T., Lignin valorization through integrated biological funneling and chemical catalysis. *Proceedings of the National Academy of Sciences* **2014,** 111, (33), 12013-12018.

251. Radoykova, T.; Nenkova, S.; Stanulov, K., Production of phenol compounds by alkaline treatment of poplar wood bark. *Chemistry of natural compounds* **2010,** 46, (5), 807-808.

252. Sasaki, M.; Goto, M., Conversion of biomass model compound under hydrothermal conditions using batch reactor. *Fuel* **2009,** 88, (9), 1656-1664.

253. Thring, R., Alkaline degradation of ALCELL® lignin. *Biomass and Bioenergy* **1994,** 7, (1-6), 125-130.

254. Jones, S. B.; Zhu, Y. *Preliminary economics for the production of pyrolysis oil from lignin in a cellulosic ethanol biorefinery*; Pacific Northwest National Laboratory (PNNL), Richland, WA (US): 2009.

255. Li, C.; Zhao, X.; Wang, A.; Huber, G. W.; Zhang, T., Catalytic transformation of lignin for the production of chemicals and fuels. *Chem. Rev* **2015,** 115, (21), 11559-11624.

256. Qi, S.-C.; Hayashi, J.-i.; Kudo, S.; Zhang, L., Catalytic hydrogenolysis of kraft lignin to monomers at high yield in alkaline water. *Green Chemistry* **2017,** 19, (11), 2636-2645.

257. Zhang, J.; Teo, J.; Chen, X.; Asakura, H.; Tanaka, T.; Teramura, K.; Yan, N., A series of NiM (M= Ru, Rh, and Pd) bimetallic catalysts for effective lignin hydrogenolysis in water. *Acs Catalysis* **2014,** 4, (5), 1574-1583.

258. Macala, G. S.; Matson, T. D.; Johnson, C. L.; Lewis, R. S.; Iretskii, A. V.; Ford, P. C., Hydrogen transfer from supercritical methanol over a solid base catalyst: A model for lignin depolymerization. *ChemSusChem* **2009,** 2, (3), 215-217.

259. Rensel, D. J.; Rouvimov, S.; Gin, M. E.; Hicks, J. C., Highly selective bimetallic FeMoP catalyst for C–O bond cleavage of aryl ethers. *Journal of catalysis* **2013,** 305, 256-263.

260. Jongerius, A. L.; Bruijnincx, P. C.; Weckhuysen, B. M., Liquid-phase reforming and hydrodeoxygenation as a two-step route to aromatics from lignin. *Green chemistry* **2013,** 15, (11), 3049-3056.

261. Xu, W.; Miller, S. J.; Agrawal, P. K.; Jones, C. W., Depolymerization and hydrodeoxygenation of switchgrass lignin with formic acid. *ChemSusChem* **2012,** 5, (4), 667-675.

262. Galkin, M. V.; Dahlstrand, C.; Samec, J. S., Mild and Robust Redox-Neutral Pd/C-Catalyzed Lignol β-O-4′ Bond Cleavage Through a Low-Energy-Barrier Pathway. *ChemSusChem* **2015,** 8, (13), 2187-2192.

263. Deng, W.; Zhang, H.; Wu, X.; Li, R.; Zhang, Q.; Wang, Y., Oxidative conversion of lignin and lignin model compounds catalyzed by CeO 2-supported Pd nanoparticles. *Green Chemistry* **2015,** 17, (11), 5009-5018.

264. Fargues, C.; Mathias, Á.; Rodrigues, A., Kinetics of vanillin production from kraft lignin oxidation. *Ind. Eng. Chem. Res.* **1996,** 35, (1), 28-36.

265. Cui, F.; Dolphin, D., Metallophthalocyanines as possible lignin peroxidase models. *Bioorganic & Medicinal Chemistry* **1995,** 3, (5), 471-477.

266. Liu, L.; Sun, J.; Li, M.; Wang, S.; Pei, H.; Zhang, J., Enhanced enzymatic hydrolysis and structural features of corn stover by FeCl 3 pretreatment. *Bioresource Technology* **2009,** 100, (23), 5853-5858.

267. Lü, J.; Zhou, P., Optimization of microwave-assisted FeCl 3 pretreatment conditions of rice straw and utilization of Trichoderma viride and Bacillus pumilus for production of reducing sugars. *Bioresource technology* **2011,** 102, (13), 6966-6971.

268. Chen, L.; Chen, R.; Fu, S., Preliminary exploration on pretreatment with metal chlorides and enzymatic hydrolysis of bagasse. *biomass and bioenergy* **2014,** 71, 311-317.

269. Gong, J.; Liu, W.; Du, X.; Liu, C.; Zhang, Z.; Sun, F.; Yang, L.; Xu, D.; Guo, H.; Deng, Y., Direct Conversion of Wheat Straw into Electricity with a Biomass Flow Fuel Cell Mediated by Two Redox Ion Pairs. *ChemSusChem* **2017,** 10, (3), 506-513.

270. Alekhina, M.; Ershova, O.; Ebert, A.; Heikkinen, S.; Sixta, H., Softwood kraft lignin for value-added applications: Fractionation and structural characterization. *Ind. Crop. Prod.* **2015,** 66, 220-228.

271. Singh, S. K.; Ekhe, J. D., Solvent effect on HZSM-5 catalyzed solvolytic depolymerization of industrial waste lignin to phenols: superiority of the water–methanol system over methanol. *RSC Advances* **2014,** 4, (95), 53220-53228.

272. Saito, T.; Perkins, J. H.; Vautard, F.; Meyer, H. M.; Messman, J. M.; Tolnai, B.; Naskar, A. K., Methanol fractionation of softwood kraft lignin: Impact on the lignin properties. *ChemSusChem* **2014,** 7, (1), 221-228.

273. Nowakowski, D. J.; Bridgwater, A. V.; Elliott, D. C.; Meier, D.; de Wild, P., Lignin fast pyrolysis: results from an international collaboration. *Journal of Analytical and Applied Pyrolysis* **2010,** 88, (1), 53-72.

274. Zeng, J.; Yoo, C. G.; Wang, F.; Pan, X.; Vermerris, W.; Tong, Z., Biomimetic Fenton-Catalyzed Lignin Depolymerization to High-Value Aromatics and Dicarboxylic Acids. *ChemSusChem* **2015,** 8, (5), 861-871.

275. Himmel, M. E.; Ding, S.-Y.; Johnson, D. K.; Adney, W. S.; Nimlos, M. R.; Brady, J. W.; Foust, T. D., Biomass recalcitrance: engineering plants and enzymes for biofuels production. *science* **2007,** 315, (5813), 804-807.

276. Sanderson, K., Lignocellulose: a chewy problem. *Nature* **2011,** 474, (7352), S12-S14.

277. Kim, T. H.; Kim, T. H., Overview of technical barriers and implementation of cellulosic ethanol in the US. *Energy* **2014,** 66, 13-19.

278. Cotana, F.; Cavalaglio, G.; Gelosia, M.; Coccia, V.; Petrozzi, A.; Nicolini, A., Effect of double-step steam explosion pretreatment in bioethanol production from softwood. *Applied biochemistry and biotechnology* **2014,** 174, (1), 156-167.

279. Li, X.; Luo, X.; Li, K.; Zhu, J.; Fougere, J. D.; Clarke, K., Effects of SPORL and dilute acid pretreatment on substrate morphology, cell physical and chemical wall structures, and subsequent enzymatic hydrolysis of lodgepole pine. *Applied biochemistry and biotechnology* **2012,** 168, (6), 1556-1567.

280. Loow, Y.-L.; Wu, T. Y.; Tan, K. A.; Lim, Y. S.; Siow, L. F.; Md. Jahim, J.; Mohammad, A. W.; Teoh, W. H., Recent advances in the application of inorganic salt

pretreatment for transforming lignocellulosic biomass into reducing sugars. *Journal of agricultural and food chemistry* **2015,** 63, (38), 8349-8363.

281. Arora, A.; Carrier, D. J., Understanding the pine dilute acid pretreatment system for enhanced enzymatic hydrolysis. *ACS Sustainable Chemistry & Engineering* **2015,** 3, (10), 2423-2428.

282. Zhao, Y.; Wang, Y.; Zhu, J.; Ragauskas, A.; Deng, Y., Enhanced enzymatic hydrolysis of spruce by alkaline pretreatment at low temperature. *Biotechnology and bioengineering* **2008,** 99, (6), 1320-1328.

283. Pan, X.; Xie, D.; Gilkes, N.; Gregg, D. J.; Saddler, J. N., Strategies to enhance the enzymatic hydrolysis of pretreated softwood with high residual lignin content. *Applied biochemistry and biotechnology* **2005,** 124, (1), 1069-1079.

284. Pielhop, T.; Amgarten, J.; Rohr, P. R.; Studer, M. H., Steam explosion pretreatment of softwood: the effect of the explosive decompression on enzymatic digestibility. *Biotechnology for Biofuels* **2016,** 9, (1), 152.

285. Diaz, A. B.; de Souza Moretti, M. M.; Bezerra-Bussoli, C.; Nunes, C. d. C. C.; Blandino, A.; da Silva, R.; Gomes, E., Evaluation of microwave-assisted pretreatment of lignocellulosic biomass immersed in alkaline glycerol for fermentable sugars production. *Bioresource technology* **2015,** 185, 316-323.

286. Bussemaker, M. J.; Zhang, D., Effect of ultrasound on lignocellulosic biomass as a pretreatment for biorefinery and biofuel applications. *Ind. Eng. Chem. Res.* **2013,** 52, (10), 3563-3580.

287. Yu, G.; Yano, S.; Inoue, H.; Inoue, S.; Endo, T.; Sawayama, S., Pretreatment of rice straw by a hot-compressed water process for enzymatic hydrolysis. *Applied Biochemistry and Biotechnology* **2010,** 160, (2), 539-551.

288. Zhang, L.; Pu, Y.; Cort, J. R.; Ragauskas, A. J.; Yang, B., Revealing the Molecular Structural Transformation of Hardwood and Softwood in Dilute Acid Flowthrough Pretreatment. *ACS Sustainable Chemistry & Engineering* **2016,** 4, (12), 6618-6628.

289. Li, Y.; Merrettig-Bruns, U.; Strauch, S.; Kabasci, S.; Chen, H., Optimization of ammonia pretreatment of wheat straw for biogas production. *J. Chem. Technol. Biotechnol.* **2015,** 90, (1), 130-138.

290. Kang, K. E.; Park, D.-H.; Jeong, G.-T., Effects of inorganic salts on pretreatment of Miscanthus straw. *Bioresource technology* **2013,** 132, 160-165.

291. Ayeni, A.; Hymore, F.; Mudliar, S.; Deshmukh, S.; Satpute, D.; Omoleye, J.; Pandey, R., Hydrogen peroxide and lime based oxidative pretreatment of wood waste to enhance enzymatic hydrolysis for a biorefinery: Process parameters optimization using response surface methodology. *Fuel* **2013,** 106, 187-194.

292. Hou, X.-D.; Li, N.; Zong, M.-H., Facile and simple pretreatment of sugar cane bagasse without size reduction using renewable ionic liquids–water mixtures. *ACS Sustainable Chemistry & Engineering* **2013,** 1, (5), 519-526.

293. Chang, V. S.; Holtzapple, M. T., Fundamental factors affecting biomass enzymatic reactivity. *Applied biochemistry and biotechnology* **2000,** 84, (1), 5-37.

294. Ryu, D. D.; Lee, S. B.; Tassinari, T.; Macy, C., Effect of compression milling on cellulose structure and on enzymatic hydrolysis kinetics. *Biotechnology and Bioengineering* **1982,** 24, (5), 1047-1067.

295. Rivers, D. B.; Emert, G. H., Factors affecting the enzymatic hydrolysis of bagasse and rice straw. *Biological wastes* **1988,** 26, (2), 85-95.

296. Li, C.; Cheng, G.; Balan, V.; Kent, M. S.; Ong, M.; Chundawat, S. P.; daCosta Sousa, L.; Melnichenko, Y. B.; Dale, B. E.; Simmons, B. A., Influence of physico-chemical changes on enzymatic digestibility of ionic liquid and AFEX pretreated corn stover. *Bioresource technology* **2011,** 102, (13), 6928-6936.

297. Chen, L.; Chen, R.; Fu, S., FeCl3 pretreatment of three lignocellulosic biomass for ethanol production. *ACS Sustainable Chemistry & Engineering* **2015,** 3, (8), 1794-1800.

298. Rabemanolontsoa, H.; Saka, S., Holocellulose determination in biomass. In *Zero-Carbon Energy Kyoto 2011*, Springer: 2012; pp 135-140.

299. Weihe, H.; Phillips, M., THE QUANTITATIVE ESTIMATION OF HEMICELLULOSES BY DIRECT ISOLATION! *Journal of Ag; ricultural Research Vol* **1947,** 74, (3).

300. Oakley, E. T., Determination of the" cellulose index" of tobacco. *Journal of Agricultural and Food Chemistry* **1984,** 32, (5), 1192-1194.

301. Ezeonu, C. S.; Onwurah, I. N.; Ubani, C. S.; Ejikeme, C. M.; Ogodo, A. C., Trichophyton Soudanense and Trichophyton Mentagrophyte-treated Rice Husk Biomass Components and Effect of Yeast on the Bioethanol Yield. *Achievements in the Life Sciences* **2016,** 10, (1), 72-79.

302. Moosavi-Nasab, M.; Majdi-Nasab, M., Utilization of sugar beet pulp as a substrate for the fungal production of cellulase and bioethanol. *African Journal of Microbiology Research* **2010,** 4, (23), 2556-2561.

303. Miller, G. L., Use of dinitrosalicylic acid reagent for determination of reducing sugar. *Analytical chemistry* **1959,** 31, (3), 426-428.

304. Brahim, M.; El Kantar, S.; Boussetta, N.; Grimi, N.; Brosse, N.; Vorobiev, E., Delignification of rapeseed straw using innovative chemo-physical pretreatments. *Biomass and Bioenergy* **2016,** 95, 92-98.

305. Adney, B.; Baker, J. *Measurement of cellulase activities: laboratory analytical procedure (LAP). National Renewable Energy Laboratory*; Technical Report: 2008.

306. Nitsos, C. K.; Matis, K. A.; Triantafyllidis, K. S., Optimization of hydrothermal pretreatment of lignocellulosic biomass in the bioethanol production process. *ChemSusChem* **2013,** 6, (1), 110-122.

307. Zheng, A.; Zhao, K.; Jiang, L.; Zhao, Z.; Sun, J.; Huang, Z.; Wei, G.; He, F.; Li, H., Bridging the gap between pyrolysis and fermentation: improving anhydrosugar production from fast pyrolysis of agriculture and forest residues by microwave-assisted organosolv pretreatment. *ACS Sustainable Chemistry & Engineering* **2016,** 4, (9), 5033-5040.

308. Salehian, P.; Karimi, K.; Zilouei, H.; Jeihanipour, A., Improvement of biogas production from pine wood by alkali pretreatment. *Fuel* **2013,** 106, 484-489.

309. Pu, Y.; Hu, F.; Huang, F.; Davison, B. H.; Ragauskas, A. J., Assessing the molecular structure basis for biomass recalcitrance during dilute acid and hydrothermal pretreatments. *Biotechnology for biofuels* **2013,** 6, (1), 15.

310. Hu, F.; Ragauskas, A., Pretreatment and lignocellulosic chemistry. *Bioenergy Research* **2012,** 5, (4), 1043-1066.

311. Nitsos, C. K.; Choli-Papadopoulou, T.; Matis, K. A.; Triantafyllidis, K. S., Optimization of hydrothermal pretreatment of hardwood and softwood lignocellulosic residues for selective hemicellulose recovery and improved cellulose enzymatic hydrolysis. *ACS Sustainable Chemistry & Engineering* **2016,** 4, (9), 4529-4544.

312. Xu, J.; Cheng, J. J.; Sharma-Shivappa, R. R.; Burns, J. C., Lime pretreatment of switchgrass at mild temperatures for ethanol production. *Bioresource Technology* **2010,** 101, (8), 2900-2903.

313. Chen, L.; Fu, S., Enhanced cellulase hydrolysis of eucalyptus waste fibers from pulp mill by tween80-assisted ferric chloride pretreatment. *Journal of agricultural and food chemistry* **2013,** 61, (13), 3293-3300.

314. Ong, H. C.; Jan, B. M.; Tong, C. W.; Fauzi, H.; Chen, W.-H., Effects of organosolv pretreatment and acid hydrolysis on palm empty fruit bunch (PEFB) as bioethanol feedstock. *Biomass and Bioenergy* **2016,** 95, 78-83.

315. Mooney, C. A.; Mansfield, S. D.; Touhy, M. G.; Saddler, J. N., The effect of initial pore volume and lignin content on the enzymatic hydrolysis of softwoods. *Bioresource Technology* **1998,** 64, (2), 113-119.

316. Li, C.; Knierim, B.; Manisseri, C.; Arora, R.; Scheller, H. V.; Auer, M.; Vogel, K. P.; Simmons, B. A.; Singh, S., Comparison of dilute acid and ionic liquid pretreatment of switchgrass: biomass recalcitrance, delignification and enzymatic saccharification. *Bioresource technology* **2010,** 101, (13), 4900-4906.

317. Du, X.; Lucia, L. A.; Ghiladi, R. A., Development of a highly efficient pretreatment sequence for the enzymatic saccharification of loblolly pine wood. *ACS Sustainable Chemistry & Engineering* **2016,** 4, (7), 3669-3678.

318. Poletto, M.; Zattera, A. J.; Forte, M. M.; Santana, R. M., Thermal decomposition of wood: Influence of wood components and cellulose crystallite size. *Bioresource Technology* **2012,** 109, 148-153.

319. He, Z.; Wang, Z.; Zhao, Z.; Yi, S.; Mu, J.; Wang, X., Influence of ultrasound pretreatment on wood physiochemical structure. *Ultrasonics Sonochemistry* **2017,** 34, 136-141.

320. Santoni, I.; Callone, E.; Sandak, A.; Sandak, J.; Dirè, S., Solid state NMR and IR characterization of wood polymer structure in relation to tree provenance. *Carbohydrate polymers* **2015,** 117, 710-721.

321. Liu, H.; Zhu, J.; Fu, S., Effects of lignin− metal complexation on enzymatic hydrolysis of cellulose. *Journal of agricultural and food chemistry* **2010,** 58, (12), 7233-7238.

322. Nzokou, P.; Pascal Kamdem, D., X-ray photoelectron spectroscopy study of red oak-(Quercus rubra), black cherry-(Prunus serotina) and red pine-(Pinus resinosa) extracted wood surfaces. *Surface and interface analysis* **2005,** 37, (8), 689-694.

323. Johansson, L.-S.; Campbell, J.; Koljonen, K.; Stenius, P., Evaluation of surface lignin on cellulose fibers with XPS. *Applied surface science* **1999,** 144, 92-95.

324. Kamdem, D.; Riedl, B.; Adnot, A.; Kaliaguine, S., ESCA spectroscopy of poly (methyl methacrylate) grafted onto wood fibers. *J. Appl. Polym. Sci.* **1991,** 43, (10), 1901-1912.

325. Ma, X.; Yang, X.; Zheng, X.; Chen, L.; Huang, L.; Cao, S.; Akinosho, H., Toward a further understanding of hydrothermally pretreated holocellulose and isolated pseudo lignin. *Cellulose* **2015,** 22, (3), 1687-1696.

326. Hallac, B. B.; Ragauskas, A. J., Analyzing cellulose degree of polymerization and its relevancy to cellulosic ethanol. *Biofuels, Bioproducts and Biorefining* **2011,** 5, (2), 215-225.

327. Ziebell, A.; Gracom, K.; Katahira, R.; Chen, F.; Pu, Y.; Ragauskas, A.; Dixon, R. A.; Davis, M., Increase in 4-coumaryl alcohol units during lignification in alfalfa (Medicago sativa) alters the extractability and molecular weight of lignin. *J Biol Chem* **2010,** 285, (50), 38961-38968.

328. Nitsos, C.; Stoklosa, R.; Karnaouri, A.; Voros, D.; Lange, H.; Hodge, D.; Crestini, C.; Rova, U.; Christakopoulos, P., Isolation and characterization of organosolv and alkaline lignins from hardwood and softwood biomass. *ACS Sustainable Chemistry & Engineering* **2016,** 4, (10), 5181-5193.

329. Wang, K.; Xu, F.; Sun, R., Molecular characteristics of kraft-AQ pulping lignin fractionated by sequential organic solvent extraction. *International journal of molecular sciences* **2010,** 11, (8), 2988-3001.

330. Passoni, V.; Scarica, C.; Levi, M.; Turri, S.; Griffini, G., Fractionation of industrial softwood kraft lignin: Solvent selection as a tool for tailored material properties. *ACS Sustainable Chemistry & Engineering* **2016,** 4, (4), 2232-2242.

331. Mohtar, S.; Busu, T. T. M.; Noor, A. M.; Shaari, N.; Yusoff, N.; Bustam, M.; Mutalib, M. A.; Mat, H., Extraction and characterization of lignin from oil palm biomass

via ionic liquid dissolution and non-toxic aluminium potassium sulfate dodecahydrate precipitation processes. *Bioresource technology* **2015,** 192, 212-218.

332. Sun, S.-N.; Li, M.-F.; Yuan, T.-Q.; Xu, F.; Sun, R.-C., Effect of ionic liquid/organic solvent pretreatment on the enzymatic hydrolysis of corncob for bioethanol production. Part 1: Structural characterization of the lignins. *Industrial crops and products* **2013,** 43, 570-577.

333. Jääskeläinen, A.; Sun, Y.; Argyropoulos, D.; Tamminen, T.; Hortling, B., The effect of isolation method on the chemical structure of residual lignin. *Wood Science and Technology* **2003,** 37, (2), 91-102.

334. Adney, B.; Baker, J., Measurement of cellulase activities. *Laboratory analytical procedure* **1996,** 6, 1996.